Characterization of novel hydrophobic surface binding proteins in *Mucor circinelloides*

PhD Thesis

Amanda Grace Vaz

Supervisors:
Prof. Dr. Tamás Papp
Dr. Gábor Nagy

Doctoral School of Biology

Department of Microbiology
Faculty of Science and Informatics
University of Szeged

Szeged
2020

TABLE OF CONTENTS

TABLE OF CONTENTS 1
LIST OF ABBREVIATIONS 3
SUMMARY 6
1. INTRODUCTION 7
1.1 General characterization of Mucorales fungi 7
1.2 Mucormycosis 10
1.3 Virulence factors of mucormycosis-causing fungi 12
1.4 Significance of cell surface and cell wall structure in the pathogenicity of filamentous fungi 14
1.4.1 Cell wall composition of fungi 15
1.4.2 Specific features of the Mucorales cell wall 17
1.5 Hydrophobic surface binding protein 18
2. AIMS 22
3. MATERIALS AND METHODS 23
3.1 Strains used in the study 23
3.2 Composition of the applied media 23
3.3 Isolation of fungal genomic DNA and agarose gel electrophoresis 24
3.4 PCR amplification for gene cloning 25
3.5 Construction of plasmids 25
3.6 Design and construction of the guide RNA (gRNA) and the template DNA for CRISPR-Cas9 gene disruption 26
3.7 Preparation of *E. coli* DH5α competent cells and bacterial transformation 27
3.8 PEG mediated protoplast transformation of *M. circinelloides* 28
3.9 Quantitative real-time reverse transcription PCR (qRT-PCR) 28
3. 10 Whole genome sequencing 29
3.11 Sequence analysis 30
3.12 Light microscopy 30
3.13 Scanning electron microscopy (SEM) 30
3.14 Sporulation assay 31
3.15 Germination assay 31
3.15 Biofilm Assay 31
3.16 Alcohol percentage test 32
3.17 Phagocytosis assay 32
3.18 Infection of *Galleria mellonella* with *hsbA* mutants of *M. circinelloides* 33
3.19 Heterologous expression of the HsbA1 and HsbA2 proteins in *Pichia pastoris* 33
3.19.1 Construction of the expression vector and transformation of P. pastoris 33
3.19.2 DNA isolation from P. pastoris 34
3.19.3 Production and purification of HsbA proteins from the P. pastoris transformants 35
3.19.4 Sodium Dodecyl Sulphate Polyacrylamide Gel Electrophoresis (SDS- PAGE) 35
3.19.5 Purification of the recombinant HsbA proteins 36
3.19.6 *Mass spectrometric analysis of purified protein* 37
3.20 Statistical analysis 37
4. RESULTS AND DISCUSSION 39

4.1 Identification of *hsbA* genes in the *M. circinelloides* genome 39
4.2 Transcription of the *hsbA* genes of *M. circinelloides* 43
4.2.1 Relative transcript levels of the hsbA genes during the cultivation period 43
4.2.2 Relative transcript levels of the hsbA genes at different temperatures 43
4.2.3 Effect of the serum on the transcription of the hsbA genes 44
4.2.4 Transcription of the hsbA genes under aerobic and anaerobic conditions 46
4.2.5 Effect of the presence of lignocellulosic materials on the transcription of the hsbA genes 47
4.3 Construction of disruption and overexpression mutants for the genes *hsbA1*, *hsbA2* and *hsbA3* 49
4.3.1 Disruption of hsbA1, hsbA2 and hsbA3 using the CRISPR-Cas9 method 49
4.3.2 Overexpression of hsbA1, hsbA2 and hsbA3 52
4.4 Characterization of the *hsbA* mutants 54
4.4.5 Colony growth of the hsbA mutants at different temperatures 54
4.4.6 Sporulation ability of the hsbA mutants 55
4.4.7 Germination ability of the spores of the hsbA mutants 55
4.4.8 Effect of cell wall stressors on the growth of the hsbA mutants 56
4.4.9 Effect of detergents on the growth of the hsbA mutants 57
4.5 Effect of the *hsbA* genes on the biofilm formation of *M. circinelloides* 59
4.6 Overexpression of the *hsbA* genes influenced the hydrophobicity of the *M. circinelloides* mycelium 60
4.7 Scanning electron microscopic analysis of mutants 62
4.8 Phagocytosis assay 64
4.8 Virulence of the *hsbA* mutants in *Galleria mellonella* non-vertebrate model 64
4.9 Heterologous expression of *M. circinelloides* HsbA1 in *P. pastoris* KM71H 66
5. CONCLUSION 68
6. ÖSSZEFOGLALÓ 71
7. AKNOWLEDGEMENT 74
8. REFERENCES 76
9. LIST OF PUBLICATIONS 88
SUPPLEMENTARY MATERIALS 92

LIST OF ABBREVIATIONS

CaN	Calcineurin
Cas9	CRISPR associated protein 9
CBS	Centraalbureau voor Schimmelcultures, Utrecht, Netherlands
cDNA	Complementary DNA
CFW	Calcofluor White
CR	Congo Red
CotH	Inner spore coat protein H
CRISPR	Clustered, regularly interspaced, short palindromic repeat
crRNA	CRISPR RNA
CutL1	Cutinase 1
Cys	Conserved L-cysteine residues
EDTA	Ethylene diamine tetra acetic acid
FTR1	High-affinity iron permease
gRNA	Guide RNA
HDR	Homology driven repair
HsbA	Hydrophobic surface binding protein A
LB	Lysogeny broth
MEA	Malt extract agar
MH-S	Murine Alveolar macrophage, SV40 transformed
MOPS	3-(N-morpholino) propanesulfonic acid
NCBI	National Center for Biotechnology Information
OD	Optical density
PAM	Protospacer adjacent motif
PAMPs	Pathogen associated molecular patterns
PBS	Phosphate buffered saline
PBSA	Polybutylene succinate-*co*-adipate
PCR	Polymerase chain reaction
PEG	Polyethylene glycol
PI	Phagocytic index
PMC	PEG-sorbitol-MOPS-calcium chloride buffer

PRRs	Pathogen recognition receptors
qRT-PCR	Quantitative real-time reverse transcription PCR
SDS-PAGE	Sodium Dodecyl Sulphate Polyacrylamide Gel Electrophoresis
SEM	Scanning electron microscopy
SMC	Sorbitol-MOPS-calcium chloride buffer
SNP	Single-point nucleotide polymorphisms
SZMC	Szeged Microbiology Collection, Hungary
TAE	Tris acetic acid-disodium EDTA buffer
TCA	Trichloroacetic acid solution
TRIS	Tris (hydroxymethyl) aminomethane
WB	Wheat bran
WGS	Whole genome sequencing
YEG	Yeast extract-glucose medium
YNB	Yeast nitrogen base
YPD	Yeast extract-peptone-dextrose medium
YPG	Yeast extract-peptone-glucose broth

Mucor circinelloides strains, genes, and encoded proteins

MS12	*M. circinelloides* f. *lusitanicus* auxotrophic mutant (*leuA*$^-$ and *pyrG*$^-$)
MS12+*pyrG*	MS12 containing a functional *pyrG* complement
MS12+pAV1	*hsbA1* overexpressed mutant
MS12+pAV2	*hsbA2* overexpressed mutant
MS12+pAV3	*hsbA3* overexpressed mutant
MS12+Δ*hsbA1*	*hsbA1* deletion mutant
MS12+Δ*hsbA2*	*hsbA2* deletion mutant
MS12+Δ*hsbA3*	*hsbA3* deletion mutant
pyrG	Gene encoding orotidine-5-monophosphate decarboxylase
leuA	Gene encoding α-Isopropylmalate isomerase
hsbA	Gene encoding hydrophobic surface binding protein A
hsbA1	Gene encoding hydrophobic surface binding protein A1

hsbA2	Gene encoding hydrophobic surface binding protein A2
hsbA3	Gene encoding hydrophobic surface binding protein A3

SUMMARY

Hydrophobic surface binding protein A (HsbA) is a small secreted protein found in eukaryotes. It was firstly isolated from the culture broth of *Aspergillus oryzae* RIB40. These proteins were found to be able to recruit enzymes to hydrophobic surfaces and could promote the activity of degradative extracellular enzymes. In case of some human pathogenic fungi, HsbA-like proteins were found to be expressed at high level during infection. The objective of the current study was to identify and characterize *hsbA* genes and the encoded proteins in *Mucor circinelloides*, which is a wildly used model organism of studies on Mucorales fungi.

Six potential *hsbA* genes named as *hsbA1a*, *hsbA1b*, *hsbA2*, *hsbA3*, *hsbA4* and *hsbA5* were identified in the genome of *M. circinelloides*. The *in silico* analysis of these genes showed that some of the proteins may be secreted and other can be cell wall bound molecules. We also found that *hsbA1b* can be a pseudogene. Four genes were selected for transcription analysis which indicated that the tested genes are expressed throughout the whole life cycle, especially in the hyphae. The genes were found to be upregulated at higher temperatures and downregulated under anaerobiosis. Presence of human serum upregulated *hsbA1a*, *hsbA2* and *hsbA4* but did not affect *hsbA3*, which were induced by lignocellulosic material indicating different regulations and functions for the four genes. Using the CRISPR-Cas9 technique *hsbA1a*, *hsbA2* and *hsbA3* were disrupted; overexpression mutants for these genes were also created. Altered expression of the three genes had only a slight effect on the growing abilities of the fungus. Overexpression of *hsbA2* led to increased spore production. Besides, overexpression of all three genes decreased the germination ability of the sporangiospores. We also found that increased expression of the genes increased the hydrophobicity of the cell surface and caused sensitivity to cell wall and membrane stressors. Biofilm forming capacity of the mutants, in which the *hsbA* genes were disrupted decreased indicating that HsbA may contribute to the biofilm formation of *M. circinelloides.*

In the non-vertebrate infection model *Galleria mellonella*, overexpression of *hsbA2* associated with decreased virulence while that of all deletion mutants significantly increased. This result may suggest that the HsbA level and/or the hydrophobicity of the mycelium may affect the pathogenicity of *M. circinelloides*.

For future analysis of the proteins and their functions, recombinant HsbA1 was expressed in *Pichia pastoris* and the produced protein was purified.

1. INTRODUCTION

1.1 General characterization of Mucorales fungi

The order Mucorales belonging to the phylum Mucoromycota (**Figure 1**) contains filamentous fungal species, which are most frequently saprotrophs and widely distributed in nature growing on decaying organic substances, such as remnants of food, dead plants, or animal waste in soil. These moulds are characterized by rapidly growing mycelium, which is typically aseptate or irregularly septate (**Richardson and Rautemaa-Richardson, 2019**). Some species of the mucoralean group exhibit dimorphism, possessing the ability to switch from a filamentous, multi-cellular state to a yeast form depending on the available oxygen level (**Lee et al., 2013; Vellanki et al., 2018**). In *Mucor* species, yeast-like growth is generally induced by anaerobiosis in the presence of fermentable hexoses, whereas hyphal growth is induced by the presence of oxygen. Some of the dimorphic *Mucor* species behave differently in response to the environmental conditions, like *Mucor genevensis*, which can grow as a yeast under aerobic condition in the presence of high hexose concentration (**Lax et al., 2020**).

Mucorales fungi can reproduce by sexual and asexual means (**Mendoza et al., 2014)**. They can reproduce asexually by chlamydospores or sporangiospores and sexually by zygospores. Sexual reproduction occurs during unfavourable condition by gametangial conjugation. When hyphal fusion occurs between two different thalli (the compatible mating types are designated as + and –) to form a zygospore, the fungi are called as heterothallic, in comparison to homothallism, which is the formation of zygospores within a single thallus. Before the zygospore germinates, it undergoes a long period of dormancy. During germination, the zygospores form a single aerial hypha with a sporangium at its apex, which in turn harbours the sporangiospores (**Lee and Heitman, 2014**). Asexual reproduction occurs during favourable conditions by formation of sporangiospores and during unfavourable conditions by formation of chlamydospores. Sporangiospore is produced at the tip of the sporangiophore inside the sporangium, which disperses and germinates to produce mycelia (**Mendoza et al., 2014)**. Chlamydospores are thick-walled resting spores, that are formed when mature hyphae become septate and accumulate nuclei and cytoplasm at the septate region and thick wall is formed around them (**Lin and Heitman, 2005**).

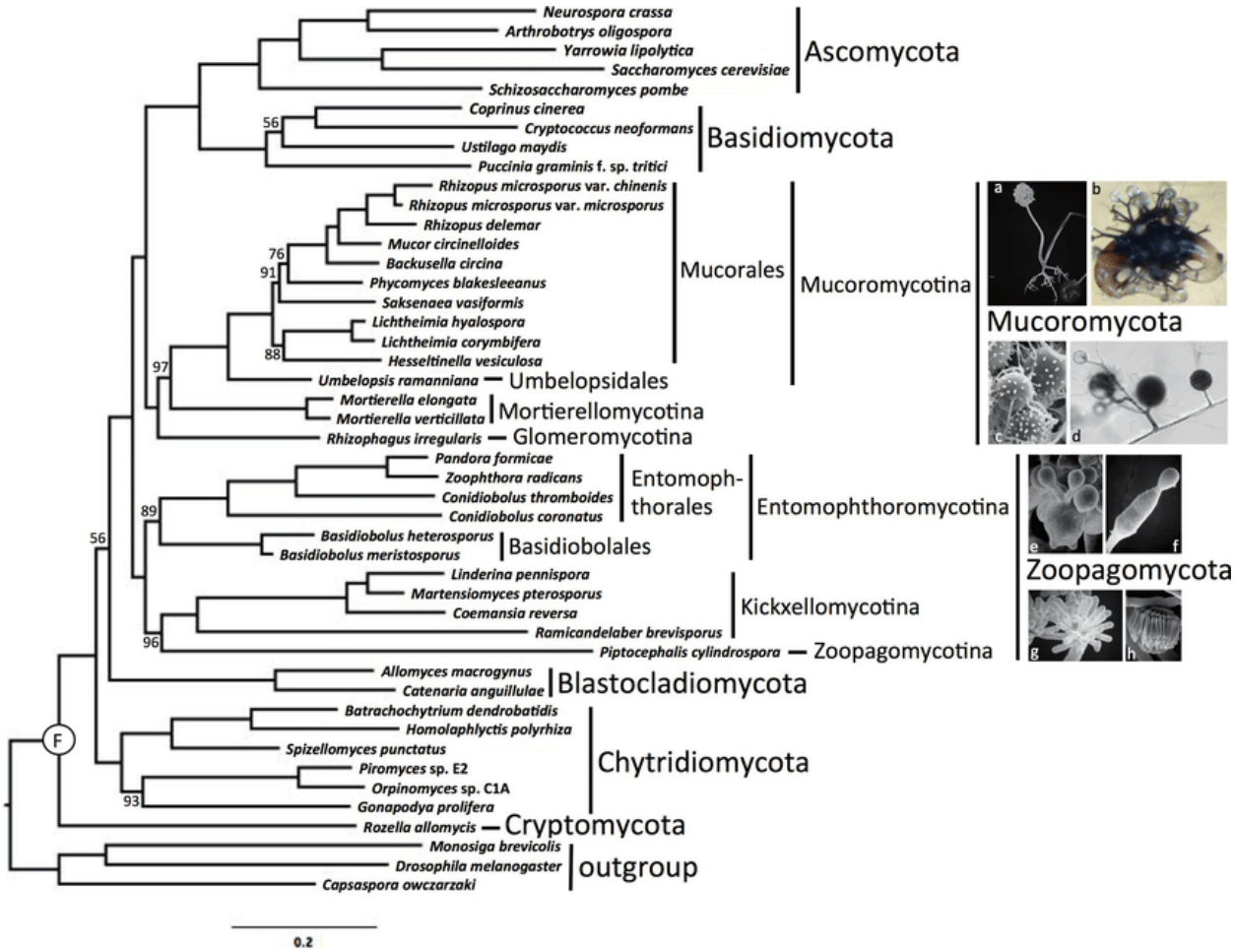

Figure 1: Phylogeny of the kingdom fungi based on the concatenated alignment of 192 conserved orthologous proteins (**Spatafora et al., 2016**)**.** Example images of species include: a. *Rhizopus* sporangium (Scanning electron micrograph, SEM), b. *Phycomyces* zygospore (Light microscope, LM), c. *Mortierella* chlamydospores (SEM), d. *Rhizophagus* spores and hyphae (LM), e. *Conidiobolus* secondary conidia forming on primary conidium (SEM), f. *Basidiobolus ballistosporic* conidium (SEM), g. *Piptocephalis* merosporangia (SEM), h. *Linderina* merosporangium (SEM).

Various characters presented by the Mucorales species including high growth rates in a wide range of temperatures (**Morin-Sardin et al., 2016**), thermophilic capacity of several species, existence in a yeast state of certain species (**Orlowski, 1991**) and high proteolytic and lipolytic enzymatic activities (**Ma et al., 2011**) make them good candidates for biotechnological developments. Many species are known for their economic importance as producers of carotenoids

or enzymes, such as amylase, protease, lipase, phytase and polygalacturonase, as well as fermenting agents for various products of soybean (**Voigt et al., 2016; Nguyen and Lee, 2018 and Walther et al., 2019**).

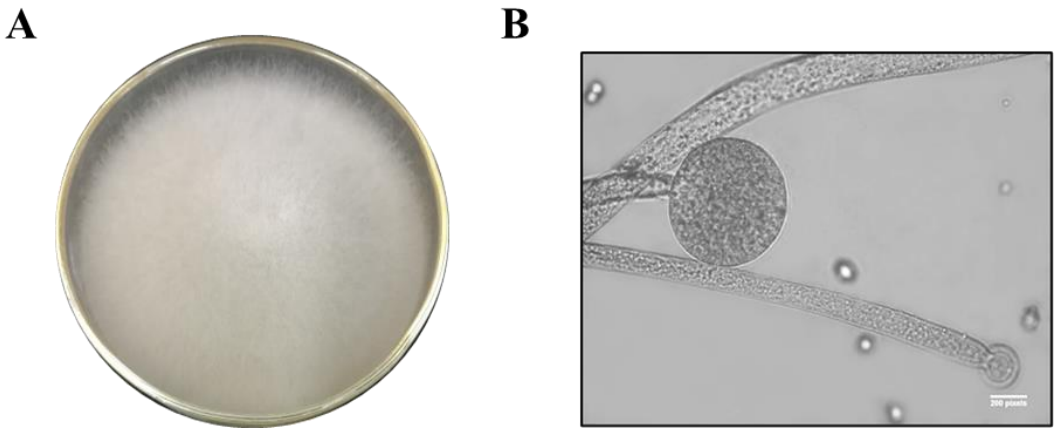

Figure 2: (A) Colony and (**B**) sporangium of of *Mucor circinelloides* f. *lusitanicus* MS12 strain grown on malt extract agar (MEA) after 4 days at 25 °C.

Some Mucorales species, such as *Mucor circinelloides* and *Rhizopus oryzae* are widely used as model organisms in various genetic and molecular biological studies (**Roncero et al., 1989; Skory, 2002; Ma et al., 2009** ; **Lee et al., 2013; López-Fernández et al., 2018 and Ibrahim et al; 2010**). It have also been applied in various studies addressed to the production of enzymes, carotenoids (**Naz et al., 2020**) and other metabolites, the genetic and molecular background of the pathogenicity of Mucorales (**Charles et al., 2011**), mechanism and role of morphological dimorphism and the role of RNA interference in the fungal cells (**Cervantes et al., 2013 and Ruiz-Vazquez et al., 2015**). Since, *M. circinelloides* accumulates all these features and is also readily transformable (**Garre et al., 2014; Gracia et al., 2017 and Nagy et al., 2017**) thus enabling opportunities for genetic modification, hence *M. circinelloides* f. *lusitanicus* (**Figure 2**) was used in our studies.

Certain species belonging to the order Mucorales are considered as human pathogenic fungi, causing superficial or invasive infections known as mucormycosis (**Spellberg and Ibrahim, 2010 and Singh et al., 2016**). Members of the genera *Rhizopus* (e.g. *R. oryzae*), *Mucor* (e.g. *M. circinelloides*) and *Lichtheimia* (e.g. *L. corymbifera*) are the most frequently isolated from

clinical samples (**Prabhu and Patel, 2004 and Petrikkos et al., 2012)** while species belonging to the genera *Rhizomucor*, *Saksenaea*, *Cunninghamella*, *Cokeromyces*, *Syncephalastrum* and *Apophysomyces* are less reported as agents of mucormycosis cases.

Despite current treatment options pertaining to mucormycosis, there has been poor outcomes and high mortality rates due to the insufficient knowledge on the physiology and virulence factors that are associated with mucoralean fungi. This is mainly due to the heterogeneity of this group and difficulties of genetically modifying the members in this group. However, *M. circinelloides* differs from the members of Mucormycetes through the ability to carry out genetic manipulations by various molecular tools. Hence *M. circinelloides* is more favourably used as a base model for understanding fungal genetics and host-pathogen interactions in mucormycosis (**Gracia et al., 2018**). The genome of *M. circinelloides* f. *lusticanicus* of the size 36.6Mb, was the third publicly available Mucorales genome. Genomic investigations of *M. circinelloides* was carried out through transforming *M. circinelloides* protoplasts with plasmid by polyethylene glycol (PEG) and calcium chloride and remains as a gold standard (**van Heeswijck and Roncero, 1984**).

1.2 Mucormycosis

Mucormycosis is a life-threatening infection, caused by a group of moulds belonging to the order Mucorales (**Ribes et al., 2000 and Spellberg et al., 2005**). It is the third most commonly occurring invasive fungal infection, followed by aspergillosis and candidiasis (**Torres-Narbona et al., 2007; Bitar et al., 2009; Saegman et al., 2010; Petrikkos et al., 2012; Chakrabarti and Dhaliwal, 2013 and Prakash et al., 2019**). A review study conducted on 851 cases from a period of January 2000 to January 2017 indicated that mucormycosis burden is higher in Europe than in Asia, as they reported 34% cases in Europe, followed by 31% in Asia, 28% in North and South America, 3% in Africa and 3% in Australia and New Zealand (**Jeong et al., 2019**). However, there is a drastic rise in the number of mucormycosis infection that are reported from India, hence this data obtained may be due to the under-reporting that could have occurred during this period from Asian countries (**Chakrabarti et al., 2009; Chakrabarti and Dhaliwal, 2013 and Prakash et al., 2019)**. Mucormycosis is characterized by the tendency of fungi to invade the vasculature, resulting in thrombosis and subsequent tissue necrosis. Tissue necrosis can further contribute to the severity of the infection by restriction of phagocytic cells from fungal clearance or antifungal agents to access to the infected loci (**Ibrahim et al., 2012**). Mucorales are opportunistic pathogens

that affect mostly immunocompromised hosts, most particularly those suffering from haematological malignancies or received bone marrow or organ transplantation (**Gonzalez et al., 2002, Pak et al., 2008)**. Other risk factors for this disease include uncontrolled diabetes mellitus, deferoxamine therapy, other forms of metabolic acidosis, neutropenia, corticosteroid therapy, skin trauma and other conditions that impairs the immune system (**Spellberg et al., 2005 and Ibrahim et al., 2016).**

The importance of Mucoralean species has grown in recent years since there is an increase in the number of patients with predisposing factors for mucormycosis (**Petrikkos and Skiada et al., 2012 and Prakash and Chakrabarti, 2019**). Most human infections are resulted by the inhalation of fungal spores that have been released into the surrounding air or by direct inoculation of organisms into disrupted skin or mucosa (**Ibrahim et al., 2004 and Petrikkos et al., 2012).** Some species of Mucorales are thermotolerant, such as *Rhizopus microsporus* (**Cheng et al., 2009**) and *Lichtheimia corymbifera* (**Hoffman and Voigt, 2007)**, with cases of mucormycosis being reported worldwide (**Richardson, 2009 and Petrikkos et al., 2012).**

Mucormycosis can be classified in different forms based on the anatomic localization of the infection, i.e. rhinocerebral, pulmonary, cutaneous, gastrointestinal, disseminated, and uncommon presentations (**Petrikkos et al., 2012**). Common features of rhinocerebral, pulmonary, and disseminated diseases include blood vessel invasion, haemorrhagic necrosis, thrombosis and, without treatment, a rapid fatal outcome (**Rogers, 2008 and Petrikkos et al., 2012**). To treat mucormycosis the following four factors are critical: early diagnosis, reversal of the underlying predisposing factor, surgical debridement of infected loci, and appropriate antifungal therapy (**Ellie et. al., 2009 and Gomes et al., 2011**). Early diagnosis is critical for the immediate treatment before the progression of the disease to a disseminate form. To reverse or control mucormycosis-predisposing factors in the host, various immunosuppressive medications such as corticosteroids can be administered at reduced dosage or stopped based on the requirements. In case of diabetic ketoacidosis patients, hyperglycaemia and acidaemia must be corrected. In previous studies, iron was shown to aggravate mucormycosis infection in animal models (**Ibrahim et. al., 2007**) hence iron administration to patients with active mucormycosis (for example, by treatment with certain iron chelators, such as deferoxamine) should be avoided. New iron chelators, deferiprone and deferasirox have shown not to be associated with the increased risk of mucormycosis and have thus been used as a therapeutic agent in experimental mucormycosis (**Reed et al., 2006; Ibrahim**

et al., 2009 and Bennett et al., 2019). Surgery is usually implemented for the control of mucormycosis in cases where the host suffers from multiple sites of infection, rhinocerebral infection, skin and soft tissue infection, various species causing the disease and the different duration for therapy (**Kontoyiannis and Lewis, 2011 and Skiada et al., 2012;**).

For first-line chemotherapy of mucormycosis, liposomal amphotericin B and amphotericin B lipid complex are administered. Since lipid formulations of amphotericin B are significantly less nephrotoxic, they can be more safely administered at high dosage for longer period compared to amphotericin B deoxycholate (**Petrikkos, 2009**). As for the second line treatment, posaconazole and a combination of liposomal amphotericin B or amphotericin B lipid complex with caspofungin are administered (**Skida et al., 2013**).

Very poor outcome has been observed despite the current treatment options, like correction of the underlying risk factors, antifungal therapy, and aggressive surgery. Mortality rates of mucormycosis infections are very high of approximately 50% and can approach to 100% in patients with disseminated disease, persistent neutropenia, and cerebral invasion (**Katragkou et al., 2013 and Skiada et al., 2019**). This is mainly due to less knowledge or poor understanding on the pathogenesis of the infection, as well as the role of specific virulence factors and the interaction with host immune system (**Morace and Borghi, 2012**). Hence researchers are trying to identify various virulence factors of these pathogenic fungus that could pose as a potential diagnostic and therapeutic target.

1.3 Virulence factors of mucormycosis-causing fungi

Virulence factors of pathogens are known to play a key role in damaging the host cells by enabling the pathogen to survive, colonize, spread, and suppress the immune response of host during an infection. Some of the virulence factors specific to Mucorales are the followings:

High-affinity iron permease (FTR1) plays a role in the uptake and transport of iron in Mucorales (**Ibrahim et al., 2007**). The *FTR1* gene was shown to be highly expressed during the infection of immunodeficient mice with *R. oryzae* (**Navarro-Mendoza et al., 2018**). Knock-out of *FTR1* reduces iron uptake and the virulence in *R. oryzae*. Infected mice were passively immunized by using an antibody against the FTR1 protein, that resulted in diminished mortality rate and enhanced survival rate (**Ibrahim et al., 2007**). Fob1 and Fob2 proteins are receptors for iron uptake and are present on the surface of Mucorales fungi. Both receptors were shown to be

highly expressed in the presence of ferrioxamine in the fungal cells, which mediates iron transfer through the reductase/permease system without the internalization of siderophore-iron complex. These receptors played a key role in the pathogenesis of *R. oryzae* in mice treated with the iron chelator deferoxamine (**Liu et al., 2015**). *M. circinelloides* also harbours ferroxidases for iron acquisition, which may have role in fungal dimorphism and virulence (**Navarro-Mendoza et al., 2018**).

CotH (spore coat protein H) proteins, which are homologous with the spore coat proteins of bacteria, were shown to be present on the spore surface of all Mucorales fungi (**Gebremariam et al., 2014**). In *R. oryzae*, CotH2 and CotH3 are known to play a key role as invasins in the pathogenesis of mucormycosis. CotH3 of Mucorales were found to be a ligand for the endothelial cell glucose-regulated protein 78 (GRP78) during host invasion (**Gebremariam et al., 2014**).

Alkaline *Rhizopus* protease enzyme (Arp) of *R. microsporus* var. *rhizpodiformis* was detected in the culture filtrate of its clinical isolate and found that it plays a role in enhancing the coagulation process in patients suffering from mucormycosis (**Spreer et al., 2006**).

ADP-ribosylation factors (Arf) are key regulators of the vesicular trafficking process and are necessary for growth, fungal dimorphism, and virulence in *M. circinelloides* (**Patiño-Medina et al., 2018**).

Calcineurin (CaN) is a calcium and a calmodulin-dependent serine/threonine protein phosphatase, which serves as a critical virulence factor of Mucorales. CaN has a tangible role in the transition from yeast to hyphal forms in *M. circinelloides* (**Lee et al., 2013 and Lee et al., 2015**). CaN is closely linked to protein kinase A activity, both of which are necessary for *M. circinelloides* pathogenicity. Disturbance of the CaN encoding gene resulted in the production of larger spores compared to the wild-type by expressing a spore size-dependent role in the virulence. It was previously shown that sporangiospore-size dimorphism was linked to virulence in *M. circinelloides* f. *lusitanicus*, where the (-) mating isolates which produced larger asexual sporangiospores were shown to be more virulent in the wax moth (*Galleria mellonella*) host model than the (+) isolates that produce small sporangiospores (**Li et al., 2011**).

1.4 Significance of cell surface and cell wall structure in the pathogenicity of filamentous fungi

The fungal cell wall, being the most external layer surrounding the cellular components, is essential for various functions such as cell viability (osmotic stability, metabolism and ion exchange), morphology (provides rigidity to cell), pathogenicity (plays a role in interaction with the host) of a cell and acts as a barrier against environmental stress (**Latgé and Calderone, 2002 and Yoshimi et al., 2017)**. The fungal cell wall of fungi also provides protection against toxic molecules and participates in the regulation of enzyme secretion (**Latgé, 2010**).

In the host system, during an immune response, the specific receptors of the immune cells called pathogen recognition receptors (PRRs) recognise and interacts with specific components of the cell wall of pathogens called pathogen associated molecular patterns (PAMPs) that are normally not found in the host (**Arana et al., 2009**). Upon binding to the PAMPs, the PRRs initiates a signalling cascade that activates downstream responses including phagocytosis, microbial killing mechanisms, and cytokine production (**Hopke et al., 2018**). Fungal cell wall PAMPs include chitin, mannan and β-glucan, which are recognized by the hosts' innate immune PRRs, such as Toll-like receptors (TLRs) and the C-type lectin receptors (CLRs) (**Erwig and Gow, 2016**). The cell wall can therefore contribute to the outcome of a fungal infection by affecting both the fungal viability and the host responses.

The cell wall of pathogenic fungi can sometimes act as an immune decoy or shield from being recognised as foreign by the host system. Identification of the potential key cell wall components of fungal pathogens can help to develop better diagnostic and therapeutic approaches for fungal infections.

The cell wall of medically important opportunistic fungal pathogens (i.e., for *Aspergillus fumigatus*, *Candida albicans*, *Pneumocystis* species, *Cryptococcus neoformans*, *Histoplasma capsulatum*, and *Blastomyces dermatitidis*) has been studied and well described previously. However, little is known about the cell wall of Mucorales species (**Lecointe, 2019**). The fungal cell wall (**Figure 3**) is mainly composed of mannoproteins on its surface, a protective layer of chitins and α- and β- linked glucans. Cell wall composition and proportion of the components usually vary between the different fungal species, but the β-1,3-glucan remains to be the major component of the cell wall of most fungi. The molecular composition of the cell wall is critical for the biology of each fungal species.

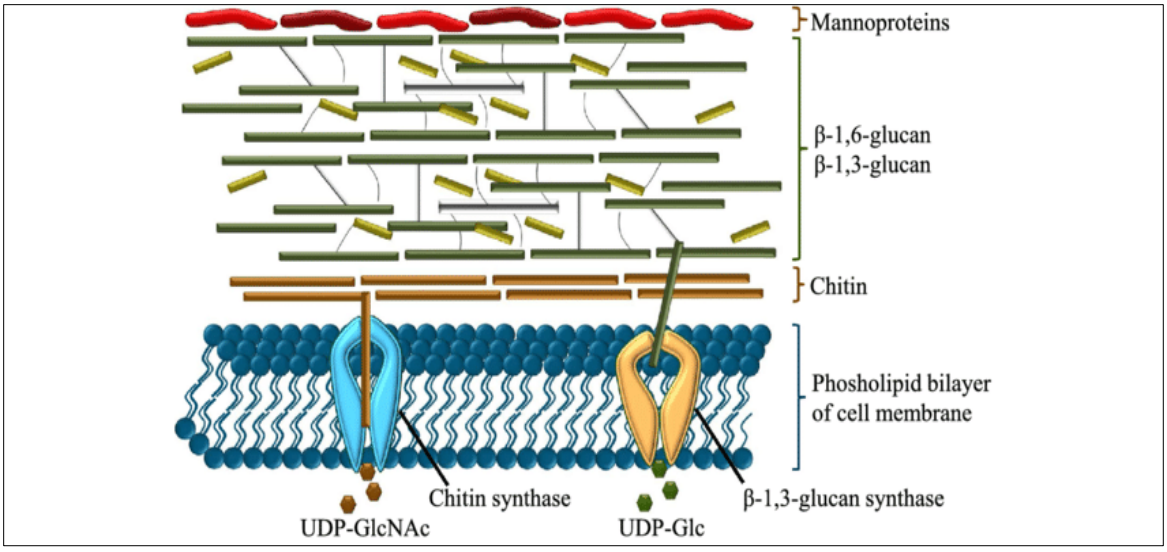

Figure 3: Fungal cell wall components (**Fesel and Zuccaro, 2016**).

Whole genome analysis carried out on virulent CBS 277.49 and avirulent NRRL 3631 strains of *M. circinelloides* showed that several genes encoding extracellular enzymes in the avirulent strain were absent, discontinuous, and truncated (**López- Fernández et al., 2018**). The phenotypic variation carried out on these strains showed that avirulent strains were more susceptible to heat stress and cell wall stress (calcofluor white and sodium dodecyl sulphate) when compared to the virulent strain. These variations suggest the possible effect of cell wall in the pathogenesis of *M. circinelloides*. Further studies were conducted by deletion of an extracellular protein-coding gene ID 112092 of unknown function, which resulted in a significantly reduced virulence in murine models. Based on this study, development of new therapeutic targets can be achieved through studying novel proteins and their role in the pathogenicity of Mucorales (**López-Fernández et al., 2018**).

1.4.1 Cell wall composition of fungi

Glucans comprise a diverse group of glucose polymers that differ in the glycosidic bond position, which confers them to be short or long, alpha or beta isomers, branched or unbranched, and soluble or particulate (**Goodridge et al., 2009**). The long β-1,3- or short β-1,6-linked chains and α-1,3 glucan chains provide the main bulk of the cell wall (**Osherov and Yarden, 2010**). The elasticity and strength of the cell is obtained through the β-1,3-glucan, whereas the cross-linking

between glucans, chitin and mannoprotein is enabled by β-1,6- glucans. In the pathogenic fungus *A. fumigatus*, the cell wall polysaccharides such as β-1,3-glucan and chitin are recognized by the host immune cells as PAMPs, which results in the immune clearance of the fungal cells. The α-1,3-glucan of *A. fumigatus* was shown to contribute to the masking of the PAMPs from hosts immune system recognition (**Fujikawa et al., 2012 and Beauvais et al., 2013)**

Chitin is a long β-1,4-linked homopolymer of an amino sugar called N-acetylglucosamine, which is arranged into fibres held together by hydrogen bonds (**Yamazaki et al., 2008**). It provides strength to the cell wall.

In the cell wall, components are continuously synthesized, degraded and structures are rearranged to provide plasticity to the rigid layer during conidial germination, hyphal growth and branching. This digestion process of the pre-existing cell wall is brought about by chitinolytic enzymes and glucanases to allow cell wall remodelling and expansion by synthases. Both enzymes are known to cleave the glycosidic linkages that holds their polymer together (**Alcazar-Fuoli et al., 2011**). Chitinolytic enzymes are a group of proteins that falls under two categories, i.e. endo- and exo-acting enzymes (**Hamid et al., 2013**). The endo-chitinases cleaves randomly at the β-1,4-links within the chitin chains, releasing the chito-oligomers and random-length products. Whereas the exo-chitinases cleaves the N, N'- diacetylchitobiose dimers (GlcNAc)2 from the non-reducing ends. The final step of chitin degradation is carried out by N-acetylglucosaminidases, which hydrolyse the dimers to monomers (**Sahai et al., 1993 and Rathore and Gupta, 2015**). Enzymes are also required for the processing of mannans and glycoproteins that are embedded in the cell walls of fungi.

Mannans are polymers of D-mannose, which are linked together by specific linkages through multiple mannosyltransferases that resides in the endoplasmic reticulum and Golgi. During post-translational modification events, it was found that mannans are added to extracellular proteins to stabilize and protect the proteins in an extracellular environment (**Filomena, 2013**).Most microorganisms are often covered by a protective proteinaceous external surface layer that serves as a shield from the pressures of the external environment and as a sieve for the surrounding molecular influx. Hydrophobins are known and characterized in Ascomycota fungi and are yet unknown in case of Mucorales. These are low molecular weight small secreted proteins characterized by various levels of hydrophobicity and the presence of eight conserved L-cysteine residues (Cys), which are responsible for the formation of four disulphide bridges (**Bayry et al.,**

2012). These proteins assemble into amphipathic monolayers at the hydrophobic and hydrophilic interfaces (**Wösten, 2001**). Hydrophobins are divided into two main groups (i.e. Class I and II) based on their hydropathy plots, solubility in solvents, inter-Cys spacing and type of the layers they form. In class I, high variability is observed in the inter-Cys spacing. Such molecules assemble into insoluble polymeric monolayers composed of fibrillar structures called rodlets and these structures can only be solubilized with strong acids. Class II hydrophobins have more conserved amino acid sequences and inter-Cys spacing. They lack the fibrillar rodlet morphology making them able to solubilise using mild treatment with organic solvents and detergents (**Bayry et al., 2012**).Hydrophobins have various functions, such as conferring hydrophobicity and water resistance helping the spread of the hyphae, formation of aerial mycelium and the dispersion of spores in air (**Bayry et at., 2012**). In *Aspergillus nidulans*, it was found that during conidiophore development, the *dewA* and *rodA* hydrophobin-encoding genes were expressed. Hydrophobins can facilitate the adherence of fungi to their substrate, especially during an infection where pathogenic fungi can penetrate the host tissues (**Wösten, 2011**). Hydrophobin layer of the spores can mask them from the recognition of the host immune system and thus, assists to the survival of the spores (**Bayry et al., 2012**). Previously, in case of *A. fumigatus*, Rod A was implicated in protecting the conidia from alveolar macrophages (**Pedersen et al., 2011**).

1.4.2 Specific features of the Mucorales cell wall

Studies conducted on the structural composition of Mucorales cell are scarce and have been mainly focused on *Mucor mucedo* and *M. circinelloides*. Mucoran, mucoric acid, chitin, and chitosan are some of the polysaccharides that have been described for these species **(Lecointe et al., 2019**).

It was previously shown that the cell wall components of *R. oryzae* and other Mucorales contained high concentrations of chitin and chitosan (**Ma et al., 2009**). In Mucorales, the proportion of chitin or chitosan varies between species, spore, and hyphal forms (**Campos- Takaki et al., 2014**). Previous analysis on the cell wall components of *L. corymbifera* showed presence of high amounts of β-1,6-glucosytransferases (GT24) and β-1,3-N-acetylglucosaminyltransferases (GT49), but fewer chitin synthases, chitin deacetylases and chitinase than in *R. oryzae* and *M. circinelloides* **(Mélida et al., 2015 and Lecointe et al., 2019**).

Glucan was shown to be the major component of the spore cell wall in *M. circinelloides* along with melanin, glucosamine, mannans and proteins. During the germination of spores, glucan synthesis was shown to decreases suggesting its role in modifying the glycoshield of the cell wall **(Lecointe et al., 2019**). Microscopic analysis of *Mucor ramannianus* spores during lysis by β-glucanase, showed the presence of an outer electron dense layer and a thick inner layer of myofibrils containing glucans (**Jones et al., 1968 and Lecointe et al., 2019**). A recent study revealed the role of β-glucans of *R. oryzae* in the production of interleukin-23 (IL-23) and activates dectin-1 of dendritic cells that triggers T_H-17 responses (**Lecointe et al., 2019**). Therefore, the exposure of the fungal cell wall polysaccharide β-glucan is essential for regulation of protective immunity to host during invasive growth of opportunistic fungal pathogen (**Chamilos et al., 2010**).

It has been shown in previous studies that several *Rhizopus* and *Mucor* species can secrete extracellular polysaccharides (EPS). The structure and molecular mass of these EPS varies in different species. The EPS are composed of mannose (8-30%), galactose (4-13%), fucose (9-25%), glucose (0-30%) and glucuronic acid (32-55%) mainly β-1,4-linked glucuronic acid. Currently, the role of the EPS is unknown in moulds. In Mucorales the extracellular matrix comprises of carbohydrates (50-90%) and proteins (10-50%) (**Lecointe et al., 2019)**.

Fungal polysaccharides that are usually located on the surface of the cell wall possess antigenic properties, due to their ability to be recognised by immune cells and trigger an immune response in the host system (**Snarr et al., 2017**). In *Absidia cylindospora*, antigenic substances were found mainly in the supernatant of disrupted cells and in purified mycelium it could be isolated in low yields. Hence suggesting the presence of antigenic substances of Mucorales cell walls to be loosely bound to the surface of mycelia and can be easily released from the surface (**Miyazaki et al., 1979**).

1.5 Hydrophobic surface binding protein

Hydrophobic surface binding protein A (HsbA) belongs to the galactomannoprotein family **(Muszewska et al., 2017)**. Galactomannans comprise of a mannose polymer with galactose side groups and is covalently bound to the β-1,3-glucan-chitin core. It is a major component of the fungal cell wall that is released during the growth of fungal hyphae (**Muszewska et al., 2017**). In case of invasive infections, such as aspergillosis, this antigen may be found in the blood circulation. This protein family has evolved through multiple duplications, leading to group formation of

species-specific paralogs in Eurotiales and Mucoromycota (**Muszewska et al., 2017**). Majority of the HsbA proteins are known as antigenic cell wall galactomannoproteins (**Cao et al., 1998 and Muszewska et al., 2017**).

HsbA proteins (HsbA, Pfam ac. Number: 12296, **Ohtaki et al., 2006**) were shown to be secreted proteins (14.5 kDa), which was isolated from the culture broth of *Aspergillus oryzae* RIB40 grown in a medium containing poly butylene succinate-*co*-adipate (PBSA) as a sole carbon source. Hence suggesting that HsbA could either be bound to the cell wall since they belong to the galactomannoprotein family (**Muszewska et al., 2017)** or secreted. *hsbA* genes identified in *A. oryzae* have orthologs/paralogs located in several fungal genomes (e.g., in that of *A. fumigatus*). It has shown that HsbA plays a role in the degradation of PBSA by recruiting an enzyme CutL1 at the hydrophobic surface (**Ohtaki et al., 2006**). Though the amino acid sequence of HsbA proteins suggest that these proteins may be hydrophilic, HsbA proteins in the presence of sodium chloride (NaCl) or calcium chloride ($CaCl_2$) were shown to be absorbed onto hydrophobic solid PBSA surfaces, suggesting that HsbA could be hydrophobic or amphipathic in nature (**Ohtaki et al., 2006)**.

Features of HsbA appears to be similar to those of the hydrophobin RolA. Like hydrophobins, HsbA proteins are low molecular mass (≤20 kDa) secreted proteins and are unique to the fungal kingdom. (**Bayry et al., 2012**). Although HsbA is able to bind to the hydrophobic surface of PBSA and promotes its degradation by recruiting cutinases, it cannot be classified as a "classical" hydrophobin due to the absence of the characteristic cysteine residues (**Takahashi et al., 2005 and Ohtaki et al., 2006**). It is known that hydrophobins are characterized by the presence of eight conserved cysteine residues that form four disulphide bonds (**Scholtmeijer et al., 2001 and Berger and Sallada, 2019)**.The structure of HsbA and the molecular mechanisms behind the attachment to hydrophobic substrates and recruitment of cutinases are yet to be determined (**Sunde et al., 2017**).

In *Aspergillus niger*, it was shown that two genes encoding a hydrophobin and an HsbA were strongly induced by the switch from glucose to wheat straw medium, suggesting that these proteins could also play a role in recruiting degradative enzymes to the surface of straw (**Delmas et al., 2012**).

HsbA proteins were shown to play role in plant pathogenic species during the colonization and penetration of fruits. The genome analysis of the ectophytic *Ramichloridium luteum* showed

significantly higher amount of HsbA proteins compared to other penetrating plant pathogen species and 13 *hsbA* genes were encoded in the genome of *R. luteum*. In *R. luteum*, RNA-Seq analysis indicated that one *hsbA* homolog (Ramle4244) was significantly upregulated during the colonization of the surface of apple fruit (**Wang et al., 2017**). In the transcriptome of *Colletotrichum fructicola*, nine homologs of *hsbA* (Pfam ac. Number: 12296, **Ohtaki et al., 2006)** were discovered, from which eight genes were upregulated at the early phase of strawberry infection while the ninth gene was upregulated at a later stage (**Zang et al. 2018**). The transcriptome analysis of the rice blast fungus *Magnaporthe oryzae* showed that there are eight *hsbA* homologs (Pfam ac. number 12296, **Ohtaki et al., 2006**) in the genome. High-throughput SuperSAGE (HT-SuperSAGE) data analysis revealed that four of the HsbA-encoding genes were shown to be upregulated during the appressorium development and the other two were upregulated later at the 14th-16th hours of the infection (**Soanes et al., 2012**). These studies suggest the importance of the HsbA-like proteins as a virulence factor in the regulation of attachment, penetration, and degradation of components of the plant epidermis, and probable role in appressorium development however the exact mechanism is unknown and requires further investigation.

During interactions with macrophages and phagocytosis, HsbA proteins were shown to be expressed approx. 10 folds higher in *L. corymbifera* JMRC: FSU:09682 strain than without the interaction (**Park, 2016)**. In case of the dimorphic *Talaromyces* (*Penicillium*) *marneffei* that cause systemic mycosis in immunosuppressed patients, the secreted cell wall mannoprotein Mp1p was found abundantly in sera of infected patients, hence Mp1p was used in serodiagnosis of this infection (**Cao et al., 1998**). Mp1p was shown to be present in the yeast phase of *T. marneffei*. (**Cao et al., 1999 and Sze et al., 2016**). Mp1p and Afmp1 from *A. fumigatus* have been placed by NCBI conserved domain database under the conserved protein domain family of HsbA. Mp1p was shown to be a novel virulence factor of *T. marneffei*, by carrying out knockout and knockdown of its gene and using the mutants in intracellular survival assay with murine macrophage cells and mouse models (**Woo et al., 2016**). All mice treated with Mp1p (Mp1) knockout *T. marneffei* strains survived even on day 60 post intravenous infection, compared to those challenged with wild-type strains where all mice died within 21 days (**Woo et al., 2016**). Though Mp1p has been previously characterized, the virulence mechanism and its cellular target remains unknown. The GPI-anchored galactomannoproteins, Afmp1 of *A. fumigatus*, belongs to the same protein family of

cell wall galactomannans as HsbA proteins. Afmp1p is a protein with 284 amino acid residues and is homologous to antigenic cell wall mannoprotein Mp1p in *Penicillium marneffei* (**Yuen et al., 2001**). Afmp1p of *A. fumigatus* was shown to be specifically located in the cell wall, through indirect immunofluorescence and immunoelectron microscopic analysis. Antibodies specific to Afmp1p were shown to express in elevated levels in patients suffering in invasive *A. fumigatus* infection, therefore suggesting the role of Afmp1p as a cell surface target for the hosts humoral immunity. Development of antigen-based kits by using Afmp1p can be carried out and examined for the serodiagnosis of *A. fumigatus* infections (**Yuen et al., 2001**). Hence, these suggest that the possible connection between HsbA proteins and their influence on the pathogenesis of *M. circinelloides* are worth to examine in detail.

2. AIMS

Our aim was to identify and characterize the gene or genes of the novel hydrophobic surface binding protein A (HsbA) of *M. circinelloides* and examine its or their functions and role in the pathogenicity of Mucorales fungi. To reach these points our objectives were the following:

1. Identification and *in silico* characterization of putative *hsbA* genes in the *M. circinelloides* genome
2. Transcription analysis of the identified genes.
3. Overexpression of the identified genes using circular plasmids and PEG-mediated protoplast transformation.
4. Disruption of the identified genes by applying the CRISPR-Cas9 method, this objective includes:
    - Construction of donor cassettes by amplifying separately the fragments encoding for the promoter and terminator of *M. circinelloides hsbA* genes as homology arms, and the *pyrG* gene as the selection marker.
    - Application of the donor cassettes along with the corresponding guide RNA (gRNA) and the Cas9 nuclease enzyme for the transformation of *M. circinelloides* protoplasts by PEG-mediated transformation.
    - Confirmation of the gene disruption by carrying out qRT-PCR, sequencing, and whole-genome sequencing.
5. Comparative morphological and physiological characterization of the *hsbA* disruption and overexpression mutants.
6. Heterologous expression of selected genes and purification of the recombinant proteins for further analysis.

3. MATERIALS AND METHODS

3.1 Strains used in the study

A *leuA*$^{-}$ and *pyrG*$^{-}$, double auxotrophic strain of *M. circinelloides* f. *lusitanicus* (strain IDs: MS12, SZMC 12082) was used in the transformation experiments. This is a leucine and uracil auxotrophic derivative of the wild-type strain CBS 277.49 (**Nagy et al., 2014**).

To exclude the effect of the lack of the *pyrG* on the viability of the original strain, a derivative of the MS12 (MS12+*pyrG*), in which the uracil auxotrophy was complemented by expressing the functional *pyrG* gene, was used as a control for the morphological and physiological studies of the overexpressed and deletion *hsbA* mutants.

Plasmid construction and propagation were performed in *Escherichia coli* DH5α.

Pichia pastoris KM71H strain (arg4 aox1: ARG4) (Thermo Scientific) was used in the heterologous protein expression studies.

3.2 Composition of the applied media

YNB minimal medium: 1% D-glucose, 0.15% ammonium sulphate, 0.15% sodium L-glutamate, 0.05% YNB (yeast nitrogen base) without amino acids (Sigma) supplemented with 0.05% uracil and/or 0.05% leucine (w/v), if required. For solid medium 2% (w/v) agar was added. YNB solidified with 1 and 2% agar and supplemented with 0.05% leucine and 0.8 M sorbitol was used as a selection medium during the transformation experiments. To test various cell wall stressors, YNB (supplemented with leucine and uracil, as required) containing 1 µl/ml of Triton X-100, 0.004 % (w/v) sodium dodecyl sulphate (SDS), 0.001 % (w/v) calcofluor white (CFW), or 0.002 % (w/v) Congo red (CR) was used.

Malt extract agar (MEA): 1% D-glucose, 0.5% yeast extract, 1% malt extract, 2% agar (w/v).

Yeast extract - glucose medium (YEG): 1% D-glucose, 0.5% yeast extract, 2% agar (w/v) for protoplast formation.

Yeast extract-peptone-glucose broth (YPG): 2% D-glucose, 1% peptone, 0.5% yeast extract (w/v) supplemented with 0.8 M sorbitol to regenerate the protoplasts after transformation.

Yeast extract-peptone-dextrose medium (YPD): 2% Dextrose,1% yeast extract, 2% peptone, 2% agar (optional, for making solid medium). For selecting *P. pastoris* KM71H transformants, YPD medium was supplemented with 100 μg/ml Zeocin as a selection marker.

Lysogeny broth (LB): 1% Sodium chloride, 1% tryptone, 0.5% yeast extract (w/v) (pH 7.0) supplemented with 2% (w/v) agar for making solid medium. For selecting *E. coli* transformants, LB medium was supplemented with 50 μg/ml ampicillin as a selection marker.

Roswell Park Memorial Institute 1640 (RPMI 1640; Sigma): 1.04% RPMI-1640 medium powder (with phenol red, without glutamine), 3.453% of 3-(N-morpholino) propanesulfonic acid (MOPS), 0.1% L-glutamine (30 mg/ml; w/v), supplemented with 0.05% uracil and/or 0.05% leucine (w/v), if required (pH 7.2).

Buffered minimal glycerol or methanol medium containing histidine (BMGH/BMMH): 100 mM potassium phosphate (pH 6.0), 1.34% yeast nitrogen base (YNB), biotin, 4 x 10^{-5}% biotin, 1% glycerol or 0.5% methanol and 0.004% histidine.

3.3 Isolation of fungal genomic DNA and agarose gel electrophoresis

Genomic DNA of the fungal strains was purified using the Gene Elute Plant Genomic DNA Miniprep Kit (Sigma Aldrich) according the manufacturer's instructions.

For agarose gel electrophoresis, 0.8 - 2% (w/v) agarose was dissolved in TAE buffer (40 mM Tris-acetic acid (pH: 7.6); 1 mM Sodium EDTA). DNA was stained with 0.5 mg/ml ethidium bromide (Sigma). As the sample buffer, 1 × DNA loading dye (Thermo Scientific) and to determine the size of the bands, the GeneRuler 1 kb DNA ladder (Thermo Scientific) were used. The electrophoretic separation was carried out in TAE buffer, with current of 80-110 V for 1 to 4 hours. Visualization of the DNA was done by exposing the agarose gel to UV light.

To isolate the DNA fragments from the agarose gel, the appropriate DNA band was cut from the gel using a sterile scalpel under UV light. The DNA was then purified from the gel using the Zymoclean Large Fragment DNA recovery Kit (Zymo Research) according to manufacturer's instructions.

3.4 PCR amplification for gene cloning

Details of the primers used in the study are shown in **Table S1.** All primers were synthesized by Integrated DNA Technologies (IDT). Phusion Flash High-Fidelity PCR Master Mix (Thermo Scientific) was used in the PCR experiments according the manufacturer's recommendations. The reactions were prepared in a final volume of 20 µl as follows:

- Template DNA (10 to 100 ng) – 0.8 µl
- Specific primers (10 µM final concentration) – 0.8 µl each
- 2X Phusion High Fidelity DNA Polymerase Master mix – 10 µl
- Molecular water (RNAse and DNAse free) – 7.6 µl

Amplification conditions were as follows: 98 °C for 10 s, 98 °C for 1 s, 60-72 °C for 5 s, 72°C for 30 s, repeat for 35 cycles, 72 for 1 min. The annealing temperature and extension time varied and were modified according to the length of the expected amplicon and the primers used.

3.5 Construction of plasmids

For the overexpression of the *hsbA1, hsbA2* and *hsbA3* genes, the plasmids pAV1, pAV2 and pAV3 were constructed, respectively. Firstly, the corresponding gene was amplified from the genomic DNA of *M. circinelloides* by using the primer pairs McHSB1oefw and McHSB1oerev for *hsbA1,* McHSB2oefw and McHSB2oerev for *hsbA2* and McHSB3oefw and McHSB3oerev for *hsbA3* (Table S1). The amplified fragments were ligated between the promoter and terminator regions of the *M. circinelloides* glyceraldehyde-3-phosphate dehydrogenase 1 gene (European Molecular Biology Laboratory (EMBL) Acc. No.: AJ293012) in the pPT81 vector (**Csernetics et al., 2011 and Nagy et al., 2014**). This vector also harbours the *M. circinelloides pyrG* gene (CBS277.49v2.0 genome database ID: Mucci1.e_gw1.3.865.1) encoding, which encodes the orotidine-5'-monophosphate decarboxylase and can complement the uracil auxotrophy of the *M. circinelloides* MS12 strain.

For the heterologous expression of the HsbA proteins in *P. pastoris*, the EasySelect™ Pichia Expression Kit (Thermo Scientific) was used according the manufacturer's recommendations. Accordingly, the plasmid pPICZα A (Thermo Scientific) was used as the expression vector. The plasmid pPICZα A contains the zeocin resistance gene, which allows to select the transformants.

3.6 Design and construction of the guide RNA (gRNA) and the template DNA for CRISPR-Cas9 gene disruption

Protospacer sequences designed to target the DNA cleavage in the *hsbA1, hsbA2* and *hsbA3* genes were the followings, 5'-ACTGACTGCTGTGCAGTCGC-3'; 5'-GAAACGCGTCTCAAGAAAGC-3' and 5'- GAATTTGATGCCGTTCTTT-3', respectively, which correspond to the fragments of the nucleotide positions between 310 and 330 downstream from the start codon of the *hsbA1*gene, between the positions 282 and 302 downstream from the start codon of *hsbA2* and between the positions 426 and 446 downstream from the start codon of *hsbA3,* respectively. Using these sequences, the Alt-R CRISPR crRNA and Alt-R CRISPR-Cas9 tracrRNA molecules were designed and purchased from Integrated DNA Technologies (IDT). To form the crRNA: tracrRNA duplexes (i.e. the gRNAs), the Nuclease-Free Duplex Buffer (IDT) was used according to the instructions of the manufacturer.

Homology driven repair (HDR) was applied for all gene disruptions following the strategy described previously (**Nagy et al., 2017**). Gene disruption strategy and the template DNA is presented in **Figure 4**. Disruption cassettes functioning also as the template DNA for the HDR were constructed by PCR using the Phusion Flash High-Fidelity PCR Master Mix (Thermo Scientific). In case of the *hsbA1* gene, at first, two fragments being 1109 and 1129 nucleotides upstream and downstream from the protospacer sequence and the *M. circinelloides pyrG* gene (CBS277.49v2.0 genome database ID: Mucci1.e_gw1.3.865.1) along with its promoter and terminator sequences were amplified using the primers listed in **Table S1**. The amplified fragments were fused in a subsequent PCR using the nested primers McHSB1/7 and McHSB1/8 (**Table S1**); the ratio of concentrations of the fragments was 1:1:1 in the reaction. Disruption of *hsbA2* using the *pyrG* gene was carried out in the same way as follows: two fragments, which were 1108 and 1138 nucleotides upstream and downstream from the protospacer sequence, respectively, were fused with the *pyrG* gene by PCR using the nested primers McHSB2/7 and McHSB2/8 (**Table S1**). In case of *hsbA3*, two fragments, 1155 and 1106 nucleotides upstream and downstream from the protospacer sequence, respectively, were fused with the *pyrG* using the nested primers McHSB3/7 and McHSB3/8 (**Table S1**).

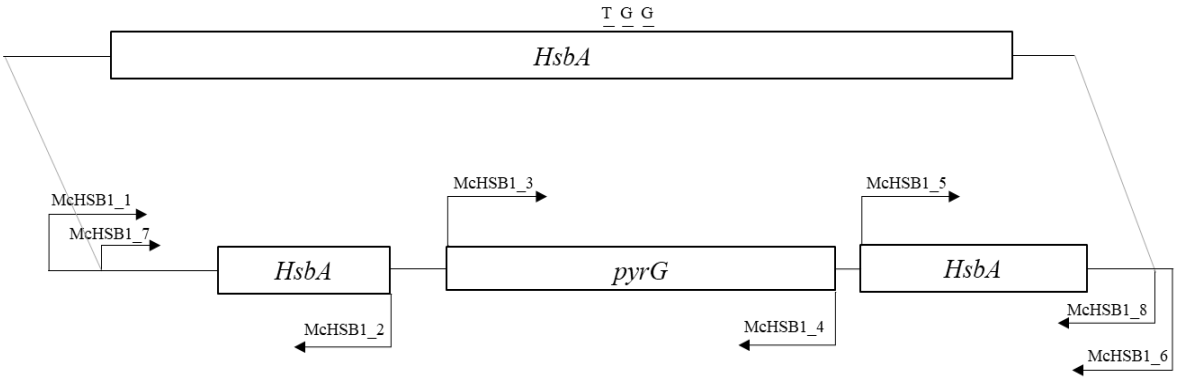

Figure 4: Strategy designed to disrupt the *hsbA* genes of *M. circinelloides* using the CRISPR-Cas9 method. HDR was performed using the disruption cassette/template DNA containing the *pyrG* gene as the selection marker. Positions of the primers used to analyze or amplify the constructs are presented (for the nucleic acid sequences of the primers, see **Table S1**). TGG indicates the PAM sequence while the arrows show the orientations of the primers.

3.7 Preparation of *E. coli* DH5α competent cells and bacterial transformation

E. coli DH5α competent cells (0.2 ml of previous stock) was inoculated into 30 ml LB and incubated overnight at 37 °C. After incubation, 1 ml of *E. coli* was inoculated into another 30-ml LB and incubated at 37 °C until the optical density of the culture at 600 nm (OD_{600}) reached 0.6. After that, the entire culture was centrifuged at 3,000 rpm for 10 min at 4 °C and the pellet was placed on ice. The pellet was resuspended in 30 ml of 100 mM CaCl2 and centrifuged at 3,000 rpm for 10 min at 4 °C. The pellet was resuspended again in 30 ml of 100 mM CaCl2 and incubated on ice for 1 h. After centrifuging the sample at 3,000 rpm for 10 min at 4 °C, the pellet was resuspended in 1.5 ml CaCl2. From this stock, 116 µl of competent cells and 34 µl of 87% sterile glycerol were aliquoted into 1.5 ml sterile microcentrifuge tubes and kept at -80 °C until use.

For transformation, DNA was added to the DH5α competent cells along with 80 µl Tris-calcium chloride-magnesium chloride (TCM) buffer (10mM Tris, 10mM $CaCl_2$ and 10mM $MgCl_2$; pH: 7.5). The components were then mixed by tapping the tube and incubated on ice for 30 min. After that, the mixture was transferred to 37 °C for 3 min (heat shock). Then, the cells were kept at room temperature for 10 min. From the cell mixtures, 30 or 100 µl were inoculated onto the surface of LB plates and incubated at 37 °C for 16 h.

3.8 PEG mediated protoplast transformation of *M. circinelloides*

This method is a modified version of that described by **van Heeswijck and Roncero (1984)**. Sporangiospores of the MS12 strain were collected after cultivating the fungus for 4 days on YNB and plated onto 20 YEG plates covered by cellophanes and incubated for 16 h at 25 °C (**Csernetics et al., 2011 and Nagy et al., 2017**). The developed colonies were then transferred into 30 ml of snail enzyme mix (17 ml sterile distilled water, 3 ml sodium-phosphate buffer (pH 6.4)(100 mM sodium phosphate buffer: 25 mM Na_2HPO_4 and 75 mM NaH_2PO_4), 10 ml of 2.4 M sorbitol and 0.45 g snail enzyme) and incubated at 25 °C for approx. 3 h with gentle shaking. Protoplasts were then filtered through a sterile gauze, washed with 5 ml SMC buffer (2.5 ml of 1 M CaCl2, 1 ml of 0.5 M MOPS (3-(N-morpholino) propanesulfonic acid), 16.65 ml of 2.4 M sorbitol, 38.5 ml distilled water) and centrifuged for 15 min at 3,200 rpm. The pelleted protoplasts were resuspended again in 3 ml SMC buffer and centrifuged under the same conditions. For transformation with plasmids, 200 µl SMC, 20 µl plasmid and 20 µl PMC (13.33 ml of 40% PEG, 400 ml of 0.5 M MOPS, 6.6 ml of 2.4 M sorbitol and 1 ml of 1 M CaCl2) were added to the protoplasts. For CRISPR-Cas9 mutagenesis, 200 µl SMC, 10 nM gRNA (IDT), 10 nM Cas9 enzyme (IDT), 10 µg template DNA (i.e. the gene disruption cassette) and 20 µl PMC were added to the protoplasts. After incubation on ice for 30 min, 2.5 ml PMC was added to the cells, which were then incubated at room temperature for 30 min. After that 25 ml SMC was added to the sample, which was centrifuged at 3,200 rpm for 10 min at 4 °C. The supernatant was discarded and 5 ml YPG supplemented with 0.8 M sorbitol was added to the protoplasts. After incubation at room temperature for 30 min, protoplasts were pelleted from the solution and washed with 20 ml SMC. Protoplasts were resuspended in YNB containing 1% agar and spread onto YNB supplemented with 0.8 M sorbitol, as well as with leucine, if required.

3.9 Quantitative real-time reverse transcription PCR (qRT-PCR)

For qRT-PCR analysis, total RNA samples were purified using the Direct-zol™ RNA Mini-Prep kit (Zymo Research) by following the manufacturer's instructions. The quality of each RNA samples was checked in 2% agarose gel. cDNA synthesis was performed by using either the Maxima H Minus First Strand cDNA Synthesis Kit (Thermo Scientific) or RevertAid H Minus First Strand cDNA Synthesis Kit (Thermo Scientific). Oligo (dT)18 and random hexamer primers were used in the reaction mixture according to manufacturer's instructions.

The qRT-PCR experiments were performed in a CFX96 real-time PCR detection system (Bio-Rad) using the Maxima SYBR Green qPCR Master Mix (Thermo Scientific) and the primers presented in **Table S1**. The relative quantification of the copy number and the gene expression was carried out by the $2^{-\Delta\Delta Ct}$ method (**Livak and Schmittgen, 2001**) using the actin gene (scaffold_07: 2052804-2054242; *M. circinelloides* CBS277.49v2.0 genome database; http://genome.jgi-psf.org/Mucci2/Mucci2.home.html) of *M. circinelloides* as a reference.

The amplification conditions for the qRT-PCR were as follows: 95 °C for 3 min, (95 °C for 15 sec, 60 °C for 30 sec, 72 °C for 30 sec was carried out for 40 cycles). Melting curve analysis was performed at 65 °C to 95 °C, with a 0.5 °C increment.

3. 10 Whole genome sequencing

Whole genome sequencing was performed at the Department of Biochemistry and Molecular Biology (University of Szeged) by the research group of Dr. László Bodai. Samples were the following: MS12, MS12-*ΔhsbA1a* and MS12-*ΔhsbA2*.

The reference genome was Mucor_circinelloides_v2_masked_scaffolds.fasta at https://genome.jgi.doe.gov/portal/pages/projectStatus.jsf?db=Mucci2. Fastq files were checked and quality controlled by the FastQC, TrimGalore program. The "Pair-end fastq read" files were trimmed by the TrimGalore program, which performed a quality analysis based on the database inside after recognizing the adapter sequences. After specifying the minimum read length (36 bp), reads that proved to be smaller after trimming were excluded. The selected reads were mapped to the reference genome using the "bwa-mem" tool, and the results were visualized using a Qualimap program. Before the variant analysis, technical duplicates were screened using the GATK / Picard MarkDuplicates tool (**van der Auwera et al., 2013**). After generating BAM files from the mapping output, duplicate reads were excluded from the variant analysis by marking with the "SAMtools flag" procedure (**Etherington et al., 2015**). Based on the obtained sequences, the targeted regions identified in the mutant strains can be validated by searching with the Basic Local Alignment Search Tool (BLAST). If the corresponding sample BAM file does not show an overlap (coverage) compared to the genomic position of the targeted region, then that region can be considered as corrupted. Variant analysis was performed with SAMtools / bcftools (**Li et al., 2009**), FreeBayes, and Bedops v2.4.39 (**Neph et al., 2012**).

3.11 Sequence analysis

Sequencing of the amplified or cloned DNA fragments was carried out commercially by the LGC Genomics (Berlin, Germany).

Oligonucleotide sequences were designed based on the sequence data available in the *M. circinelloides* CBS277.49v2.0 genome database (DoE Joint Genome Institute; http://genome.jgi-psf.org/Mucci2/Mucci2.home.html) (**Corrochano et al., 2016**).

Sequences obtained after DNA sequencing was analysed by using the Basic Local Alignment Search Tool (BLAST) at the site of the National Center for Biotechnology Information (NCBI) (https://blast.ncbi.nlm.nih.gov/Blast.cgi). Sequences were evaluated and aligned by using the PreGap and Gap4 programs of the Staden Package (**Staden et al., 2000**).

Motifs, domains, and main features of the HsbA proteins were predicted using the tools available at the Expasy Bioinformatics Resource Portal (http://www.expasy.ch), such as Compute pI/Mw, MyHits, PROSITE and ProtScale (**Gasteiger et al., 2005**). The GPI-Som software (http://gpi.unibe.ch; **Fankhauser and Mäser, 2005**) was used to identify the glycosylphosphatidylinositol (GPI)-anchors in the amino acid sequence of HsbA proteins.

3.12 Light microscopy

Microscopic examinations were carried out with a DMI 4000B (Leica) inverted light. Micromorphology was examined on the second and fourth days of cultivation.

3.13 Scanning electron microscopy (SEM)

Small pieces were cut from the 4-days grown mycelia with sterilized cork borer. Samples were soaked in 2.5% glutaraldehyde in 0.05 M cacodylate buffer (pH: 7.5) for 2 h at room temperature and then washed by adding 1 ml of 50, 70 and 80% ethanol for 15 min each. The samples were then stored in 80% ethanol at 4 °C overnight. On the next day, the samples were washed with 90% ethanol, 95% ethanol and 96% ethanol for 15 min, twice each at room temperature. Then, they were incubated in t-butyl alcohol:100% ethanol (1:2) for 1 h, t-butyl alcohol:100% ethanol (1:1) for 1 h and t-butyl alcohol:100% ethanol (2:1) for 1 h at room temperature. Finally, the samples were incubated in absolute t-butyl alcohol for 2 h at room temperature. After changing the t-butyl alcohol to a fresh solution, samples were placed at 4 °C for 15 min. Freeze drying was performed overnight under vacuum. After coating with gold

nanoparticles, the samples were examined using an S-4700 scanning electron microscope (Hitachi).

3.14 Sporulation assay

Mucor circinelloides sporangiospores were collected on the 7th day of cultivation on solid YNB plates (supplemented with leucine and uracil, if required) at 25 °C. To examine the sporulation capacity, spore with final concentration of 5x 10^4 spores/ml were inoculated into malt extract agar (MEA) media and incubated at 25 °C for 4 days. After 4 days the spores were washed with 5ml of sterile distilled water and count the spores produced using a Bürker chamber.

3.15 Germination assay

M. circinelloides sporangiospores were collected on the 7th day of cultivation on solid YNB plates (supplemented with leucine and uracil, if required) at 25 °C. Spores were then stored in liquid YNB medium at 4 °C for 16 h to synchronize their physiological state. To examine the germination ability, 10^7 spores were inoculated into 10 ml liquid YNB medium and incubated at 25 °C under continuous shaking (150 rpm). Germination of the spores was examined by light microscopy at 4, 5 and 6 h post-inoculation, by using 10 µl of spore suspension in a Bürker chamber and counted for 10 focus areas.

3.15 Biofilm Assay

A spore suspension (10^4 spores/ml) was prepared in RPMI 1640 (pH 7.2) buffered with 165 mM MOPS. Two hundred µl of this suspension was inoculated into the wells of a 96-wells microtiter plate and incubated at room temperature for 24 or 48 h. After incubation, the formed biofilms were washed twice with phosphate buffered saline (PBS) (1x PBS for 1 litre: 0.08% NaCl, 0.02% KCl, 0.144% Na_2HPO_4, 0.024% KH_2PO_4; pH 7.0) and fixed with 95% ethanol for 15 min. After removing the ethanol carefully, biofilms were stained with 200 µl of 0.1% safranin for 5 min and examined by light microscopy. Quantification of the bound safranin was carried out by eluting it with 200 µl of 30% glacial acetic acid and measuring the absorbance of the eluted solution at 490 nm with a SPECTROstar Nano plate reader (BMG LABTECH). For biofilm formation analysis, MS12+*pyrG* cultivated in RPMI 1640 medium was used as the control. To test the biofilm inhibition, cultures of each tested strain grown in RPMI 1640 was used as the control for their

respective treated sample. The biofilm formation and inhibition in terms of percentage (%) was calculated as follows:

Biofilm formation (%) = (O.D. of test/O.D. of control) x 100.

Biofilm inhibition (%) = {(O.D. of control-O.D. of test)/ O.D. of control} x 100.

3.16 Alcohol percentage test

Alcohol percentage test (APT) more commonly referred as molarity of ethanol method (MED) makes use of aqueous ethanol solutions with different concentrations to determine the lowest concentration of ethanol solution that is absorbed or wets the surface (**Watson and Letey, 1970 and Chau et al., 2010**).The higher the concentration of ethanol that wets the surface, the more severe the degree of hydrophobicity (**Letey et al., 2000**). Due to the delicate nature of fungi, a reference point of approximately 5 s or less is more reasonable for assessing the hydrophobicity on fungal surfaces because of the effect of hydrophobicity degradation (**Crockford et al., 1991**). Fungal cultures were inoculated onto slide YNB media supplemented with leucine and uracil (if required) and were incubated in the dark at 25°C. Fungal growth was assessed daily until the growth covered the glass slide completely (7 days).

A series of aqueous ethanol solutions (20, 40, 60, 80 and 90% ethanol) were prepared. Four-µl drops of ethanol were applied on the surface of the fungal colonies; a time interval of <5 s was used for infiltration of the solution droplets. This short penetration time was vital to ensure that the hydrophobicity decay of the mycelium did not affect the experiment (**Crockford et al., 1991**). Inner and outer zones of fungal colony were distinguished by the observation of two distinct zones, with difference in colour, structure, and aerial mycelia (**Chau et al., 2010**). Three droplets per concentration were placed on each zone and assessed on two technical replicates and three biological repeats of fungal cultures.

3.17 Phagocytosis assay

Murine macrophage-like cell line J774.2 (Invitrogen) was cultured in Dulbecco's modified Eagle's medium (DMEM, Lonza) supplemented with 10% heat-inactivated fetal bovine serum (FBS, Biosera) and 1% 100x penicillin-streptomycin solution (Lonza) at 37 °C in a humidified incubator with 5% CO_2. Phagocytosis assays were performed using the same culture conditions in DMEM medium supplemented with FBS, without penicillin-streptomycin. J774.2 cells (10^5

cells/ml) were placed on 24-well cell culture plates with flat bottoms in 1 ml DMEM medium supplemented with 10% heat-inactivated FBS and without antibiotics for 16 h before the experiment. Four hours before the infection, cells were stained with CellMask Deep Red Plasma Membrane stain. Briefly, 0.5 µl CellMask Deep Red Plasma Membrane stain (Thermo Scientific) was added to each well of the plate and incubated in the dark for 10 min at 37 °C, 5% CO2 and 100% relative humidity. Then, the cells were washed twice with PBS and incubated for four hours in 1 ml/well fresh DMEM medium. Afterwards, fungal spores were collected from 1-week-old MEA cultures and stained with 0.1 mg/ml fluorescein-isothiocyanate (FITC, Sigma Aldrich) for 15 min at room temperature and washed with PBS. Stained fungal spores were added to the J774.2 cells at an effector: target (E:T) ratio of 1:5. For analysis, collected samples were centrifuged with 1000 rpm for 15 min and resuspended in 200 µl PBS supplemented with 0.05 % Tween-20 (Reanal). Interaction and phagocytosis were measured after 3 h using a FlowSight Imaging Flow Cytometer (Amnis) and evaluated with the IDEAS Software (Amnis). Phagocytosis assay was performed by Dr. Homa Mónika. Phagocytic index (PI) was calculated according to the followings:

Phagocytic index (PI) = (Total number of engulfed cells/ Total number of counted macrophages) x (Number of macrophages containing engulfed cells/Total number of counted macrophages) x 100.

3.18 Infection of *Galleria mellonella* with *hsbA* mutants of *M. circinelloides*

Spores were resuspended in an insect physiological saline (IPS). 20 µl IPS containing 10^5 spores were injected into the last right or left proleg of wax moth (*Galleria mellonella;* BioSystem Technology, TruLarv) larvae (20 larvae per strain) using a sterile insulin needle (BD Micro-Fine). The controls were injected with 20 µl of IPS and we used untreated controls as well. After infection, the larvae were kept at 28 °C in dark and the survival was monitored every day for 6 days. Survival curves were made by the Kaplan-Meier method.

3.19 Heterologous expression of the HsbA1 and HsbA2 proteins in *Pichia pastoris*

3.19.1 Construction of the expression vector and transformation of P. pastoris

Total RNA was purified from the mycelium of the *M. circinelloides* MS12 strain grown on YNB medium at 25 C for 4 days using the DNA/RNA extraction kit (Viogene) according the

manufacturer's instruction. cDNA synthesis was performed by the Maxima H Minus First Strand cDNA Synthesis Kit (Thermo Scientific). The *hsbA1 and hsbA2* genes were amplified by PCR using the primer pairs McHSB1HEfw-McHSB1HErev and McHSB2HEfw-McHSB2HErev, respectively (**Table S1**). The PCR products were then cloned into pJET 2.1 blunt end cloning vector (Invitrogen), according the manufacturer's instruction. pJET 2.1 plasmids containing the *hsbA* genes were digested by the restriction enzymes Xho1 and Xba1 and the cut fragments containing the genes were ligated into the pPICZα A vector (Invitrogen), according the manufacturer's instruction (**Figure 5**).

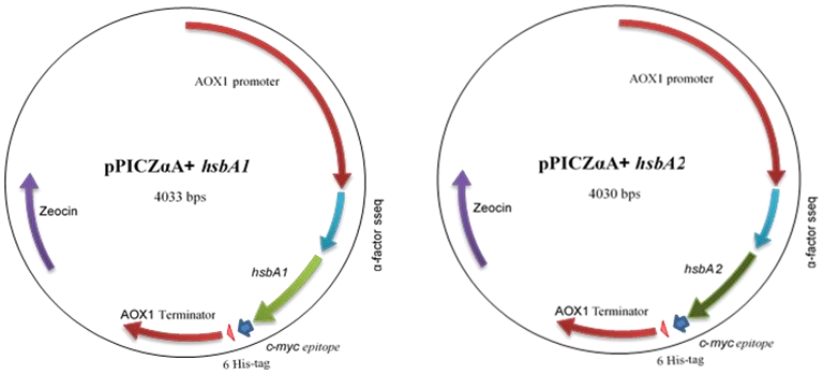

Figure 5: Schematic map of the constructed vectors for heterologous expression of *Mucor* HsbA proteins in *P. pastoris*.

Transformation of *P. pastoris* KM71H strain (Invitrogen) with the constructed vectors was performed by electroporation according to manufacturer's instruction (EasySelect *Pichia* Expression Kit, Invitrogen). Selection of clones was carried out by cultivating the transformants on YPD + Zeocin (YPDZ; Invitrogen) selective media.

3.19.2 DNA isolation from P. pastoris

The appropriate *Pichia* strain was inoculated into 2ml YPD/YPDZ liquid media (Invitrogen) and incubated on a shaker at 28°C, overnight. Then, the culture was centrifuged at 5,000 rpm for 5 min. The supernatant was discarded and 500 µl lysis buffer (5 g SDS, 9.3 g EDTA (50 mM), 6.05 g TRIS (100 mM, pH: 8.0), sterile distilled water) was added to the pellet. The sample was then vortexed with glass beads for 3 min. After addition of 270 µl ammonium acetate (7 M), it was incubated at 65 °C for 5 min. The sample was then extracted with 500 µl chloroform:

isoamyl alcohol (24:1) and centrifuged for 10 min at 13,000 rpm. The upper phase was pipetted into a new tube and an equal amount of isopropanol was added to it. After incubating for 20 min at -20 °C, the sample was centrifuged for 10 min at 13,000 rpm. To the pellet, 500 µl 70%-ethanol was added and it was centrifuged at 13,000 rpm for 5 min. The supernatant was carefully removed and, after drying, the pellet was re-suspended in 50 µl sterile distilled water.

3.19.3 Production and purification of HsbA proteins from the P. pastoris transformants

For expression of the proteins in *P. pastoris*, a single yeast colony was inoculated into 25 ml BMGH medium and incubated at 28 °C on a shaker (250 rpm) for 16 h (i.e. until it reached an OD_{600} = 2-6). The cells were harvested by centrifuging at 1,500 ×g for 5 min at room temperature. The pellet was then re-suspended in 100ml BMMH medium to an OD_{600} = 1.0 in a 1 liter flask, which was incubated at 28 °C on a shaker (250 rpm) for 7 days. After every 24 hours, 100% methanol to a final concentration of 0.5% was added to maintain the induction. One ml of the expression culture was transferred to a 1.5-ml microcentrifuge tube at each time point, i.e. at 0 h and 1-7 days post-inoculation, and these samples were used to analyse the expression levels of HsbA proteins and to determine the optimal time to harvest. Each culture was centrifuged at 13,000 rpm for 3 min at room temperature and the supernatant was transferred to a separate tube.

Protein expression was analysed by precipitating 1 ml of culture supernatant with 100% trichloroacetic acid (TCA) and carrying out an SDS-PAGE gel electrophoresis. After addition of TCA, the sample was incubated on ice for 30 min and centrifuged again at 13,000 rpm for 10 min at room temperature. To the pellet, 500 µl acetone was added and the sample was mixed by vortexing briefly. After centrifuging again at 13,000 rpm for 10 min, the wash step with 500 µl acetone was repeated. After centrifuging, the pellet was dried for 20 min in a drier and re-dissolved in 22.5 µl of nuclease free water.

3.19.4 Sodium Dodecyl Sulphate Polyacrylamide Gel Electrophoresis (SDS- PAGE)

As a resolving gel a 12% SDS-PAGE gel containing 1.68 ml ProSieve 50 gel solution (Lonza), 1.75 ml of 1.5 M Tris-HCl (pH: 8.8), 70 µl 10% SDS, 70 µl of 10% APS (BioRad), 2.8 µl TEMED (BioRad) and 3.4 ml of sterile deionized water was prepared. The stacking gel contained 300 µl ProSieve 50 gel solution (Lonza), 390 µl of 1M Tris-HCl (pH: 6.8), 30 µl of 10% SDS, 30 µl of 10% APS (BioRad), 3 µl TEMED (BioRad) and 2.25 ml of sterile deionized water.

Samples were prepared for loading into the SDS-PAGE gel by adding 2.5 µl of Loading dye (Thermo Scientific) to 22.5 µl sample and kept the samples at 80 °C for 10 min. The whole volume of samples was loaded into the well of the 12% SDS-PAGE gel. Running was carried out with a constant voltage of 150 V and a current of 90 mA for 1 h in 1x Tris-glycine-SDS running buffer (pH: 8.3) (BioRad).

Gels were then stained with either Coomassie stain or by silver nitrate. Coomassie staining was carried out by incubating the SDS-PAGE gel in a solution of 0.0025% Coomassie, 40% methanol and 7% acetic acid overnight at room temperature. After that, the staining solution was carefully removed and de-stained the gel twice with destaining solution I containing 40% methanol and 7% acetic acid for 30 min. Then, the gel was treated twice with destaining solution II containing 3.5% acetic acid and 5% methanol for 45 min. Silver nitrate staining was carried out by fixing the gel in a fixation solution of 50% ethanol, 12% acetic acid and 0.05% formaldehyde for 2 h. Then, the gel was washed three times with 20% ethanol for 20 min. Sensitization of the gel was carried out by using 0.02% disodium sulphate for 2 min. After washing the gel twice with sterile distilled water for 1 min, it was treated with 0.02% silver nitrate solution for 20 min. Then, it was washed again with sterile distilled water for 1 min. Development of the gel was carried out in 6% sodium carbonate, 0.05% formalin and 0,02% sodium thiosulphate, until bands were visible. Reaction was stopped by using 100 µl of glacial acetic acid.

3.19.5 Purification of the recombinant HsbA proteins

Culture supernatants (10 ml) obtained from the 7-days culturing of *Pichia* transformants in BMMH were initially loaded into a 50-ml Bioscale Mini Bio-Gel P-6 Desalting Cartridge (BioRad) equilibrated previously with 50 mM acetate buffer (pH: 4.5). The flow rate for desalting was 9 ml/min. After desalting, 10 ml of the sample was subjected on chromatography using a Nuvia cPrime cation exchange chromatography column (8 mm ID x 100 mm H, V=5.0 ml; BioRad) equilibrated with acetate buffer (pH: 4.5). Unbound proteins were washed with acetate buffer (50 mM, pH: 4.5). For elution of protein samples, 25 mM Tris buffer (4.4 g/L Tris-HCl, 2.65 g/L Tris base; pH: 8.0) was added in an isocratic flow with a flow rate of 2 ml/min. Five ml of elutes were then used for further purification by using size exclusion chromatography with a HI prep 16/60 Sephacryl S200HR column (M_r 5 x 10^3 - 2.5 x 10^5 Da; GE Healthcare) and 50 mM phosphate buffer (pH: 7.0). The flow rate for elution was 0.5 ml/min in an isocratic flow.

3.19.6 *Mass spectrometric analysis of purified protein*

Mass spectrometric identification of HsbA1 was based on enzymatic digestion. Proteins from *P. pastoris* supernatant was initially precipitated with 100% trichloroacetic acid, then the precipitated proteins were run on a 12% polyacrylamide gel. The polyacrylamide gel containing protein was cut in the expected size, sliced into small pieces and 100 µl of 25 mM NH_4HCO_3 in 50% acetonitrile was added for the sample. After the sample was vortexed for 10 min and centrifuged for 1 min at 800xg. After discarding supernatant, the sample was dried by vacuum centrifugation. To reduce disulphide bridges of dried sample, 25 µl of 10 mM dithiothreitol in 25 mM dithiothreitol NH_4HCO_3 was added. Sample was incubated for 1 hour at 56 °C and centrifuged (1 min, 800x*g*).

To alkylate the sample, 25 µl of iodoacetamide was added to the gel cube and incubated at room temperature for 45 min in dark. After incubation, the sample was centrifuged, and the supernatant was removed. The gel cube was dehydrated with 100 µl of 25 mM NH_4HCO_3 in 50% acetonitrile, then the sample was dried by vacuum centrifugation. 25 µl of trypsin was added to the dried sample and incubated for 10 min at 4 °C, then 25 µl of mM NH_4HCO_3 was added and incubated for 16 hours at 37 °C. After trypsin digestion, 5% formic acid: 50% acetonitrile in 1:1 ration was added to the sample. Analysis of the digested sample with MS (quadrupole flight time mass spectrometer, Micromass® Q-TOF, Waters) connected with ultra-high performance liquid chromatograph (UPLC, Nano Aquity Ultraperformance Liquid Chromatography System, Waters) was performed using BEH130 C18 column (column length 250 mm, column diameter: 75 µm, particle size: 1.7 µm, Waters). The composition of mobile phase was 3% "eluent B". The flow rate was 350 nl/min and the temperature of column thermostat was 40 °C. The mass spectrometer used in MSE mode with electrospray ionization with positive polarity. WATER Biopharmalynx softer (Waters) was used to evaluate the data. Mass spectrometric measurements and data evaluation were performed by Dr. Zoltán Kele (Szeged University, Faculty of General Medicine, Institute of Medical Chemistry).

3.20 Statistical analysis

Values presented in the thesis are mean ± standard deviation for the technical and biological replicates. Significance was calculated and assessed by unpaired t test and one-way ANOVA using

GraphPad Prism version 5.01 and Microsoft excel software of the Microsoft Office package for Windows. A probability (P) values less than ≤ 0.05 was considered as statistically significant.

4. RESULTS AND DISCUSSION

4.1 Identification of *hsbA* genes in the *M. circinelloides* genome

BLAST searches using the *L. corymbifera hsbA1* gene (NCBI GenBank accession number: CDH54577) in the *Mucor* genome database (DoE Joint Genome Institute; *M. circinelloides* CBS277.49v2.0; http://genome.jgi-psf.org/Mucci2/Mucci2.home.html) found six potential *hsbA* genes, which were named as *hsbA1a*, *hsbA2*, *hsbA1b*, *hsbA3*, *hsbA4* and *hsbA5*, respectively. Location and some features of the encoded putative proteins are presented in **Table 1**. Interestingly the coding sequences of *hsbA1a* and *hsbA1b* are totally the same, though they have differences between their promoter and terminator regions (**Figure S1**). This finding may indicate a recent duplication of the *hsbA1* gene in *M. circinelloides*. *hsbA5* was the least similar to *L. corymbifera hsbA* gene.

Table 1: Location of the six *hsbA*-like genes identified in the *M. circinelloides* genome and main features of the encoded putative proteins.

Protein ID	Location	Name in this study	Length (aa)	Weight of matured protein (kDa)	Signal sequence cleavage site	GPI-anchor
166852	scaffold_08: 1405558-1406179	HsbA1a	185	17.15	between aa 19 and 20; ANA-AA	yes
92193	scaffold_05: 2170704-2171323	HsbA2	185	17.33	between aa 19 and 20; AHA-AA.	yes
166851	scaffold_08: 1402687-1403308	HsbA1b	185	17.15	between aa 19 and 20; ANA-AA.	yes
157923	scaffold_01: 1093150-1093764	HsbA3	184	16.9	between aa. 18 and 19; VNA-AA	no
158131	scaffold_01: 1800078-1800698	HsbA4	185	17.75	between aa 18 and 19; VNA-AA	no
84535	scaffold_08: 1977158-1977774	HsbA5	185	17.08	between aa 19 and 20; ANA-AA	no

As expected, all putative proteins contain a signal sequence (**Table 1**) indicating that they are secreted proteins similarly to other known HsbA proteins (**Muszewska et al., 2017)**. The putative HsbA1a, HsbA1b and HsbA2 also harbour a GPI-anchor (**Table 1**). This is a lipid anchor, which is added to the C-terminus of certain proteins during their posttranslational modification (**Paulick and Bertozzi, 2008**). In fungi, proteins with GPI-anchor are eventually incorporated into the cell wall (**Kinoshita, 2016**). These results suggest that HsbA1a, HsbA1b and HsbA2 are cell wall bound proteins while the other identified HsbA proteins are secreted into the extracellular space.

Figure 6 shows the multiple alignment of the hypothetic HsbA proteins of *M. circinelloides.* The protein 166852 (HsbA1a) and 166851 (HsbA1b) have identical amino acid sequences.

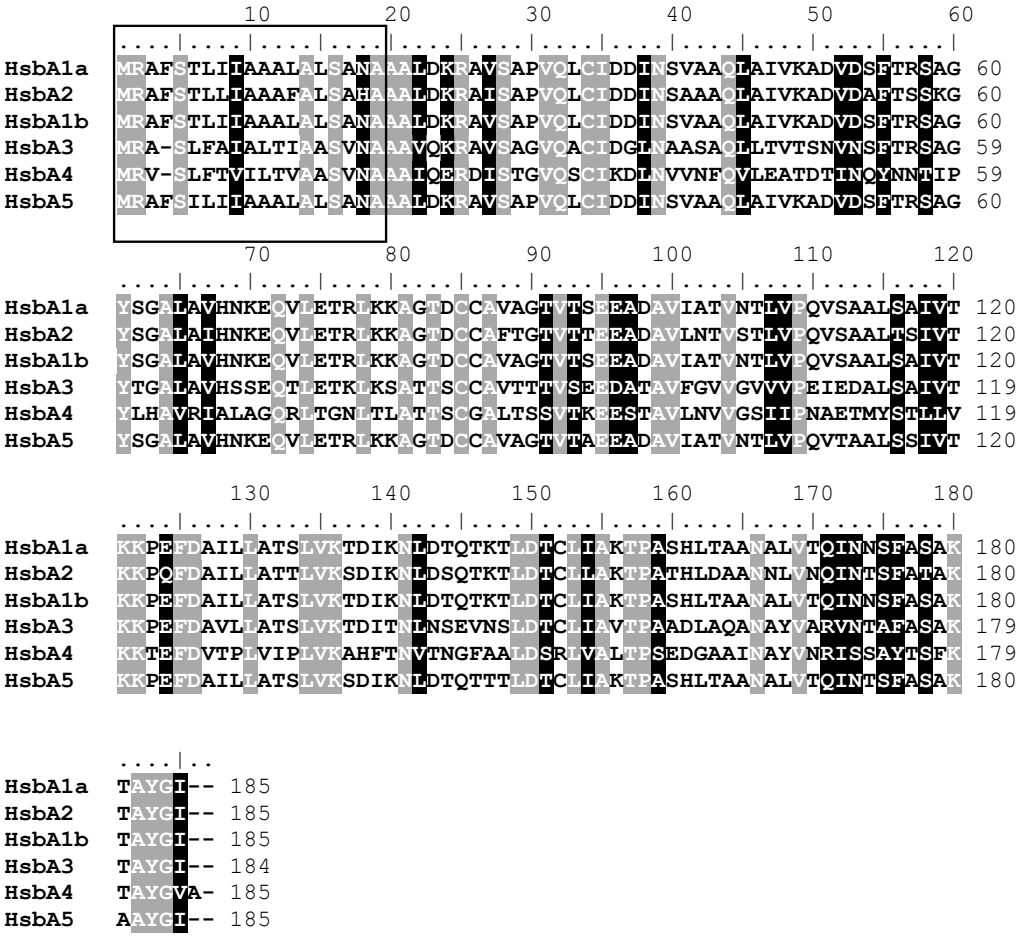

Figure 6: Sequence alignment of HsbA proteins of *M. circinelloides.* Signal sequences are highlighted in the box. Area's shaded in grey represent identical amino acid residues, whereas those shaded in black represent similar amino acid residues.

Table 2: Proteins homologues to the different HsbA proteins of *M. circinelloides* found by BLASTp search in the NCBI GenBank database.

Protein	Protein homologues (80-100% identity)	Similar proteins with known function (25-50% identity)
HsbA1a	• HsbA domain containing protein *Mucor lusitanicus* (**KAF1802751.1** and **KAF1806709.1**). • Hypothetical protein- *M. circinelloides* 1006PhL (**EPB85214.1**, **EPB87478.1** and **EPB86827.1**). • Hsb protein- *Mucor ambiggus* (**GAN11327.1**).	• Antigenic cell wall- *Moniliophthora roreri* MCA 2997 (**ESK86092.1**). • Cell wall galactomannoprotein- *Cordyceps fumosorosea* ARSEF 2679 (**XP_018702310**.1) and *Akanthomyces lecanii* RCEF 1005 (**OAA70820.1**). • Cell wall galactomannoprotein- *Cordyceps militaris* (**ATY65847.1**). • Antigenic cell wall galactomannoprotein- *C. militaris* CM01 (**XP_006672052.1**).
HsbA2	• HsbA domain containing protein- *M. lusitanicus* (**KAF1806709.1**, **KAF1802751.**1 and **KAF1802566.1**). • Hsb protein- *M. ambiggus* (**GAN11327.1**). • Hypothetical protein- *M. circinelloides* 1006PhL (**EPB86885.1**, **EPB87478.1**, **EPB85214.1** and **EPB86827.1**).	• Hypothetical protein (**XP_018702310.1**). • Cell wall galactomannoprotein- *Ceraceosorus bombacis* (**CEH18752.1**) and *A. lecanii* RCEF 1005 (**OAA70820.1**). • Cell wall galactomannoprotein- (**ATY65847.1**). • Antigenic cell wall galactomannoprotein- (**XP_006672052.1)** and Beauveria *brongniartii* RCEF 3172 (**OAA42529.1**), • Maf- like protein (**WP_112562570.1**, **WP_112970673.1**, **WP_112544964.1** and **WP_007813806.1**). • Putative antigenic cell wall protein (**XP_007918864.1**).
HsbA1b	• HsbA domain containing protein- *M. lusitanicus* (**KAF1802751.1**, **KAF1806709.1** and **KAF1802566.1**), • Hypothetical protein- *M. circinelloides* 1006PhL (**EPB85214.1**, **EPB87478.1**, **EPB86885.1** and **EPB86827.1**), • Hsb protein- *M. ambiggus* (**GAN11327.1**)	• Antigenic cell wall (**ESK86092.1**), • Cell wall galactomannoprotein (**XP_018702310.1** and **OAA70820.1**), • Cell wall galactomannoprotein (**ATY65847.1**),
HsbA3	• HsbA domain containing protein- *M. lusitanicus* (**KAF1801797.1**), • Hypothetical protein- *M. circinelloides* 1006PhL (**EPB88576.1**), • Hsb protein- *M. ambiggus* (**GAN05215.1**).	• Putative STE/STE20/PAKA protein kinase- *Rhizopus microsporus* (**CEG83325.1**).
HsbA4	• Hypothetical protein (**KAF1802016.1**)	-
HsbA5	• HsbA domain containing protein- *M. lusitanicus* (**KAF1802566.1**, **KAF1802751.1** and **KAF1806709.1**), • Hypothetical protein- *M. circinelloides* 1006PhL (**EPB87478.1**, **EPB85214.1**, **EPB86885.1** and **EPB86827.1**), • Hsb protein - *M. ambiggus* (**GAN11327.1**).	• Processing alpha glucosidase I- *Rhizopus azygosporus* (**RCH88279.1**), • Cell wall galactomannoprotein (**XP_018702310.1** and **OAA70820.1**), • Cell wall galactomanno (**ATY65847.1**), • Antigenic cell wall (**ESK86092.1**).

Table 2 shows the most similar proteins of other fungi found by BLASTp search in the NCBI GenBank. Majority of the homologues are cell wall associated mannoproteins or secreted

proteins. However, only a few of them have been characterized and little is known about their function. HsbA proteins of *M. circinelloides* were shown to be homologous to mannans and mannoproteins are known to be major antigens of the fungal cell wall that could stimulate immune B-cell response, such anti-mannan antibodies are usually present in the serum of patients suffering from mycoses (**Ponton et al., 2001**).

The galactomannan (**ESK86092.1, XP_018702310.1**, **OAA70820.1**, **ATY65847.1**, **OAA42529.1 and XP_006672052.1)** comprises mannan and galactofuranose; it is linked to a GPI anchored precursor and located at the outermost layer of the cell wall (**Costachel et al., 2005 and Gow et al., 2017)**. The galactomannans present on the cell surface of pathogenic fungi may be involved in the infection mechanism (**Oka, 2018**).

Multicopy associated filamentation (Maf) proteins (**WP_112562570.1**, **WP_112970673.1**, **WP_112544964.1** and **WP_007813806.1)** are nucleotide binding proteins that plays role in arrest of cell division (**Tchigvintsev et al., 2013 and Weerakkody et al., 2019**).Though Maf protein have been shown to play role in inhibition of septum formation in eukaryotes, bacteria and archae, the exact biochemical activity remains unknown (**Butler et al., 1993**).

Putative STE/STE20/PAKA protein kinase (**CEG83325.1)** belongs to the family of p21 activated kinases (PAKs). The p21 activated kinases (PAKs) are serine/ threonine kinases (STE), which is involved in mitogen-activated protein kinase (MAPK) signal transduction and regulates cytokinesis and actin dependent growth, which effects morphogenesis and cellular function (**Boyce and Andrianopoulos, 2011 and Gomes et al., 2018**).

α-Glucosidases (EC3.2.1.20) (**RCH88279.1)** are a group of glycoside hydrolase enzymes, that are involved in the metabolism of oligosaccharides, and in biosynthesis and modification of glycoproteins (**de Melo et al., 2006 and Carvalho et al., 2010)**. These enzymes catalyze the hydrolysis of α-1,4 glucosidic linkages, releasing D-glucose from the non-reducing end of the substrates. α-Glycosidase enzymes were shown to be involved in processes of fungal growth, and in the synthesis and extension of cell wall (**Seidl et al., 2008**). Furthermore, the inhibitors of these enzymes were shown to impair the growth and development of fungi (**Kaur et al., 2019**).

Because they showed the highest similarity to the *L. corymbifera hsbA* gene, HsbA1a (which is referred as *hsbA1* in our further analysis), HsbA2, HsbA3 and HsbA4 were selected for further detailed analysis.

4.2 Transcription of the *hsbA* genes of *M. circinelloides*

4.2.1 Relative transcript levels of the hsbA genes during the cultivation period

Relative transcription levels of *hsbA1*, *hsbA2*, *hsbA3* and *hsbA4* of *M. circinelloides* were studied by carrying out qRT-PCR analyses using the primers shown in **Table S1**.

During the whole cultivation period, *hsbA1* and *hsbA2* showed the highest relative transcription level, especially in the second and third days (**Figure 7**). This experiment suggested that *hsbA* genes are expressed differently throughout the life cycle of the fungus.

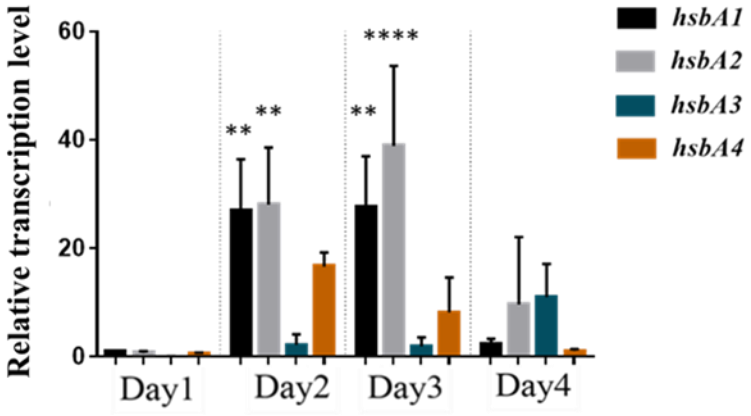

Figure 7: Relative transcription levels of four *hsbA* genes of *M. circinelloides* during cultivation at 25 °C on YNB medium. Transcript level of *hsbA1* measured after 24 h post-inoculation was taken as 1. The presented values are averages of three independent experiments; error bars indicate standard deviation. Values indicated by asterisks significantly differed from the value taken as 1 according to the statistical method one-way ANOVA (** $p < 0.01$; **** $p < 0.0001$).

4.2.2 Relative transcript levels of the hsbA genes at different temperatures

The effect of temperature on the relative transcription levels of the four tested *hsbA* genes was examined at 25 and 35 °C (**Figure 8**). At the higher temperature, all four genes proved to be upregulated compared to their transcription activity at 25 °C, indicating a clear temperature regulation in their expression.

There are only few studies concerning the regulation and function of HsbA proteins. Onaga et al. (**2017**) examined the expression of virulence related genes of *Magnaporthe oryzae* during the infection of rice by transcriptome analysis. They also found that *hsbA* genes were upregulated at elevated temperatures (i.e. at 38 °C) and concluded that temperature elevation could favour the

fungal infection. They also noticed that cutinases and other hydrolytic enzymes showed increased expression in parallel with the *hsbA* genes.

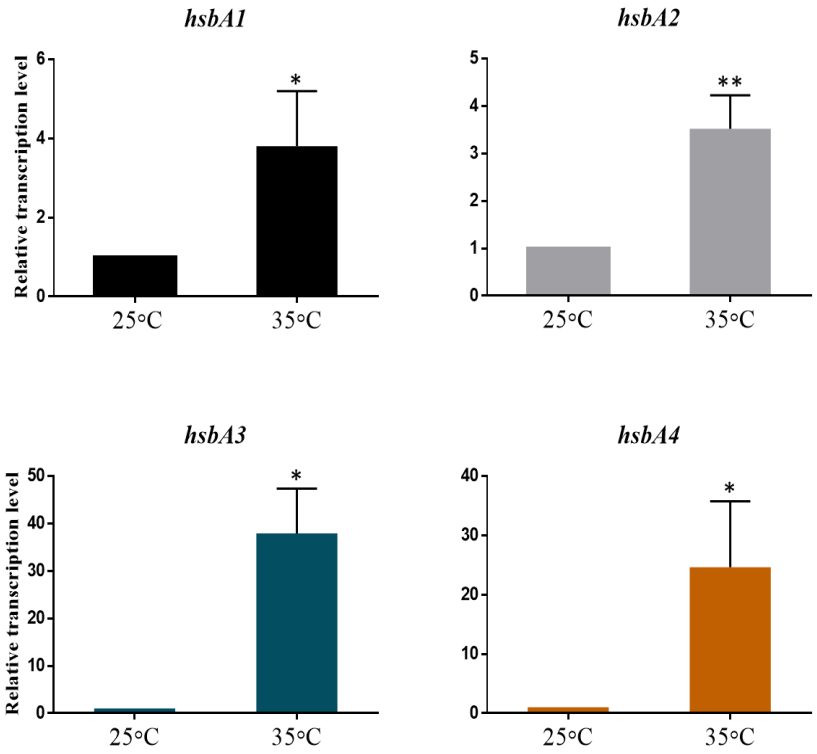

Figure 8: Relative transcription levels of the *hsbA* genes of *M. circinelloides* at different cultivation temperatures (i.e. at 25 and 35 °C). MS12 was grown on YNB for 4 days; transcript level of each gene measured at 25 °C was taken as 1. The presented values are averages of three independent experiments; error bars indicate standard deviation. Values indicated by asterisks significantly differed from the value taken as 1 according to the statistical method unpaired t- test (* $p < 0.05$; ** $p < 0.01$).

4.2.3 Effect of the serum on the transcription of the hsbA genes

Effect of the presence of serum on the relative transcription levels of the four *hsbA* genes of *M. circinelloides* was measured on the fourth cultivation day (**Figure 9**). We found that the transcription level of *hsbA1*, *hsbA2* and *hsbA4* increased in the presence of serum compared to the untreated control.

During host invasion, serum serves as an important source of protein that binds to the cell surface of pathogens on interaction and stimulates the immune system. Galactomannan is a

polysaccharide, one of the major cell wall components of *Aspergillus* spp. that is released during the growth of the fungus. Galactomannan of the human pathogenic *A. fumigatus* can be used to diagnose invasive aspergillosis where galactomannans are shown to be released in high concentration into the serum during the terminal phase of invasive aspergillosis (**Christopher et al., 2006**). In *C. albicans* it was proposed that the upregulation of cell wall mannans and mannoproteins is a requirement for defence mechanisms (**Netea et al., 2008**).

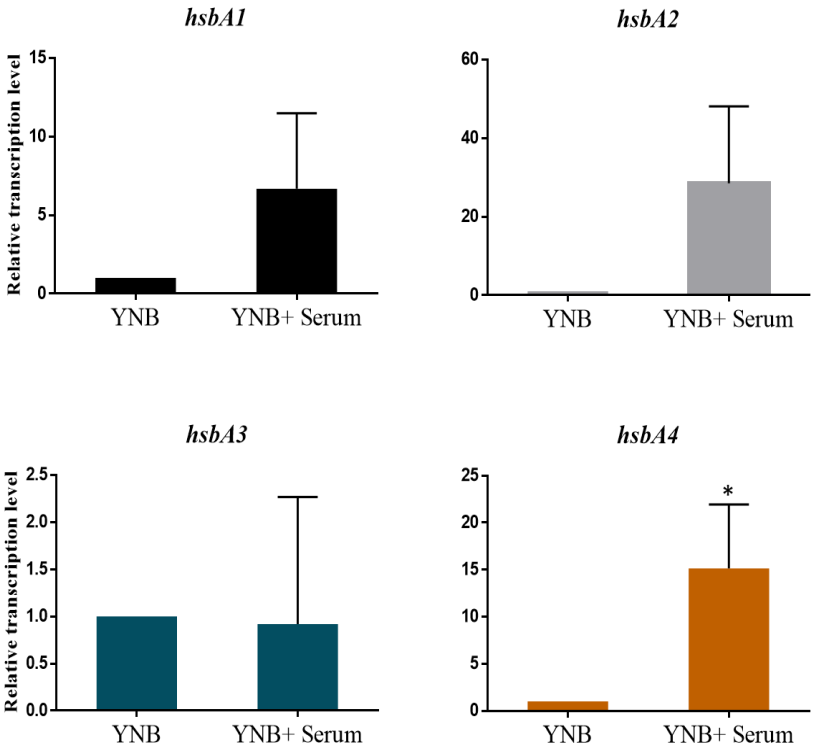

Figure 9: Relative transcription levels of the *hsbA* genes of *M. circinelloides* after cultivation with and without serum in the medium. MS12 was grown in YNB broth or YNB broth supplemented with 10% human serum (kindly provided by E.J. Tóth) at 25 °C for 4 days; transcript level of each gene measured without serum was taken as 1. The presented values are averages of three independent experiments; error bars indicate standard deviation. Values indicated by asterisks significantly differed from the value taken as 1 according to the statistical method unpaired t- test (* $p < 0.05$).

M. circinelloides spores produced on YPG medium supplemented with native blood serum showed increased virulence compared to spores that were produced on YPG supplemented with denatured blood serum or on YPG alone (**Patiño-Medina et al., 2019**). The spores produced from YPG supplemented with native blood serum showed increased death in a *Caenorhabditis elegans* model, increased survivability in the presence of macrophages, increased germination rate and longer hyphae, enhanced resistance to stress factors, such as H_2O_2, and increased thermotolerance compared to spores produced under other conditions (**Patiño-Medina et al., 2019**). Serum was shown to also enhance the virulence of *M. circinelloides* spores through increased fungal proliferations in liver and lung tissues of mice, compared to those produced in YPG alone or YPG supplemented with denatured serum. The authors suggest that presence of thermolabile components in the serum may influence the virulence capacity of *M. circinelloides*. Anyway, in our study, serum highly increased the transcription of certain *hsbA* genes suggesting that it may modify the expression of certain cell surface proteins.

4.2.4 Transcription of the hsbA genes under aerobic and anaerobic conditions

M. circinelloides grows in a filamentous form under aerobic conditions. However, its growth can switch to a yeast-like form in the lack of oxygen and at high carbon dioxide levels (**Wolff et al., 2002**). Morphological dimorphism also affects the virulence of mucormycosis-causing fungi (**Li et al., 2011; Lee et al., 2013 and Lee et al., 2015**). This switch from the filamentous to the yeast growth and vice versa requires reorganization of the cell wall and cell surface.

Effects of the presence or absence of oxygen on the transcription of the four *hsbA* genes of *M. circinelloides* were compared after two days post-inoculation (**Figure 10**).

Relative transcription levels of all tested *hsbA* genes was significantly lower under anaerobiosis than aerobiosis. Moreover, it seems that *hsbA1* and *hsbA2* are only transcribe in the presence of oxygen and/or at filamentous growth. These results suggest that these genes may be regulated by the availability of oxygen or the hyphal morphological state of the fungus. As the encoded proteins are localized on the cell surface or secreted, this regulation can be related to the reorganization of the cells during the different morphological states.

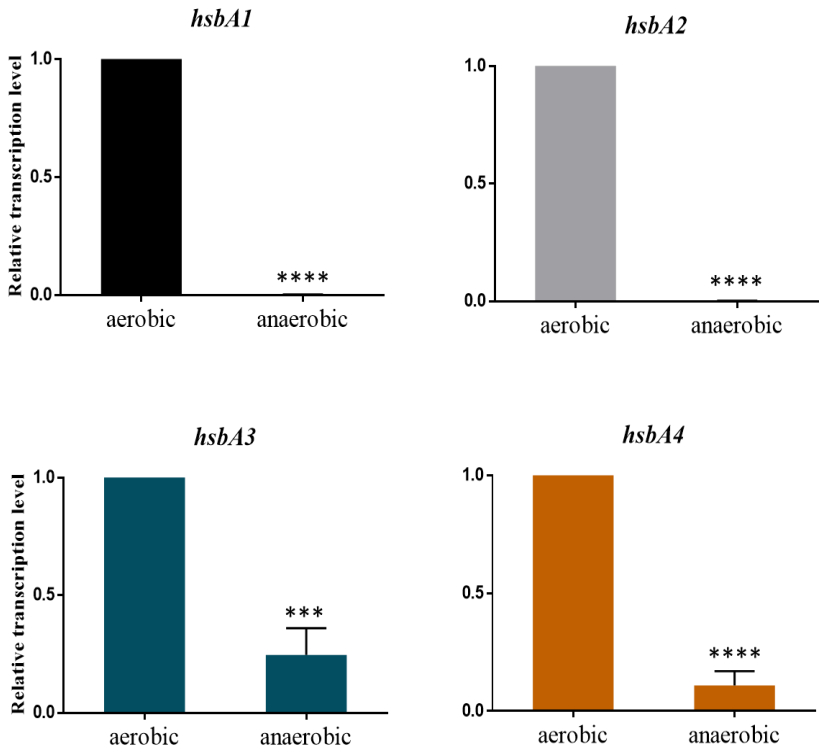

Figure 10: Relative transcription levels of the four tested *hsbA* genes under aerobic and anaerobic conditions. MS12 was grown in 30 ml YNB broth at 25 °C under aerobic or anaerobic condition for 4 days. Anaerobic cultivation was carried out in a BBL GasPak Anaerobic System (Becton Dickinson). Transcript level of each gene measured after aerobic cultivation was taken as 1. The presented values are averages of three independent experiments; error bars indicate standard deviation. Values indicated by asterisks significantly differed from the value taken as 1 according to the statistical method unpaired t- test (*** $p < 0.001$; **** $p < 0.0001$).

4.2.5 Effect of the presence of lignocellulosic materials on the transcription of the hsbA genes

The physiological response of filamentous fungus *A. niger* to wheat straw as a lignocellulosic substrate was shown to strongly induce two genes encoding a hydrophobin and HsbA, hence suggesting the role of HsbA proteins in recruiting lytic enzymes to the straw surface (**Delmas et al., 2012**). The transcription of *hsbA* was also shown to be upregulated in *A. oryzae* cells grown in the wheat bran medium (**Maeda et al., 2004**).

The effect of wheat bran on the transcription of the four tested *hsbA* genes of *M. circinelloides* was examined (**Figure 11**). *hsbA3* showed significantly higher expression gown on

minimal medium supplemented with wheat bran than on the medium, which did not contain this lignocellulosic material. Other genes did not respond to the presence of wheat bran, suggesting a possible role of *hsbA3* in the degradation of lignocellulosic substances and/or in hyphal development in plant material.

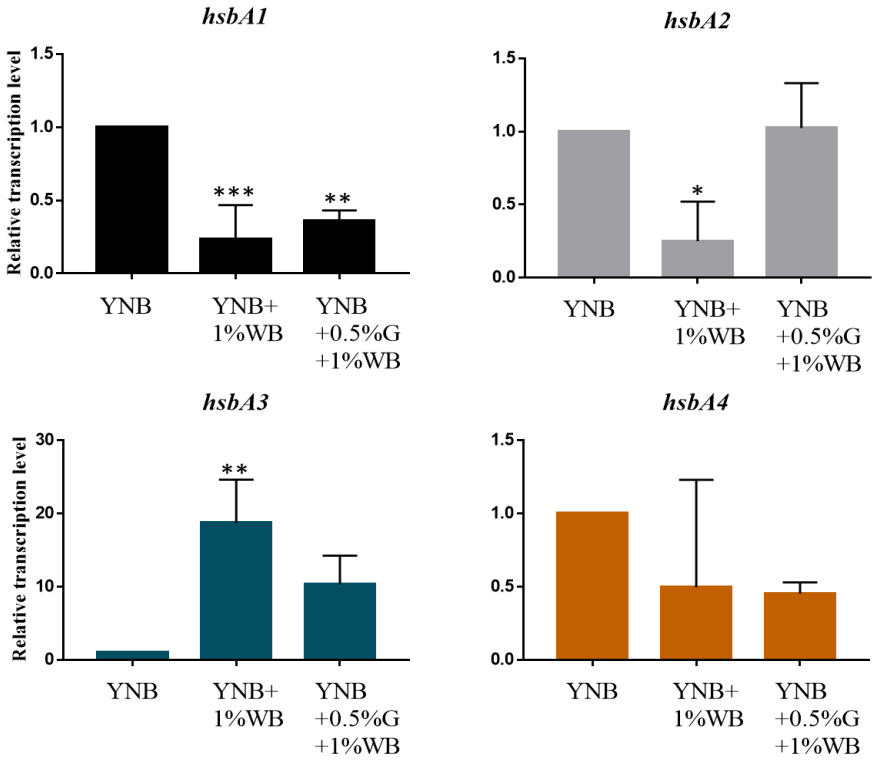

Figure 11: Relative transcription levels of the four tested *hsbA* genes after cultivation with or without wheat bran in the growing medium. MS12 was grown for 2 days in YNB, YNB supplemented with 1% wheat bran media (YNB + 1%WB) or YNB containing 0.5% glucose and 1% wheat bran (YNB + 0.5%G + 1%WB). Transcription level of each gene measured after cultivation in YNB alone was taken as 1. The presented values are averages of three independent experiments; error bars indicate standard deviation. Values indicated by asterisks significantly differed from the value taken as 1 according to the statistical one-way ANOVA (* $p < 0.05$; ** $p < 0.01$; *** $p < 0.001$).

4.3 Construction of disruption and overexpression mutants for the genes *hsbA1, hsbA2* and *hsbA3*

4.3.1 Disruption of hsbA1, hsbA2 and hsbA3 using the CRISPR-Cas9 method

Single disruptions of *hsbA1*, *hsbA2* and *hsbA3* were carried out by integrating the *pyrG* selection marker gene into the corresponding *hsbA* gene via the CRISPR-Cas9 technique (see **Figure 4**), which resulted in the strains MS12+Δ*hsbA1*, MS12+Δ*hsbA2* and MS12+Δ*hsbA3*, respectively. It should be emphasized that the *M. circinelloides* genome contains *hsbA1* in two identical copies (i.e. *hsbA1a* and *hsbA1b*). Although *hsbA1a* and *hsbA1b* have the same coding sequences, their promoter and terminator regions are different (see **Figure S1**). Template DNA to disrupt the *hsbA1* gene (e.g. the disruption cassette containing the *pyrG* gene) was designed to contain targeting regions homologous with the promoter and terminator of the *hsbA1a* gene. So, we expected that gene disruption will affect *hsbA1a.*

Transformation frequency of the *hsbA1* disruption was 8, for *hsbA2* was 2, for *hsbA3* was 14 per 10^5 protoplasts. Successful gene disruption was proven by PCR amplifying the expected fragments in each case. Sequencing of the amplified fragments indicated that integration of the *pyrG* gene occurred in the expected sites. qRT-PCR analysis proved the absence of the *hsbA1*, *hsbA2* and *hsbA3* transcripts in their respective mutants MS12+Δ*hsbA1*, MS12+Δ*hsbA2*, MS12+Δ*hsbA3* (**Figure 12**). Mutants selected for further analysis proved to be mitotically stable retaining the integrated fragment even after 20 cultivation cycles.

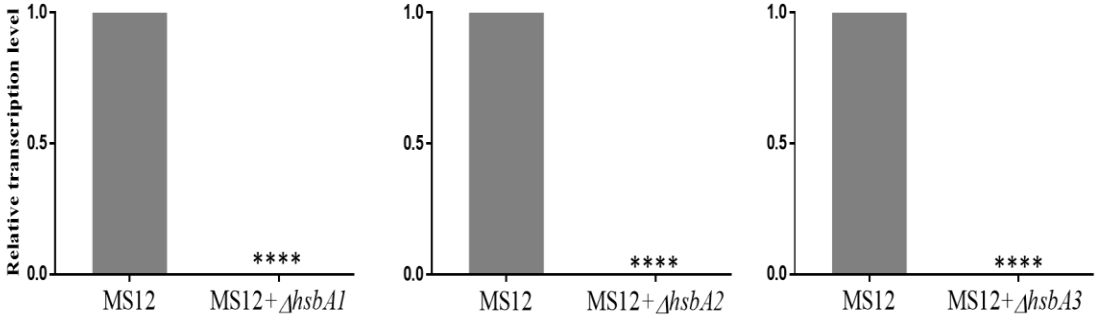

Figure 12: Relative transcription level of *hsbA1*, *hsbA2* and *hsbA3* in their respective deletion mutants and parental strain (MS12). Strains were grown on YNB at 25 °C for 2 days; transcript level of each gene measured in the MS12 strain at was taken as 1. The presented values are averages of three independent experiments; error bars indicate standard deviation. Values

indicated by asterisks significantly differed from the value taken as 1 according to the statistical method unpaired t test (**** p <0.0001).

CRISPR-Cas9 system is a highly efficient method that is widely used in biological and biomedical applications (**Song et al., 2019**). However, the possible occurrence of *off-target* effects caused by the CRISPR-Cas9 system during genome editing is a known phenomenon, hence high concentrations of Cas9:guide RNA complexes can cleave *off-target* sites containing mutations near or within the PAM that are not cleaved when enzyme concentrations are limiting (**Pattanayak et al., 2013**). Although we used a plasmid-free technique, which highly decreases the chance of any *off-target* effects, whole genome sequencing (WGS) was performed on MS12+Δ*hsbA1* and MS12+Δ*hsbA2* to determine or exclude non-specific cleavage events (**Smith et al., 2014 and Dong et al., 2019**). Another reason of the WGS was the fact that qRT-PCR clearly indicated the absence of the *hsbA1* transcripts in the MS12+Δ*hsbA1* strains despite that we targeted only one of the two *hsbA1* copies. Moreover, based on the simple PCR analysis, it was not possible to decide, which of them was affected by the gene disruption. **Table 3** summarizes the main data of the analysis.

The whole genome sequence of the mutant strains was compared with the parental strains. If there is no match in the targeted position, the mutation of the gene is confirmed. Based on the results of WGS the *hsbA1a* (**Figure 13**) and *hsbA2* (**Figure 14**) genes were disrupted, and we could not observe any mutation (insertion or deletion) in the *hsbA1b* gene (**Figure 13**).

Table 3: Strains involved in the WGS analysis, identifiers of the disrupted genes and position of the targeted chromosomes and genes.

Strain	**Examined gene**	**Gene ID of the targeted gene in the *M. circinelloides* genome database**	**Chromosome/ scaffold**	**Position (nl)**
MS12-*ΔhsbA1*	*hsbA1a*	fgenesh1_pg.08_#_422	scaffold_08	1405558-1406179 (+)
MS12-*ΔhsbA1*	*hsbA1b*	fgenesh1_pg.08_#_421	scaffold_08	1402687-1403308 (-)
MS12-*ΔhsbA2*	*hsbA2*	Mucci1.estExt_fgeneshMC_pg.C_50665	scaffold_05	68044-70136 (-)

Figure 13: Result of WGS analysis of MS12-Δ*hsbA1* mutant. We could not observe overlapping region in case of *hsbA1a* (scaffold_08: 1405558-1406179) with the reference genome, but the *hsbA1b* (scaffold_08:1402687-1403308) was intact in the mutant strain.

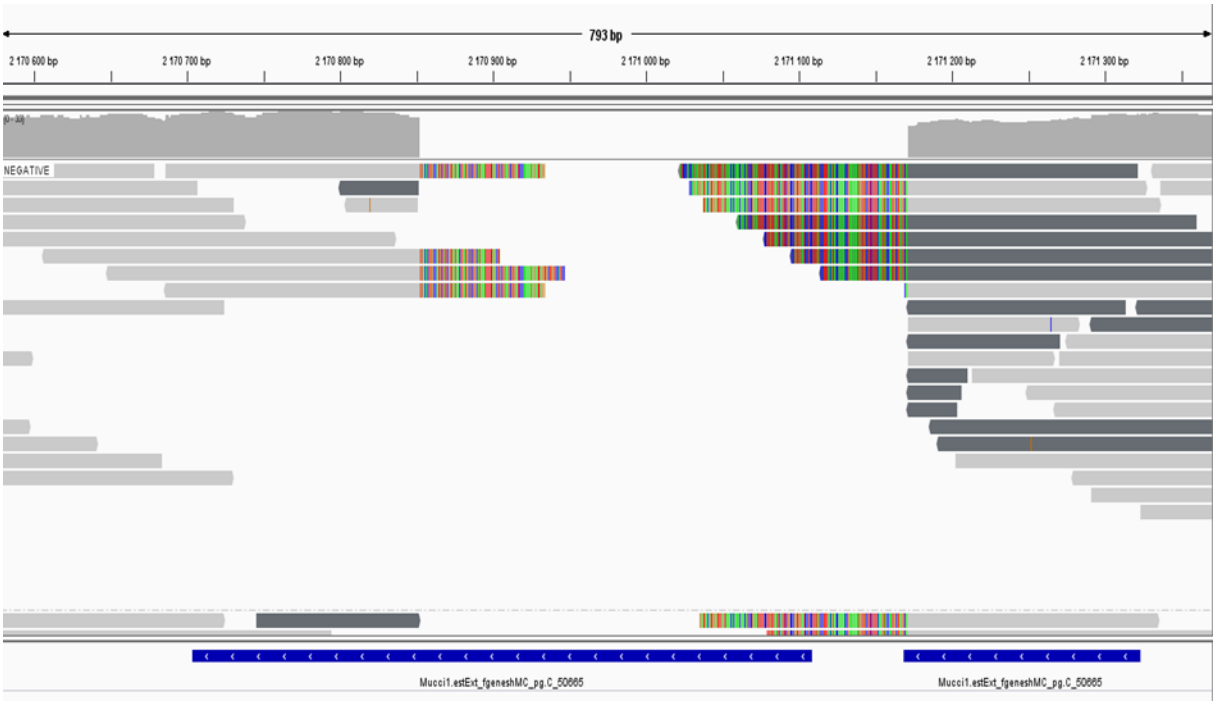

Figure 14. Result of WGS analysis of MS12-Δ*hsbA2* mutant. We could not observe overlapping region with the reference genome

The issue of specificity/accuracy (i.e. the ratio of *on-target* and *off-target* cleavage) often arises using the CRISPR-Cas9 system for genome editing. The efficiency of genome editing can be obtained by variant analysis, which can be achieved by comparing the indels and single-point nucleotide polymorphisms (SNPs) in the mutant strains and reference genome. The results of the variant analysis are summarized in **Table 4**

Table 4: The number of all identified variant in the strains.

Sample	SNP	Indel
MS12	293	51
MS12-Δhsb1A	290	46
MS12-Δhsb2A	302	43

We could not observe any off-target event using the CRISPR-Cas9 system to generate our disrupted mutant and the disruptions in the targeted regions could be observed, but interestingly somehow the *hsbA1* specific crRNA could not recognise the *hsbA1b* gene and could not cause mutation within the gene. To analyse the relative transcript level of *hsbA1* gene in MS12-Δ*hsbA1* strain using a quantitative real-time PCR, we could not detect any amplicon. Our result suggests, the *hsbA1b* gene may be a result of a recent duplication event and may be a non-functional at least under the tested conditions.

4.3.2 Overexpression of hsbA1, hsbA2 and hsbA3

M. circinelloides protoplasts were transformed with the circular plasmids pAV1, pAV2 and pAV3 giving rise the strains MS12+pAV1, MS12+pAV2 and MS12+pAV3, respectively. Transformation frequencies were 11, 2 and 7 transformant colonies per 10^5 protoplasts for MS12+pAV1, MS12+pAV2 and MS12+pAV3, respectively. PCR analysis was carried out on two transformant colonies of MS12+pAV1 and MS12+pAV2 (**Figure 15A**) and one colony for MS12+pAV3 (**Figure 15B**), which demonstrated the presence of the transferred plasmids. Sequencing of the PCR products also verified the presence of the corresponding plasmids. The expected sizes of the amplicons were 720 bp for pAV1 and pAV2, and 722bp for pAV3, respectively.

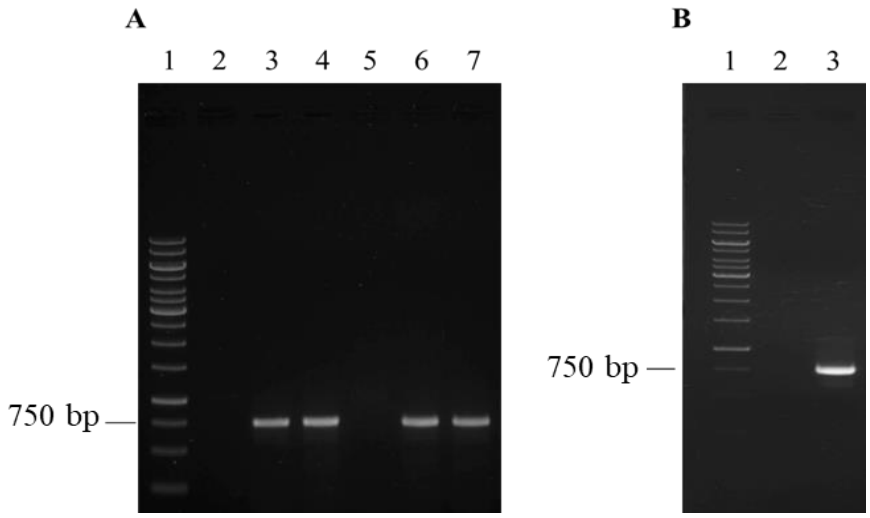

Figure 15: Confirmation of the presence of the plasmids pAV1, pAV2 and pAV3 in *M. circinelloides* transformants. PCR was carried out with the primer pairs Gpdp-McHSB1oerev, Gpdp-McHSB2oerev and Gpdp-McHSB3oerev for pAV1, pAV2 and pAV3, respectively (**Table S1**). Panel **A**: lane 1, GeneRuler 1 kb DNA ladder (Thermo Scientific); lane 2, MS12 (*hsbA1* control); lane 3, MS12+pAV1_1; lane 4, MS12+pAV1_2; lane 5, MS12 (*hsbA2* control); lane 6, MS12+pAV2_1; lane 7, MS12+pAV2_2. Panel **B**: lane 1, Gene Ruler 1 kb DNA ladder; lane 2, MS12 (*hsbA3* control); lane 3: MS12+pAV3.

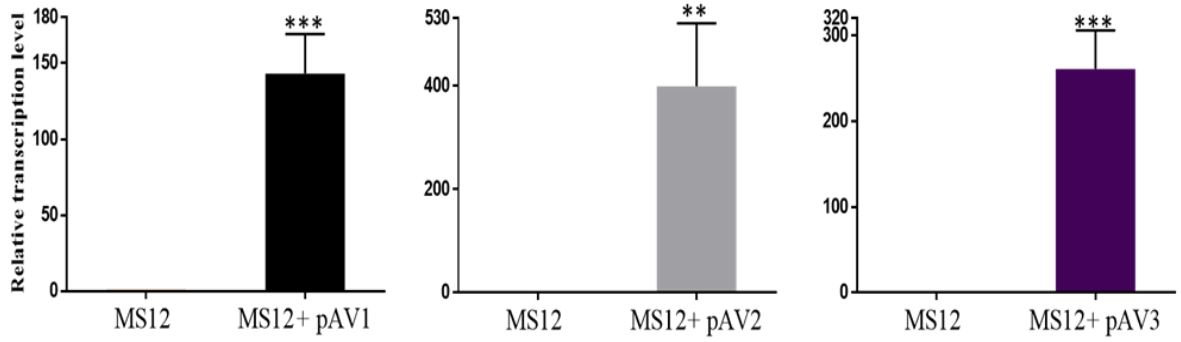

Figure 16: Relative transcription level of *hsbA1*, *hsbA2* and *hsbA3* genes in their respective overexpression mutants and parental strain (MS12). Strains were grown on YNB at 25 °C for 2 days; transcript level of each gene measured in the MS12 strain at was taken as 1. The presented values are averages of three independent experiments; error bars indicate standard deviation. Values indicated by asterisks significantly differed from the value taken as 1 according to the statistical method unpaired t test (** $p < 0.01$, *** $p < 0.001$).

qRT-PCR was carried out to check the expression levels of *hsbA1* (MS12+pAV1), *hsbA2* (MS12+pAV2) and *hsbA3* (MS12+pAV3) in the respective overexpressed mutant (**Figure 16**). Elevated amounts of *hsbA* transcripts were detected in all overexpressed transformants with significant difference compared to the parental MS12 control indicating the overexpression of the genes.

4.4 Characterization of the *hsbA* mutants

4.4.5 Colony growth of the hsbA mutants at different temperatures

Colony growth of the mutants did not differ significantly from that of the MS12+*pyrG* strain used as a control at any temperatures (**Figure S2**), except in the case of the overexpression mutants, which displayed significantly decreased colony diameter at 30 °C, especially in case of MS12+pAV1(**Figure 17**). Micromorphology of the strains did not differ from that of the MS12+*pyrG*.

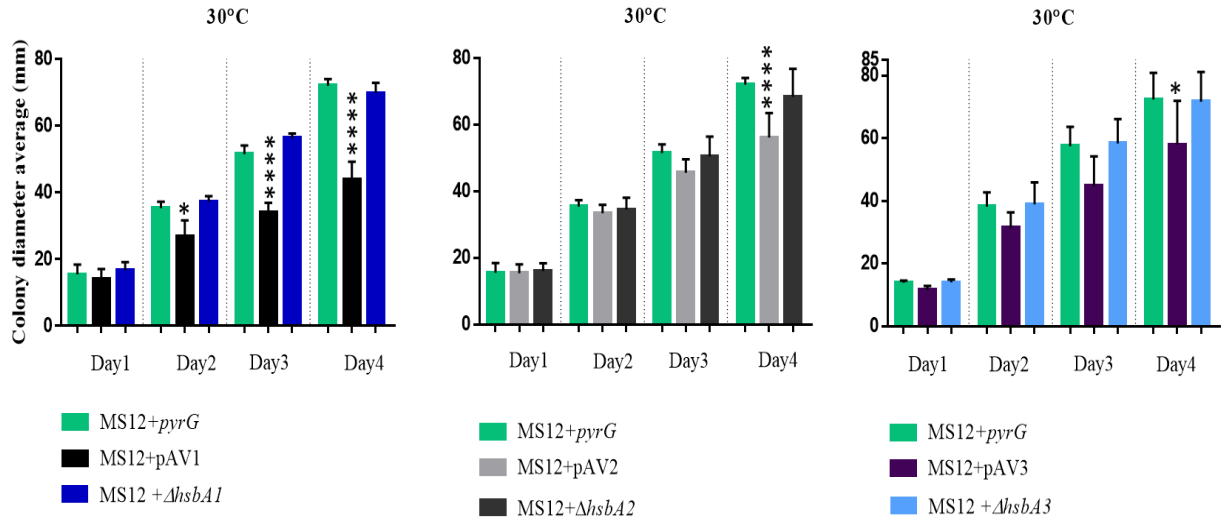

Figure 17: Colony diameter of the hsbA mutants and the MS12+*pyrG* strain at 30 °C. Strains were grown on YNB plates for four days. The presented values are averages; colony diameters were measured during three independent cultivation (error bars indicate standard deviation). Values indicated with asterisks significantly differed from the corresponding value of the MS12+*pyrG* strain according to the statistical method one-way ANOVA (*p<0.05; **p < 0.01, **** p < 0.0001).

4.4.6 Sporulation ability of the hsbA mutants

Sporulation ability of the control MS12+*pyrG* strain and the mutants, in which the *hsbA* genes were overexpressed or disrupted, were compared (**Figure 18**).

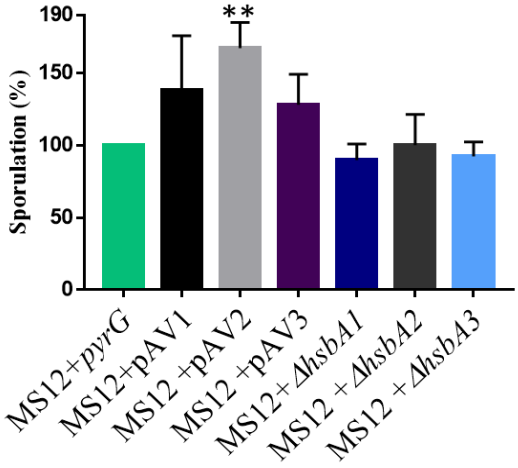

Figure 18: Sporulation of MS12+*pyrG* and the *hsbA* overexpression and disruption mutants grown on MEA plates for 4 days at 25 °C. The inoculum size was 5×10^4 in each case. The presented values are averages; Spores were counted after three independent cultivation (error bars indicate standard deviation). Values indicated with asterisks significantly differed from the corresponding value of the MS12+*pyrG* strain according to unpaired t test (**$p < 0.01$).

Spore production ability of the MS12+pAV2 overexpression mutant was significantly higher than that of the control strain suggesting that the *hsbA2* gene may have role in the sporulation of *M. circinelloides*.

4.4.7 Germination ability of the spores of the hsbA mutants

Mucorales possess the ability to elude pathogenic clearance and undergo germination to form hyphae within the host, thereby allowing the progression of infection through angioinvasion, dissemination and tissue damage (**Ghuman and Voelz, 2017**). Germination enables Mucorales to establish infection and progress to disseminated form within the compromised human host, due to inability of the immune system to supress fungal germination and to kill fungal spores (**Ibrahim et al., 2012).**

To examine the effect of HsbAs on the germination ability of *M. circinelloides*, germination rates of the overexpressed and deletion mutants were compared to that of the MS12+*pyrG* strain (**Figure 19**). There were no differences observed between deletion mutants of *hsbA* and the MS12+*pyrG* strain. However, overexpression of all three genes caused significantly reduced germination ability in the mutants.

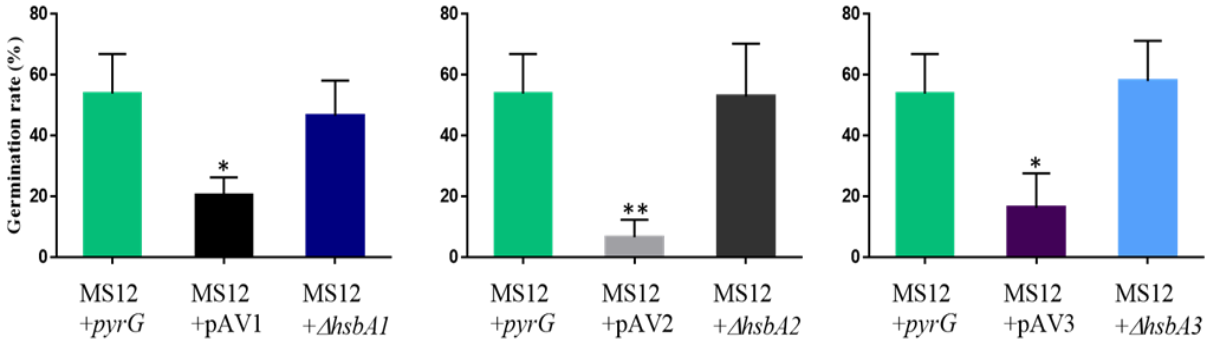

Figure 19: Germination rates of the sporangiospores of the *hsbA* mutants and the MS12+*pyrG* strain. Spores (10^6 spores/ml) were incubated in YNB broth for 6 h at 25 °C and then germinated spores were counted. Spores were counted after three independent cultivation (error bars indicate standard deviation). Values indicated with asterisks significantly differed from the corresponding value of the MS12+*pyrG* strain according to the one-way ANOVA (*$p < 0.05$, **$p < 0.01$).

4.4.8 Effect of cell wall stressors on the growth of the hsbA mutants

HsbA proteins are either secreted or cell wall bound molecules and, as mannoproteins, may participate in the formation of the surface of the spores and the hyphae. Therefore, we examined the effect of cell wall stressor dyes calcofluor white (CFW) and congo red (CR) (**Figure 20**), which can disturb the fungal cell wall structure by connecting to the chitin and β-glucan components of the cell wall (**Wood, 1980 and Nodet et al., 1990**).

No difference in the growth intensity of the deletion mutants (i.e. MS12+Δ*hsbA1*, MS12+Δ*hsbA2* and MS12+Δ*hsbA3*) was observed compared to that of the control (i.e. MS12+*pyrG*). Contrarily, cell wall stressors, especially CR affected the growth of the strains, in which the *hsbA* genes were overexpressed. Presence of CR in the medium decreased the growing ability of all overexpression mutants while CFW affected clearly only the growth of the MS12+pAV1 strain. Results suggest that HsbA1, HsbA2 and HsbA3 may have role in the

maintenance of the cell wall structure and their overexpression may cause sensitivity to cell wall stress.

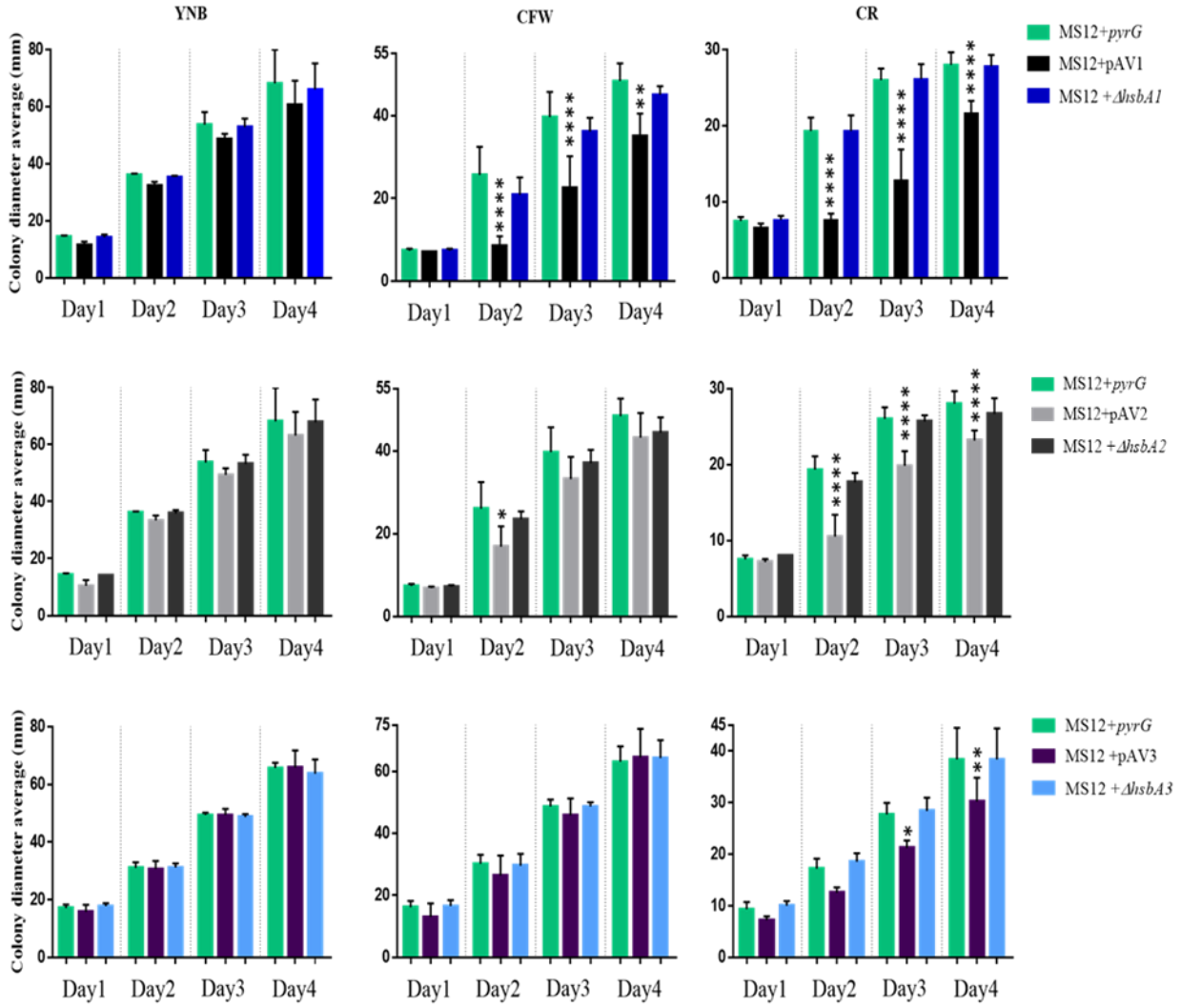

Figure 20: Effect of calcofluor white (CFW) and congo red (CR) on the colony growth of the *hsbA* mutants compared to that of the MS12+*pyrG* strain. Strains were cultivated on YNB supplemented with CFW or CR for 4 days at 25 °C. Values presented are from three independent cultivations (error bars indicate standard deviation). Values indicated with asterisks significantly differed from the value of the MS12+*pyrG* strain measured on the same day according to (*p < 0.05, **p < 0.01, ***p < 0.001, ****p < 0.0001).

4.4.9 Effect of detergents on the growth of the hsbA mutants

Membrane disruptors, SDS and Triton X-100 were also tested on the mutants (**Figure 21**).

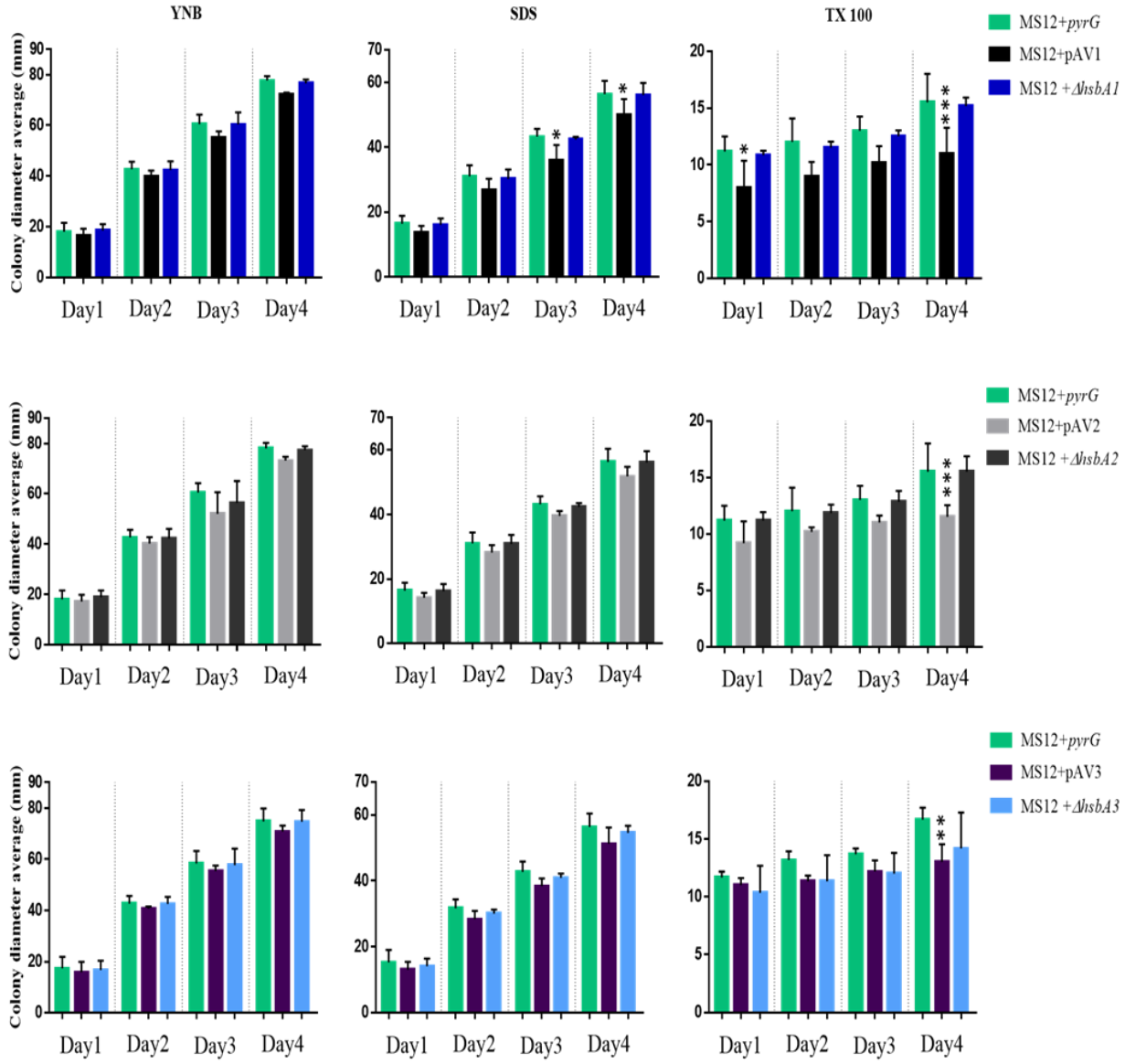

Figure 21: Effect of SDS and Triton X-100 on the colony growth of the *hsbA* mutants compared to that of the MS12+*pyrG* strain. Strains were cultivated on YNB supplemented with SDS or Triton X-100 for 4 days at 25 °C. Values presented are from three independent cultivations (error bars indicate standard deviation). Values indicated with asterisks significantly differed from the value of the MS12+*pyrG* strain measured on the same day according to the two-way ANOVA (*$p < 0.05$, **$p < 0.01$, ***$p < 0.001$, ****$p < 0.0001$).

Similarly, to cell wall stressors, detergents did not change the growing ability of the deletion mutants compared to MS12+*pyrG* strain used as the control. At the same time, SDS was

shown to effect only the growth of the *hsbA1* overexpression mutant, whereas Triton X-100 caused decreased colony growth in all the overexpression mutants on the fourth day of cultivation. These results indicate that overexpression of *hsbA* genes especially *hsbA1* causes sensitivity to membrane disrupting agents.

Summarizing the characterization of the growing and sporulation ability of the mutants, we can tell that deletion of *hsbA1*, *hsbA2* and *hsbA3* did not altered the growing and the general viability of the fungus compared to the control strain (MS12+*pyrG*). Overexpression of these genes slightly affected the colony growth and significantly decreased the germination ability of the sporangiospores. Overexpression also caused sensitivity to cell wall and membrane stressors.

4.5 Effect of the *hsbA* genes on the biofilm formation of *M. circinelloides*

Biofilms are dense, sessile communities of microbes that adheres to surfaces and to each other, that are protected from its surrounding environment by an extracellular matrix (ECM) mainly composed of polysaccharides. (**Harding et al., 2009 and Costa-Orlandi et al., 2017**). Biofilm formation was shown to be involved in the pathogenesis of implant-associated and chronic infections (**Hall-Stoodley et al., 2004 and Singh et al., 2011**).

Biofilm formation was implicated in both yeasts and filamentous fungi that are resistant to antimicrobials and environmental conditions, however, studies conducted on the filamentous fungal biofilms are limited compared to yeast biofilms (**Blankenship et al., 2006; Harding et al., 2009 and Costa-Orlandi et al., 2017**). A proposed model for filamentous fungi suggests that despite the distinct morphology, it was similar to bacterial and yeast biofilm development. In case of *A. fumigatus* biofilms, extracellular matrix is composed of α-1,3-glucans, hydrophobins, galactomannan, monosaccharides, polyols, and melanin (**Müller et al., 2011**). The extracellular matrix of *R. oryzae*, *L. corymbifera* and *Rhizomucor pusillus* was shown to be composed primarily of amino sugars (glucosamine and N-acetyl glucosamine), with glucose and proteins being present in small quantities. In filamentous fungi, hydrophobins are involved in the adhesion of hyphae to hydrophobic surfaces and may be involved in biofilm formation (**Harding et al., 2009)**.

To assess the role of HsbAs in the biofilm formation of *M. circinelloides*, on overexpressed and deletion mutants along with MS12+*pyrG* strain a biofilm assay according to Singh et al. (**2011**) was performed (**Figure 22**).

While overexpression mutants showed the same biofilm forming ability, the deletion mutants were found to form significantly lower amount of biofilm than the MS12+*pyrG* strain.

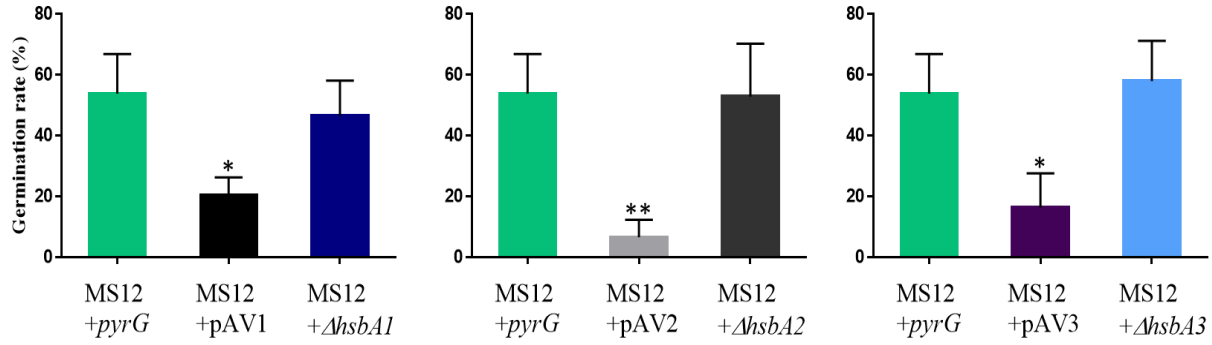

Figure 22: Biofilm assay conducted on overexpressed and deletion mutants. Values are averages from three independent experiments (error bars indicate standard deviation). Values indicated with asterisks significantly differed from the value of the MS12+*pyrG* strain (taken as 100%) according to the one-way ANOVA (*$p < 0.05$, **$p < 0.01$).

4.6 Overexpression of the *hsbA* genes influenced the hydrophobicity of the *M. circinelloides* mycelium

The overall cell wall surface hydrophobicity of the fungal cell wall is caused by the presence of certain hydrophobic moieties, such as proteins and mannoproteins and their interaction with other hydrophilic regions of the cell wall (**Hazen et al., 1990 and Singh et al., 2004**). Kyte-Doolittle hydrophobicity plots (**Kyte and Doolittle, 1982**) of HsbA amino acids using the ProtScale tool of the Expasy portal (**Gasteiger et al., 2005**) revealed that hydrophobic regions with values above 0 were more abundant in these proteins than the hydrophilic regions (**Figure 23**). Hence suggesting that HsbA proteins are more hydrophobic in nature, rather than hydrophilic.

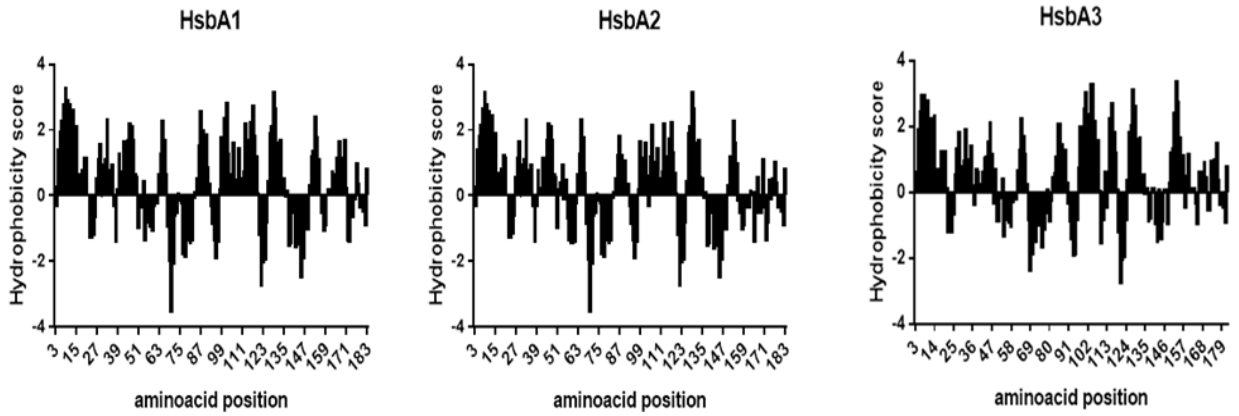

Figure 23: Kyte-Doolittle plot of HsbA1, HsbA2 and HsbA3 (http://web.expasy.org/protscale).

Alcohol percentage test (APT) measuring the wettability of the mycelial surface using different concentrations of ethanol is used to compare the hydrophobicity of different colony surfaces (**Chau et al., 2010**), hence we used APT to compare the hydrophobicity of the mycelia of the different *hsbA* mutants (**Figure 24**). Higher the concentration of ethanol that wets the fungal surface, the more severe the degree of the hydrophobicity (**Chau et al., 2010**).

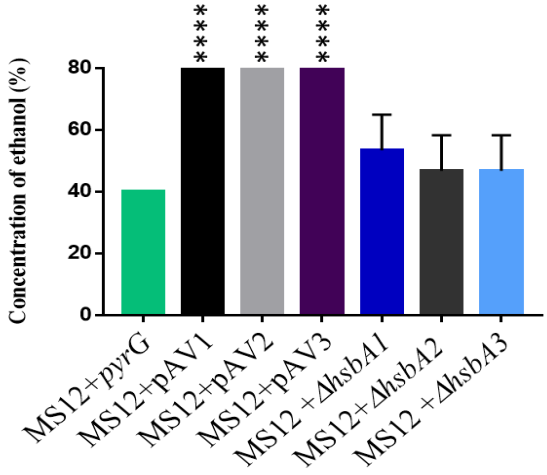

Figure 24: Ethanol concentrations that wet the mycelial surfaces of the colonies of the *hsbA* mutants and the MS12+*pyrG* strain. Strains were grown on solid YNB for 4 days at 25 °C. Values are averages from three independent experiments (error bars indicate standard deviation). Values indicated with asterisks significantly differed from the value of the MS12+*pyrG* strain according to the statistical analysis one-way ANOVA (****$p < 0.0001$).

Adhesion properties of fungal cells plays crucial role in colonization, pathogenesis, and antagonist interactions (**Kennedy, 1990; Krasowska and Sigler, 2014 and Mendes-Giannini et al., 2005)**. Greater the degree of hydrophobicity of fungal cells and substrates causes greater attractive force which results in a higher degree of adhesion. This is mainly seen in case of hydrophobins which are cysteine- rich polypeptides known to play role in dispersion of fungal spore, adhesion, and pathogenesis (**Bayry et al., 2012**). Hydrophobic microorganisms are also known to cause damage of surfaces by the formation of biofilms that allows the fungi to resist host immune response and antifungal therapy (**Kennedy, 1990 and Krasowska and Sigler, 2014**).

Absorption of HsbA proteins onto the hydrophobic material PBSA in the presence of NaCl or $CaCl_2$ was demonstrated suggesting that they can be hydrophobic in nature (**Ohtaki et al., 2006**).

Alcohol percentage test did not indicate significant difference between the deletion mutants and the MS12+*pyrG* strain. However, as the mycelial surface of MS12+pAV1, MS12+ pAV2 and MS12+ pAV3 were easily wetted with high concentrations of ethanol, the test suggested that overexpression of the *hsbA* genes increased the hydrophobicity of the mycelium.

4.7 Scanning electron microscopic analysis of mutants

To determine the effect of overexpression and deletion of HsbA on the spore wall surface of *M. circinelloides*, SEM image analysis was carried out for the overexpressed and deletion mutants of *hsbA* along with MS12 parental strain (**Figure 25**). It was previously shown by the SEM image analysis of *M. circinelloides* that larger spores had granulated surface (bumpy surfaced), whereas the smaller spores were smooth surfaced. These spore granules or bumps are resulted from vesicle trafficking processes that takes place from the cytosol to the cell surface, which is necessary for cell wall construction (**Li et al., 2011**).

We observed a subpopulation of smaller spores with granulated surfaces in the MS12+ pAV1 overexpression mutant sample (**Figure 25, B**) compared to the smaller spores of the parental MS12 strain (**Figure 25, H**). There were no differences observed between the small spores of the deletion mutants and MS12 parental strains. On comparing the large spores, the deletion mutants had large spores (**Figure 25C, F and I**) which were either less granulated or smooth when compared to the larger spore of parental MS12 strain (**Figure 25G**). There were no differences observed in case of the granulations on the larger spores surfaces of MS12+pAV1 and

MS12+pAV2 when compared with the parental MS12 larger spores. Hence suggesting that overexpression and deletion of *hsbA* genes could influence the overall surfaces of small and large spores. Although the exact mechanism behind the cause of this variations are yet to be determined.

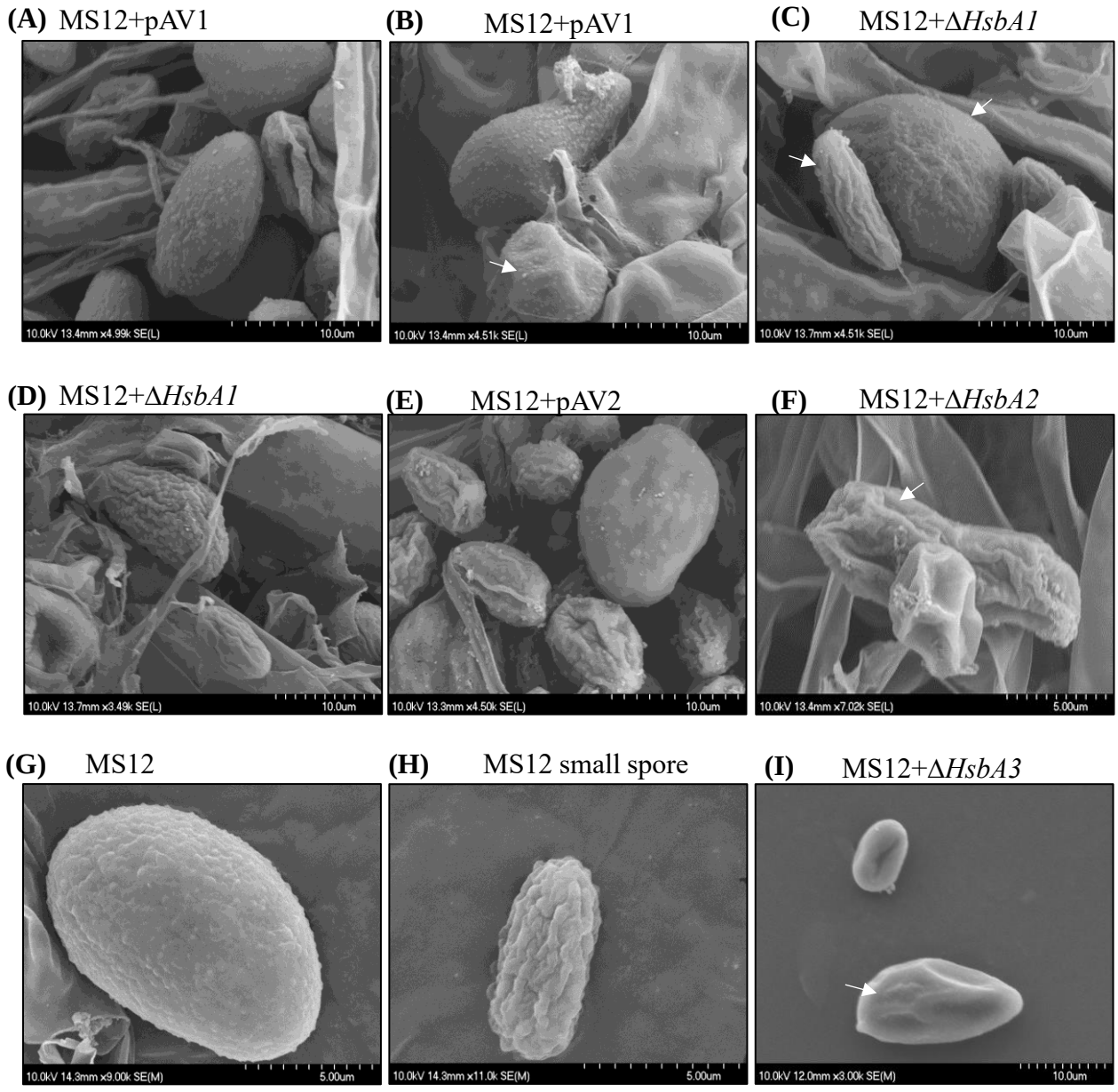

Figure 25: Spore surface variation between parental (MS12) and the overexpressed and deletion mutants. Arrows indicates surface variation of *hsbA* overexpressed and deletion mutants when compared to the MS12 parental strain.

4.8 Phagocytosis assay

Survival of fungal pathogen in host system is the most important factor for the progression of invasive fungal infection (**Missall et al., 2004**). Mucorales encounters cells of the innate immune system including macrophages, neutrophils and dendritic cells following the invasion of the host (**Ghuman and Voelz., 2017**). Phagocytic cells are known to be key players in controlling infections caused by Mucorales (**Chayakul et al., 2006 and Ibrahim et al., 2012**).

Interaction between MS12+*pyrG* and the mutant strains with J774.2 murine macrophages were carried out and examined (**Figure 26**). There was no significant difference in the phagocytosis of macrophages between overexpressed and deletion mutants when compared to MS12+*pyrG*. Hence suggesting that HsbAs play no role in the recognition and phagocytosis of *M. circinelloides* by J774.2 macrophages.

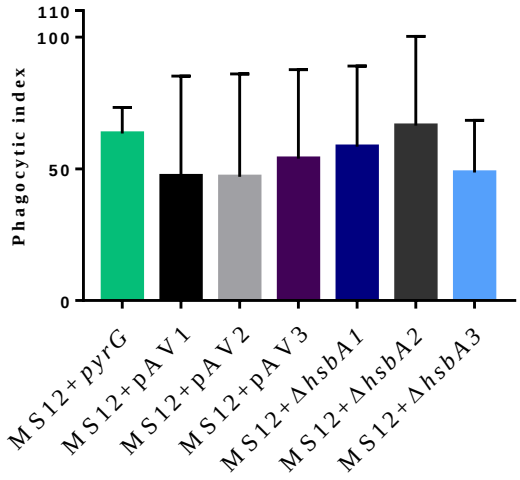

Figure 26: Phagocytosis index of overexpressed and deletion mutants with the MS12+*pyrG* strain. Values are averages from three independent experiments and 3 biological replicates (error bars indicate standard deviation). Values of mutants were compared with the value of the MS12+*pyrG* strain and significance was calculated by the one-way ANOVA.

4.8 Virulence of the *hsbA* mutants in *Galleria mellonella* non-vertebrate model

To investigate the role of HsbA proteins in pathogenicity of *M. circinelloides*, we used wax moth larvae (*G. mellonella*) as a non-vertebrate animal model. Larvae were infected with different *hsbA* mutant strains and larval survival was examined for six days. In the untreated and IPS-treated control groups, none of the larvae died by the end of the experiment. **Figure 27** shows the survival

of larvae infected with different *hsbA* mutant strains and the control strain (MS12+*pyrG*). Where, overexpression of *hsbA2* resulted significantly decreased virulence of the mutant strain, while the virulence of MS12+*ΔhsbA1*, MS12+*ΔhsbA2* and MS12+*ΔhsbA3* mutants significantly increased.

The main limitation of the use of invertebrate hosts is whether the results obtained in these models can be adapted to mammals and to the human body. However, the lack of an adaptive immune system and specific organs, such as the lung, can affect pathogenesis, so in order to get a more accurate picture of the role of mutant strains in pathogenicity, it is appropriate to study them in a vertebrate model. Although, the wax moth is a widely used non-vertebrate model organism to examine the pathogenicity of different filamentous fungi such as Mucoromycotina species (**Li et al., 2011; Xu et al., 2017; Maurer et al., 2019; Vellanki et al., 2020**).

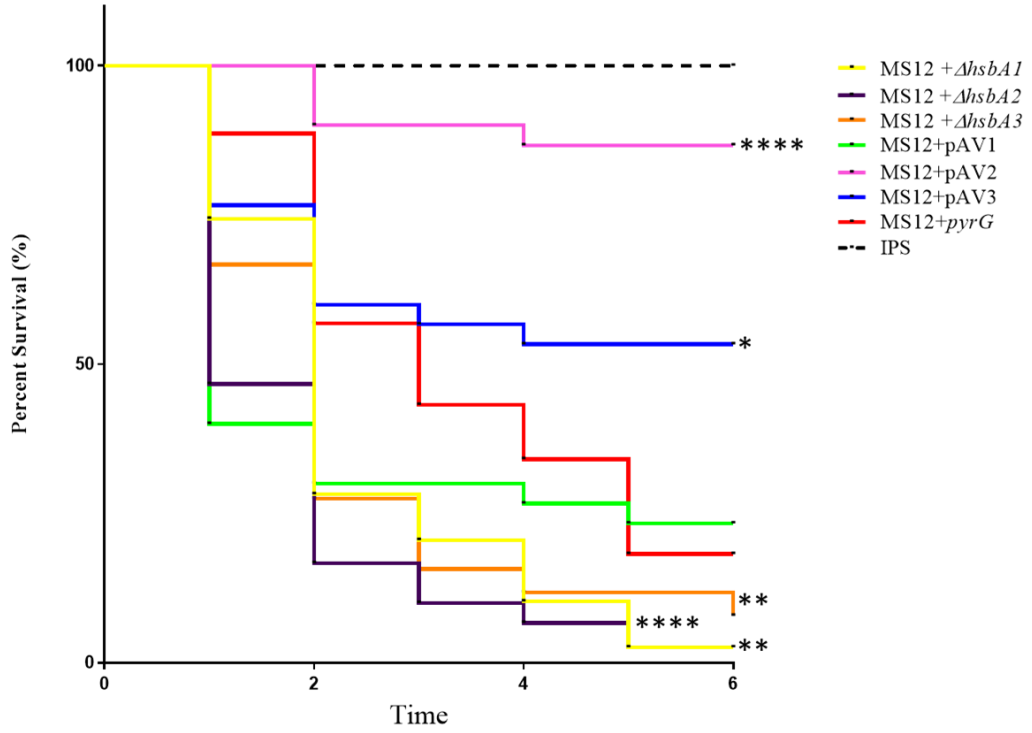

Figure 27: Survival of *G. mellonella* larvae infected with the *hsbA* mutant and the control *M. circinelloides* strains. The control strain was MS12+pyrG. Virulence of MS12+pAV1 strain decreased compared to the MS12+*pyrG* strain, while the deletion of *hsbA1*, *hsbA2* or *hsb3* resulted increased virulence. Survival curve followed by astriks were significantly differed from the control strain according to the Log-rank (Mantel-Cox) test (*$p < 0.05$, **$p < 0.01$, ***$p < 0.001$, ****$p < 0.0001$)

4.9 Heterologous expression of *M. circinelloides* HsbA1 in *P. pastoris* KM71H

Two pPICZαA+*hsbA1* and one pPICZαA+*hsbA2 Pichia* transformants were obtained. These transformants were used for expression of HsbA1 and HsbA2 in BMMH culture media, in a period of 1-7 days at 30 °C to verify the expression of HsbA1 and HsbA2 proteins. Protein of the desired size (i.e. approximately 17 kDa) was shown to be expressed on day 7 in the culture of pPICZαA+*hsbA1* positive clones at 30 °C (**Figure 28**), whereas there was not traceable expression of proteins in the culture supernatant of *Pichia* transformant harbouring the pPICZαA+*hsbA2*. Hence, we carried out large scale protein expression and purification for the pPICZαA+*hsbA1*_1 transformant. Elute 39 after size exclusion chromatography was shown to contain proteins at approximately 17 kDa (**Figure 28**). The presence of recombinant HsbA1 protein of 17.9 kDa was confirmed through mass spectrometric analysis (**Figure 29**). Hence, the purified HsbA protein obtained can be used in further studies and for example for production of monoclonal antibodies.

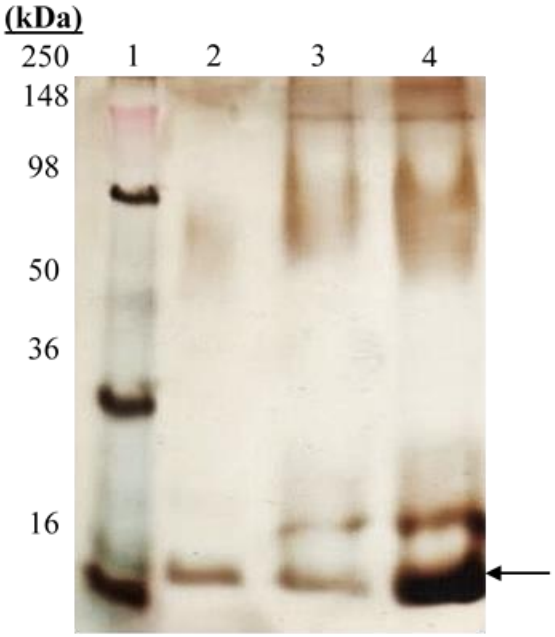

Figure 28: Silver stained 12 % SDS-PAGE gel containing protein fractions from day 7 culture supernatant of HsbA1 positive *P. pastoris* KM71H transformants. Lane 1: Protein size marker (SeeBlue Plus2); lane 2: Elute 39 after size exclusion chromatography; lane 3: 7th day culture supernatant of pPICZαA +*hsbA1*_1; lane 4: 7th day culture supernatant of pPICZαA+*hsbA1*_2.

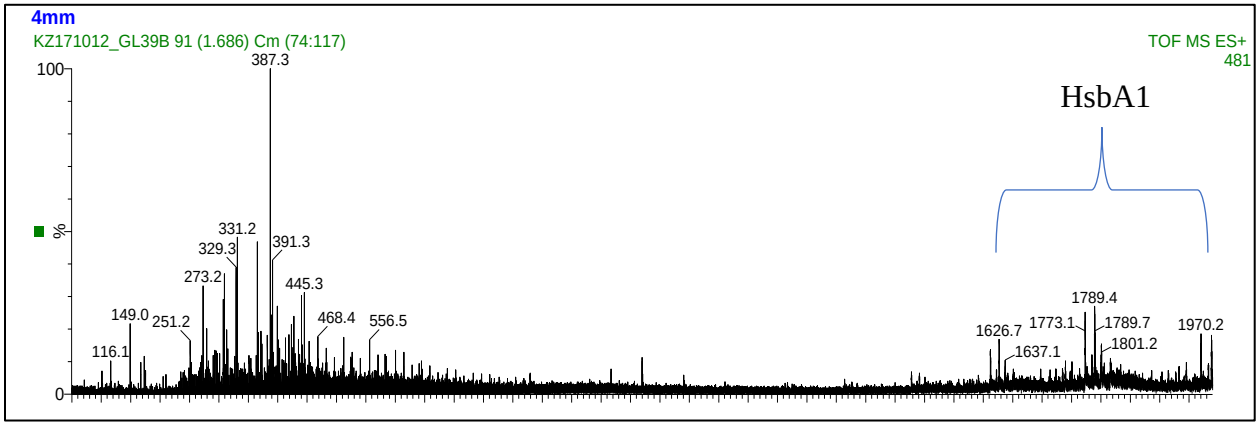

Figure 29: Mass spectrometric analysis of the heterologously expressed HsbA1 protein in *P. pastoris* KM71H.

5. CONCLUSION

Hydrophobic surface binding protein A (HsbA) are small galactomannoproteins of fungi **(Muszewska et al., 2017)** that could either be bound to the cell wall or secreted to outside the cell. It is suggested that these proteins may have role in the adhesion to hydrophobic surfaces, in recruiting cutinases and hydrolytic enzymes on hydrophobic surfaces and colonization and penetration into the plant tissues; *hsbA* genes were found to be upregulated in human pathogen fungi during the infection (**Ohtaki et al., 2006; Delmas et al., 2012; Soanes et al., 2012; Park, 2016; Wang et al., 2017and Zang et al., 2018**). The aim of the present study was to characterize the hsbA genes of the Mucoralean model organism *M. circinelloides*.

Six *hsbA* genes were found in the *M. circinelloides* genome named as *hsbA1a*, *hsbA1b*, *hsbA2*, *hsbA3*, *hsbA4* and *hsbA5*. In case of *hsbA1a* and *hsbA1b*, the coding regions were identical, and the two genes are located close together in the genome suggesting that they can be the result of a recent duplication even. Transcription activity could not be detected for *hsbA1b*, even if *hsbA1a* was disrupted, which suggest that this gene may be not functioning. Sequence analysis predicted HsbA1a, HsbA1b and HsbA2 as GPI-anchored proteins suggesting their incorporation into the cell wall while HsbA3, HsbA4 and HsbA5 seem to be secreted proteins.

qRT-PCR analysis indicated that the tested *hsbA* genes (i.e. *hsbA1a*, *hsbA2*, *hsbA3* and *hsbA4*) are expressed throughout the whole life cycle and especially from the second day of cultivation, i.e. in the late hyphal stage. All four genes responded to the changes in the cultivation temperature: they displayed elevated transcription levels at higher temperatures. All four genes were downregulated by anaerobiosis (especially *hsbA1a* and *hsbA2*, which were inactive under anaerobic growth) indicating that they are linked to the aerobic and/or hyphal growth. Presence of human serum upregulated *hsbA1a*, *hsbA2* and *hsbA4* but did not affect *hsbA3* suggesting different roles in the adaptation for environmental changes. Presence of lignocellulosic material in the cultures induced only the transcription of *hsbA3* suggesting that this gene may participate in the degradation of plant material.

For a more detailed characterization, three *hsbA* genes, i.e. *hsbA1a*, *hsbA2* and *hsbA3* were disrupted by integrating the *pyrG* selection marker into the corresponding gene using the CRISPR-Cas9 method. Molecular analysis of the transformants proved that mutations occurred in the targeted sites and no *off-target* effect was induced. qRT-PCR analysis proved the lack of transcription of the disrupted genes. Additionally, the three genes were overexpressed by using

plasmids and promoters assuring strong expression. qRT-PCR proved the elevated transcript levels in the overexpressed strains.

Disruption and overexpression of the three *hsbA* genes had only a slight effect on the growing ability of the fungus.

In case of *hsbA1a* and *hsbA3*, alterations in the gene expression did not affect the spore producing ability. However, overexpression of *hsbA2* led an increased sporulation indicating that function of this gene has a role in the sporangiospore production.

Interestingly, overexpression of all three genes decreased the germination ability of the sporangiospores while gene disruption did not affect this feature. This finding suggests that alteration in the amount of the encoded proteins influence the viability of the spores maybe because of the altered hydrophobicity of the cell surface. Overexpression mutants also displayed increased sensitivity to cell wall and membrane stressors suggesting structural alterations in the outer layers of the fungal cells. These findings correlated with those of the hydrophobicity tests where the mycelial surface of the overexpression mutants proved to be more hydrophobic than those of the disruption mutants and the control strain. All these results strongly suggest that HsbA molecules have role in the regulation of the hydrophobicity of the cellular surfaces in *M. circinelloides*.

It is known that hydrophobins participate in the biofilm formation of filamentous fungi (**Brown et al., 2016**). In our tests, we found that biofilm forming capacity of the mutants, in which the *hsbA* genes were disrupted somewhat decreased indicating that HsbA may contribute to the biofilm formation of *M. circinelloides.* SEM image analysis of overexpressed and deletion mutants further revealed that surfaces of MS12+pAV1 small spores were more granulated, when compared to the parental MS12 strain. Whereas large spores of all deletion mutants were slightly granulated or smooth surface when compared to parental strains, hence suggesting the involvement of HsbA in the cell surface integrity of small and large spores. Although the exact mechanism behind the cause of this variations are yet to be determined.

Disruption and overexpression of the three *hsbA* genes had no effect on the phagocytosis of *M. circinelloides* by J774.2 cells.

In *Galleria* non-vertebrate model, overexpression of *hsbA2* resulted in significantly decreased virulence while that of all deletion mutants significantly increased. This result may suggest that the HsbA level and/or the hydrophobicity of the mycelium may affect the pathogenicity of *M. circinelloides*.

For future analysis of the proteins and their functions recombinant HsbA1 was expressed in a *Pichia pastoris* heterologous expression system and the produced protein was purified.

In conclusion, the results of the present study suggest that HsbA proteins are hydrophobic surface-active proteins that are differentially expressed during the aerobic growth of *M. circinelloides*. In *M. circinelloides*, HsbAs have ability to influence the cell wall integrity of spores and hyphae, sporulation and germination capacity of the spores, hydrophobicity of the hyphal surfaces, biofilm formation and virulence.

6. ÖSSZEFOGLALÓ

A hidrofób felszínt kötő fehérjék (HsbA) gombák által termelt kisméretű galaktomannoproteinek **(Muszewska és mtsi., 2017)**, melyek vagy a sejtfalhoz kapcsolódnak, vagy a külső térbe szekretálódnak. A fehérjecsalád egyes tagjairól feltételezik, hogy szerepük van degradatív enzimek szilárd, hidrofób felületeken történő toborzásában és a növénypatogén gombák esetében a növényi szövetekbe történő penetrációban; humánpatogének esetében pedig a fertőzés során a *hsbA* gének felülszabályozását figyelték meg (**Ohtaki és mtsi., 2006; Delmas és mtsi., 2012; Soanes és mtsi., 2012; Park, 2016; Wang és mtsi., 2017 és Zang és mtsi., 2018**).

Jelen kutatás célja a Mucorales rendbe tartozó modellorganizmus, a *Mucor circinelloides hsbA* génjeinek azonosítása és jellemzése volt.

A *M. circinelloides* genomban hat *hsbA* gént azonosítottunk, melyeket a következőképpen neveztük el: *hsbA1a, hsbA1b, hsbA2, hsbA3, hsbA4* és *hsbA5*. A *hsbA1a* és a *hsbA1b* gén kódoló szekvenciája teljesen megegyezőnek bizonyult, noha határoló szakaszaik, így promóter és terminális régióik különbözőek voltak. A két gén a genomban egymás után, közel helyezkedik el, feltehetően egy nem túl régi duplikációs eseménynek köszönhetően. Ha a *hsbA1a* gént elrontottuk, a mutánsban nem tapasztaltunk HsbA1 transzkriptumot, ami arra utal, hogy a *hsbA1b* gén, legalábbis a vizsgált körülmények közt, nem expresszálódik, azaz feltehetően egy pszeudogénről van szó. A szekvenciák *in silico* elemzése arra enged következtetni, hogy a HsbA1a, HsbA1b és HsbA2 fehérjék glükozil-foszfatidil-inozitol (GPI) horgonyon keresztül a sejtfalhoz kapcsolódnak, míg a HsbA3, HsbA4 és HsbA5 fehérjék a külső térbe választódnak ki.

Kvantitatív valós idejű PCR (qRT-PCR) technikával kivitelezett transzkripció elemzéseket végeztünk négy génnel (*hsbA1a*, *hsbA2*, *hsbA3* és *hsbA4*). Megállapítottuk, hogy mind a négy gén a gomba teljes életciklusa során átíródik, de különösen a késői tenyésztési szakaszban (azaz legnagyobb mértékben a hifákban). Ugyancsak mind a négy génre jellemző volt, hogy magasabb hőmérsékleten erősebben, anaerob tenyésztés során gyengébben fejeződtek ki, mint alacsonyabb hőmérsékleten, illetve aerob viszonyok közt. A *hsbA1a* és a *hsbA2* gén csak aerob körülmények közt fejeződött ki. Mindez azt mutatja, hogy a gének átíródása az oxigén és/vagy a hifa morfológia jelenlétéhez kötődik. A humán szérum jelenléte fokozta a *hsbA1a, hsbA2* és *hsbA4* átíródását, de nem volt hatással a *hsbA3* génre, azt sugallva, hogy a gének eltérő szabályozás alatt állnak és eltérő a szerepük a környezeti változásokhoz történő alkalmazkodásban. Ugyanakkor növényi lignocellulóz anyag jelenléte indukálta a *hsbA3* transzkripcióját, ami arra utalhat, hogy ennek a

génnek más gombák *hsbA* génjéhez hasonlóan szerepe lehet a növényi anyag degradációjának elősegítésében.

A részletesebb funkcionális elemzések érdekében, három *hsbA* gén (*hsbA1a*, *hsbA2* és *hsbA3*) esetében olyan mutánsokat állítottunk elő, amelyekben a géneket vagy elrontottuk, vagy túlműködtettük. A gének elrontását a CRISPR-Cas9 technika alkalmazásával hajtottuk végre: a *pyrG* uracil auxotrófiát komplementáló szelekciós marker gént homológ rekombinációval a célgénbe integráltuk, ezzel elrontva azt. A transzformánsok molekuláris elemzése (PCR, szekvenálás, teljes genom szekvenálás) azt mutatták, hogy a mutációk a célzott helyen történtek és a génszerkesztés nem okozott *off-target* hatást. A mutánsok qRT-PCR elemzésével igazoltuk, hogy az elrontott génekről nem íródik át mRNS. Emellett olyan plazmidokat is építettünk, melyekkel, azokat expressziós vektorként a gombába juttatva, a gének túlműködtetése megvalósítható volt. A qRT-PCR elemzés a gének fokozott átíródását mutatta az így létrehozott mutánsokban.

Ezután a diszrupciós és a túlműködtetett mutánsokkal fiziológiai és patogenitási teszteket végeztünk. Sem a gének elrontásának, sem a túlműködtetésének nem volt lényeges hatása a növekedésre. A *hsbA1a* és a *hsbA3* esetében a mutánsok spóraképző képessége sem változott. Ugyanakkor a *hsbA2* túlműködtetése a sporangiospórák képződésének szignifikáns fokozódásával járt, azt jelezve, hogy e génnek szerepe lehet a sporuláció során.

Érdekes módon mindhárom gén túlműködtetése csökkentette a spórák csírázási képességét, míg a gének elrontásának nem volt ilyen hatása. A későbbi vizsgálatok tükrében azt feltételezzük, hogy a gének túlműködtetése talán a spórafelszín hidrofobicitásának megváltozása miatt hatott a spórák életképességére negatívan. A gének túlműködtetése a gombákat sejtfal és membrán stresszt okozó szerekre is érzékennyé tette, ami a sejtfal és a sejt külső rétegei szerkezetének megváltozására utal. Ezek az eredmények korreláltak a mutánsokkal végzett hidrofobicitási tesztek eredményeivel, melyek azt mutatták, hogy a túlműködtetett mutánsok felszínének hidrofobicitása magasabb volt az eredeti, vad típusú törzsénél és a géndiszrupciós mutánsokénál. Mindez azt sugallja, hogy a HsbA fehérjék részt vesznek a sejtfelszín hidrofobicitásának kialakításában *M. circinelloides*-ben.

Ismert, hogy a hidrofobinok részt vesznek a fonalas gombák által kialakított biofilmek képzésében (**Brown és mtsi., 2016**). Vizsgálatainkban azt tapasztaltuk, hogy azon mutánsok

biofilmképző képessége, amelyekben a *hsbA* géneket elrontottuk, szignifikánsan csökkent, ami a HsbA fehérjék biofilmképzésben játszott szerepére utalhat.

A hsbA gének elrontása és túlműködtetése nem volt hatással a mutánsok J774.2 egér makrofág sejtek általi fagocitózisára az interakciós tesztek során.

Galleria mellonella alternatív, gerinctelen patogenitási modellben, a hsbA2 gén túlműködtetése szignifikáns mértékben csökkentette a gomba virulenciáját, ugyanakkor mindhárom gén elrontása fokozta azt. Mindez azt jelzi, hogy a HsbA fehérjék jelenléte és/vagy a felszín hidrofobicitása hatással van a *M. circinelloides* patogenitására.

Végezetül a további funkcionális vizsgálatok érdekében a HsbA1 fehérje heterológ expresszióját valósítottuk meg *Pichia pastoris* expressziós rendszerben. A termelt fehérjét kitisztítottuk és megkezdtük az elemzését.

Összefoglalva a fentieket, jelen kutatás eredményei alapján azt mondhatjuk, hogy a HsbA fehérjék a *M. circinelloides* aerob növekedése során, eltérő módon expresszálódnak. A fehérjéknek szerepe lehet a spóraképzésben, a spórák csírázó képességében, a gomba felszín hidrofobicitásának szabályozásában, a biofilm képzésben és a patogenitásban.

7. AKNOWLEDGEMENT

Primarily, my sincere thanks to God Almighty for all the blessing bestowed on me and for giving me the strength and guidance to successfully my complete thesis.

I would like to thank the head of the department, Prof. Dr. Csaba Vágvölgyi for giving me the opportunity to carry out my PhD research and studies in the Department of Microbiology at the Doctoral school of biology.

I would like to express my sincere gratitude to my supervisors, Dr. Tamas Papp and Dr. Gabor Nagy, for their constant guidance and support during my PhD research and in dissertation completion.

I would like to thank Csilla Szebenyi, Dr. Miklós Takó, Dr. Zoltán Kele, Dr. László Galgóczi, Dr. Ildikó Nyilasi, Dr. Mónika Homa, Dr. Csaba Papp, Dr. Tibor Mihály Németh, Dr. Eszter Bokor and Tamás Petkovits, who helped me with their valuable time.

My sincere thanks to my colleagues, Tünde Kartali, Olivér Jáger and Rakesh Varghese and my best friend Sandugash Ibragimova for providing a fun and favourable environment to work with.

My love and thanks to my soulmate and loving husband Surya Henry, my personal mentor, whose love, and support played a major role in my PhD life. They helped me in many ways to complete my research and dissertation.

I would like to thank my mother Maria D'silva and my father Leo Vaz, who have helped me with their constant prayers and blessings and most of all with their valuable guidance and support, that has been very helpful in various phases throughout my PhD journey. I would like to my brother Savio Vaz and his wife Cassandra Almeida, my sister Luella Vaz, who were always there for me.

My humble thanks to my grandmother Helen D'silva, who has always given me true value of life and has always been my strength, she has helped me with her prayers towards my success.

My sincere thanks to my mother in law Dr. Sarumathy Masilamani and my father in law Henry Periyananyagam, who were always there to encourage and support me with their constant prayers and blessings. I would like to thank my brother in-law, his wife, and my God child, for their support and best wishes.

I would like to thank jointly The University Grant Commission New Delhi India, and Stipendium Hungaricum Tempus Public Foundation Hungary, for awarding me the Doctoral research fellowship.

I would like to dedicate my PhD thesis to my beloved father late ***Leo Vaz***
who has always been my inspiration towards my work.
With love

This study was carried out with the support of the "Lendület" Grant of the Hungarian Academy of Sciences (LP2016-8/2016), the NKFI project K131796 and the project GINOP-2.3.2-15-2016-00035.

8. REFERENCES

Alcazar-Fuoli, L., Clavaud, C., Lamarre, C., Aimanianda, V., Seidl-Seiboth, V., Mellado, E., Latgé, J.-P. (2011). Functional analysis of the fungal/plant class chitinase family in *Aspergillus fumigatus*. Fungal Genet Biol 48, 418-429.

Arana, D.M., Prieto, D., Román, E., Nombela, C., Monge, R.A., Pla, J. (2009). The role of the cell wall in fungal pathogenesis. Microbiol Biotechnol 2, 308-320.

Bayry, J., Aimanianda, V., Guijarro, J.I., Sunde, M., Latgé, J.-P. (2012). Hydrophobins-unique fungal proteins. Plos Pathog 8, E1002700

Beauvais, A., Bozza, S., Kniemeyer, O., Formosa, C., Balloy, V., Henry, C., Roberson, R. W., Dague, E., Chignard, M., Brakhage, A. A., Romani, L., Latgé, J. P. (2013). Deletion of the α-(1,3)-glucan synthase genes induces a restructuring of the conidial cell wall responsible for the avirulence of *Aspergillus fumigatus*. PLoS Pathog 9, e1003716.

Berger, B.W., Sallada, N.D. (2019). Hydrophobins: multifunctional biosurfactants for interface engineering. J Biol Eng 13, 10.

Bitar, D., Van Cauteren, D., Lanternier, F., Dannaoui, E., Che, D., Dromer, F., Desenclos, J. C., Lortholary, O. (2009). Increasing incidence of zygomycosis (mucormycosis), France, 1997-2006. Emerg Infect Dis 15, 1395-1401.

Blankenship, J.R., Mitchell, A.P. (2006). How to build a biofilm: a fungal perspective. Curr Opin Microbiol 9, 588-594.

Boyce, K.J., Andrianopoulos, A. (2011). Ste20-related kinases: effectors of signaling and morphogenesis in fungi. Trends Microbiol 19, 400-410.

Butler, Y.X., Abhayawardhane, Y., Stewart, G.C. (1993). Amplification of the *Bacillus subtilis* maf gene results in arrested septum formation. J Bacteriol 175, 3139-3145.

Campos-Takaki, G. M., Dietrich, S. M. C., Beakes, G. W. (2014). Cytochemistry, ultrastructure and x-ray microanalysis methods applied to cell wall characterization of mucoralean fungi strains in microscopy: advances in scientific research and education. Ed. Mendez-Vilas A. (Formatex), 121-127.

Cao, L., Chan, C., Lee, C., Sai-Yin Wong, S., Yuen, K. (1998). *Mp1* encodes an abundant and highly antigenic cell wall mannoprotein in the pathogenic fungus *Penicillium marneffei*. Infect Immun 66, 966-973.

Cao, L., Chan, K.M., Chen, D., Vanittanakom, N., Lee, C., Chan, C.M., Sirisanthana, T., Tsang, D.N., Yuen, K.Y. (1999). Detection of cell wall mannoprotein mp1p in culture supernatants of *Penicillium marneffei* and in sera of penicilliosis patients. J Clin Microbiol 37, 981-986.

Carvalho, A.F.A., Boscolo, M., da Silva, R., Ferreira, H., Gomes, E. (2010). Purification and characterization of the α-glucosidase produced by thermophilic fungus *Thermoascus aurantiacus* CBMAI 756. J Microbiol 48, 452-459.

Cervantes, M., Vila, A., Nicolás, F.E., Moxon, S., Haro, J.P. De, Dalmay, T., Torres-Martínez, S., Ruiz-Vázquez, R.M. (2013). A single argonaute gene participates in exogenous and endogenous rnai and controls cellular functions in the basal fungus *Mucor circinelloides*. Plos One 8, e69283.

Chakrabarti, A., Chatterjee, S. S., Das, A., Panda, N., Shivaprakash, M. R., Kaur, A., Varma, S. C., Singhi, S., Bhansali, A., Sakhuja, V. (2009). Invasive zygomycosis in India: experience in a tertiary care hospital. Postgrad Med J 85, 573-581.

Chakrabarti, A., Dhaliwal, M. (2013). Epidemiology of Mucormycosis in India. Curr Fungal Infect Rep 7, 287-292.

Chamilos, G., Ganguly, D., Lande, R., Gregorio, J., Meller, S., Goldman, W.E., Gilliet, M., Kontoyiannis, D.P. (2010). Generation of il-23 producing dendritic cells (dcs) by airborne fungi regulates fungal pathogenicity via the induction of th-17 responses. Plos One 5, e12955

Chau, H.W., Goh, Y.K., Si, B.C., Vujanovic, V. (2010). Assessment of alcohol percentage test for fungal surface hydrophobicity measurement. Lett App Microbiol 50, 295-300.

Chayakulkeeree, M., Ghannoum, M.A., Perfect, J.R. (2006). Zygomycosis: the re-emerging fungal infection. Eur J Clin Microbiol Infect Dis 25, 215-229.

Cheng, V.C., Chan, J.F., Ngan, A.H., To, K.K., Leung, S.Y., Tsoi, H.W., Yam, W.C., Tai, J.W., Wong, S.S., Tse, H., Li, I.W., Lau, S.K., Woo, P.C., Leung, A.Y., Lie, A.K., Liang, R.H., Que, T.L., Ho, P.L., Yuen, K.Y. (2009). Outbreak of intestinal infection due to *Rhizopus microsporus*. J Clin Microbiol 47, 2834-2843.

Corrochano, L.M., Kuo, A., Marcet-Houben, M., Polaino, S., Salamov, A., Villalobos-Escobedo, J.M., Grimwood, J., Álvarez, M.I., Avalos, J., Bauer, D., et al. (2016). Expansion of signal transduction pathways in fungi by extensive genome duplication. Curr Biol 26, 1577-1584.

Costachel, C., Coddeville, B., Latgé, J.-P., Fontaine, T. (2005). Glycosylphosphatidylinositol-anchored fungal polysaccharide in *Aspergillus fumigatus*. J Biol Chem 280, 39835-39842.

Costa-Orlandi, C.B., Sardi, J.C.O., Pitangui, N.S., De Oliveira, H.C., Scorzoni, L., Galeane, M.C., Medina-Alarcón, K.P., Melo, W.C.M.A., Marcelino, M.Y., Braz, J.D., et Al. (2017). Fungal biofilms and polymicrobial diseases. J Fungi 3, 22.

Crockford, H., Topalidis, S., Richardson, D.P. (1991). Water repellency in a dry sclerophyll eucalypt forest - measurements and processes. Hydrol Proc 5, 405-420.

Csernetics, Á., Nagy, G., Iturriaga, E.A., Szekeres, A., Eslava, A.P., Vágvölgyi, C., Papp, T. (2011). Expression of three isoprenoid biosynthesis genes and their effects on the carotenoid production of the zygomycete *mucor circinelloides*. Fungal Genet Biol 48, 696-703.

Delmas. S., Pullan, S.T., Gaddipati, S., Kokolski, M., Malla, S., et al. (2012). Uncovering the genome-wide transcriptional responses of the filamentous fungus *Aspergillus niger* to lignocellulose using RNA sequencing. Plos Genet 8, e1002875.

de Melo, E.G., Carvalho, A.I. (2006). α- and β-Glucosidase Inhibitors: Chemical Structure and Biological Activity. Tetrahedron 62, 10277-10302.

de Ruiter, G.A., van der Lugt A., Voragen A., Rombouts F., Notermans S. (1991). High-performance size-exclusion chromatography and ELISA detection of extracellular polysaccharides from Mucorales. Carbohydr Res 215, 47-57.

de Ruiter G. A., Josso S., Colquhoun I., Voragen A., Rombouts F. (1992). Isolation and characterization of β (1-4)-D-glucuronans from extracellular polysaccharides of moulds belonging to Mucorales. Carbohydr Polym 18, 1-7.

Dong, Y., Li, H., Zhao, L., Koopman, P., Zhang, F., Huang, J. X. (2019). Genome-Wide Off-Target Analysis in CRISPR-Cas9 Modified Mice and Their Offspring. G3 (Bethesda) 9, 3645-3651.

Erwig, L.P., Gow, N.A.R. (2016). Interactions of fungal pathogens with phagocytes. Nature Rev Microbiol 14, 163-176.

Etherington, G.J., Ramirez-Gonzalez, R.H., Maclean, D. (2015). Bio-samtools 2: a package for analysis and visualization of sequence and alignment data with samtools in ruby. Bioinformatics 31, 2565-2567.

Fesel, P.H., Zuccaro, A. (2016). B-glucan: crucial component of the fungal cell wall and elusive mamp in plants. Fungal Genet Biol 90, 53-60.

Fankhauser, N., & Mäser, P. (2005). Identification of GPI anchor attachment signals by a Kohonen self-organizing map. Bioinformatics (Oxford, England), 21(9), 1846–1852. https://doi.org/10.1093/bioinformatics/bti299.

Fujikawa, T., Sakaguchi, A., Nishizawa, Y., Kouzai, Y., Minami, E., Yano, S., Koga, H., Meshi, T., Nishimura, M. (2012). Surface α-1,3-glucan facilitates fungal stealth infection by interfering with innate immunity in plants. PLoS Pathog 8, e1002882.

Garcia, A., Adedoyin, G., Heitman, J., Lee, S. C. (2017). Construction of a Recyclable Genetic Marker and Serial Gene Deletions in the Human Pathogenic Mucorales *Mucor circinelloides*. G3 (Bethesda) 7, 2047-2054.

Garcia, A., Vellanki, S., Lee, S.C. (2018). Genetic tools for investigating Mucorales fungal pathogenesis. Curr Clin Microbiol Rep 5, 173-180.

Garre, V., Nicolás, F.E., Torres-Martínez, S., Ruiz-Vázquez, R.M. (2014). The RNAi machinery in Mucorales: the emerging role of endogenous small RNAs. In fungal RNA biology, A. Sesma, and T. von der Haar, Eds. (Cham: Springer International Publishing), pp. 291-313.

Gasteiger, E., Hoogland, C., Gattiker, A., Duvaud, S., Wilkins, M.R., Appel, R.D., Bairoch, A. (2005). Protein identification and analysis tools on the expasy server. In the proteomics protocols handbook, J.M. Walker, Ed. (Totowa, NJ: Humana Press), pp. 571–607.

Gebremariam, T., Liu, M., Luo, G., Bruno, V., Phan, Q.T. et al. (2014). Coth3 mediates fungal invasion of host cells during mucormycosis. J Clin Invest 124, 237-250.

Ghuman, H., Voelz, K. (2017). Innate and adaptive immunity to Mucorales. J Fungi 3, 48.

Goldstein, E.J.C., Spellberg, B., Walsh, T.J., Kontoyiannis, D.P., Edwards, J., Ibrahim, A.S. (2009). Recent advances in the management of mucormycosis: from bench to bedside. Clin Infect Dis 48, 1743-1751.

Gomes, E.V., Bortolossi, J.C., Sanches, P.R., Mendes, N.S., Martinez-Rossi, N.M., Rossi, A. (2018). Ste20/paka protein kinase gene releases an autoinhibitory domain through pre-mRNA alternative splicing in the dermatophyte *Trichophyton rubrum*. Int J Mol Sci 19, 3654.

Gomes, M.Z.R., Lewis, R.E., Kontoyiannis, D.P. (2011). Mucormycosis Caused By Unusual Mucormycetes, Non-*Rhizopus*, -*Mucor*, and -*Lichtheimia* Species. Clin Microbiol Rev 24, 411.

Gonzales, C.E., Rinaldi, M.G., Sugar, A.M. (2002). Zygomycosis. Infect Dis Clin North Am 16, 895-914.

Goodridge, H.S., Wolf, A.J., Underhill, D.M. (2009). B-glucan recognition by the innate immune system. Immunol Rev 230, 38-50.

Gow, N., Latge, J. P., Munro, C.A. (2017). The Fungal Cell Wall: Structure, Biosynthesis, and Function. Microbiol Spectr 5, https://doi.org/10.1128/microbiolspec.

Hall-Stoodley, L., Costerton, J.W., Stoodley, P. (2004). Bacterial biofilms: from the natural environment to infectious diseases. Nat Rev Microbiol 2, 95-108.

Hamid, R., Khan, M.A., Ahmad, M., Ahmad, M.M., Abdin, M.Z., Musarrat, J., Javed, S. (2013). Chitinases: an update. J Pharm Bioallied Sci 5, 21.

Harding, M.W., Marques, L.L.R., Howard, R.J., Olson, M.E. (2009). Can filamentous fungi form biofilms? Trends Microbiol 17, 475-480.

Hazen, K.C., Lay, J.G., Hazen, B.W., Fu, R.C., Murthy, S. (1990). Partial biochemical characterization of cell surface hydrophobicity and hydrophilicity of *Candida albicans*. Infect Immun 58, 3469-3476.

Hoffmann, K., Discher, S., Voigt, K. (2007). Revision of the genus *Absidia* (Mucorales, Zygomycetes) based on physiological, phylogenetic, and morphological characters; thermotolerant *Absidia* spp. form a coherent group, Mycocladiaceae fam. nov. Mycol Res 111, 1169-1183.

Hopke, A., Brown, A.J., Hall, R.A., Wheeler, R.T (2018). Dynamic fungal cell wall architecture in stress adaptation and immune evasion. Trends Microbiol 26, 284-295.

Ibrahim, A., Spellberg, B., Walsh, T.J., Kontoyiannis, D.P. (2012). Pathogenesis of mucormycosis. Clin Infect Dis 54 (S1), S16-S22.

Ibrahim, A.S., Gebermariam, T., Fu, Y., Lin, L., Husseiny, M.I., French, S.W., Schwartz, J., Skory, C.D., Edwards, J.E., Spellberg, B.J. (2007). The iron chelator deferasirox protects mice from mucormycosis through iron starvation. J Clin Invest 117, 2649-2657.

Ibrahim, A.S., Gebremariam, T., Schwartz, J.A., Edwards, J.E., Spellberg, B. (2009). Posaconazole mono- or combination therapy for the treatment of murine zygomycosis. Antimicrob Agents Chemother 53, 772-775.

Ibrahim, A. S., Gebremariam, T., Lin, L., Luo, G., Husseiny, M. I., Skory, C. D., Fu, Y., French, S. W., Edwards, J. E., Jr, Spellberg, B. (2010). The high affinity iron permease is a key virulence factor required for *Rhizopus oryzae* pathogenesis. Mol Microbiol 77, 587-604.

Katragkou, A., Walsh, T.J., Roilides, E. (2014). Why is mucormycosis more difficult to cure than more common mycoses? Clin Microbiol Inf 20, 74-81.

Kaur, J., Sharma, A., Sharma, M., Manhas, R. K., Kaur, S. Kaur, A. (2019). Effect of α-glycosidase inhibitors from endophytic fungus *Alternaria destruens* on survival and development of insect pest *Spodoptera litura* Fab. and fungal phytopathogens. Sci Rep 9, 11400.

Kennedy, M.J. (1990). Models for studying the role of fungal attachment in colonization and pathogenesis. Mycopathology 109, 123-137.

Kinoshita, T. (2016). Glycosylphosphatidylinositol (GPI) anchors: biochemistry and cell biology: introduction to a thematic review series. J Lipid Res 57, 4-5.

Kontoyiannis, D.P., Lewis, R.E. (2006). Invasive zygomycosis: update on pathogenesis, clinical manifestations, and management - infectious disease clinics. Infect Dis Clin North Am 20, 581-607.

Krasowska, A., Sigler, K. (2014). How microorganisms use hydrophobicity and what does this mean for human needs? Front Cell Infect Microbiol 4, 112.

Kyte, J., and Doolittle, R.F. (1982). A simple method for displaying the hydropathic character of a protein. J Mol Biol 157, 105-132.

Latgé, J-P. (2010). Tasting the fungal cell wall. Cell Microbiol 12, 863-872.

Latgé, J-P., Calderone, R. (2002). Host-microbe interactions: fungi invasive human fungal opportunistic infections. Curr Opin Microbiol 5, 355-358.

Lax, C., Pérez-Arques, C., Navarro-Mendoza, M.I., Cánovas-Márquez, J.T., Tahiri, G., Pérez-Ruiz, J.A., Osorio-Concepción, M., Murcia-Flores, L., Navarro, E., Garre, V., et al. (2020). Genes, pathways, and mechanisms involved in the virulence of Mucorales. Genes 11, 317.

Lecointe, K., Cornu, M., Leroy, J., Coulon, P., Sendid, B. (2019). Polysaccharides cell wall architecture of Mucorales. Front Microbiol 10, 469.

Lee, S.C., Heitman, J. (2014). Sex in the Mucoralean fungi. Mycoses 57, 18-24.

Lee, S.C., Li, A., Calo, S., Heitman, J. (2013). Calcineurin plays key roles in the dimorphic transition and virulence of the human pathogenic zygomycete *Mucor circinelloides*. Plos Pathog 9, e1003625.

Lee, S.C., Li, A., Calo, S., Inoue, M., Tonthat, N.K., et al. (2015). Calcineurin orchestrates dimorphic transitions, antifungal drug responses and host-pathogen interactions of the pathogenic mucoralean fungus *Mucor circinelloides.* Mol Microbiol 94: 844-865.

Letey, J., Carrillo, M.L.K., Pang, X.P. (2000). Approaches to characterize the degree of water repellency. J Hydrology 231–232, 61–65.

Li, C.H., Cervantes, M., Springer, D.J., Boekhout, T., Ruiz-Vazquet, R.M. (2011). Sporangiospore size dimorphism is linked to virulence of *Mucor circinelloides*. Plos Pathog 7, e1002086.

Li, H. (2011). A statistical framework for snp calling, mutation discovery, association mapping and population genetical parameter estimation from sequencing data. Bioinformatics 27, 2987-2993.

Lin, X., Heitman, J. (2005). Chlamydospore formation during hyphal growth in *Cryptococcus neoformans*. Eukaryot Cell 4, 1746-1754.

Liu, M., Lin, L., Gebremariam, T., Luo, G., Skory, C.D., et al. (2015). Fob1 and fob2 proteins are virulence determinants of *Rhizopus oryzae* via facilitating iron uptake from ferrioxamine. Plos Pathog 11, e1004842.

Livak, K.J., Schmittgen, T.D. (2001). Analysis of relative gene expression data using real-time quantitative PCR and the $2^{-\Delta\Delta ct}$ method. Methods 25, 402-408.

López-Fernández, L., Sanchis, M., Navarro-Rodríguez, P., Nicolás, F.E., Silva-Franco, F., Guarro, J., Garre, V., Navarro-Mendoza, M.I., Pérez-Arques, C., Capilla, J. (2018). Understanding *Mucor circinelloides* pathogenesis by comparative genomics and phenotypical studies. Virulence 9, 707.

Ma, L.J., Ibrahim, A.S., Skory, C., Grabherr, M.G., Burger,G., Butler, M., et al. (2009). Genomic analysis of the basal lineage fungus *Rhizopus oryzae* reveals a whole-genome duplication. Plos Genet 5, e1000549.

Ma L, Liu X, Liang J, Zhang Z. (2011). Biotransformations of cinnamaldehyde, cinnamic acid and acetophenone with Mucor. World J Microbiol Biotechnol. 27: 2133–2137.

Maeda, H., Sano, M., Maruyama, Y., Tanno, T., Akao, T., Totsuka, Y., Endo, M., Sakurada, R., Yamagata, Y., Machida, M., et al. (2004). Transcriptional analysis of genes for energy catabolism and hydrolytic enzymes in the filamentous fungus *Aspergillus oryzae* using cDNA microarrays and expressed sequence tags. Appl Microbiol Biotechnol 65, 74-83.

Maurer, E., Hörtnagl, C., Lackner, M., Grässle, D., Naschberger, V., Moser, P., Segal, E., Semis, M., Lass-Flörl, C., Binder, U. (2019). *Galleria mellonella* as a model system to study virulence potential of Mucormycetes and evaluation of antifungal treatment. Med Mycol 57, 351-362.

Mélida, H., Sain, D., Stajich, J. E., Bulone, V. (2015). Deciphering the uniqueness of Mucoromycotina cell walls by combining biochemical and phylogenomic approaches. Environ Microbiol 17, 1649-1662.

Mendes-Giannini, M.J.S., Soares, C.P., da Silva, J.L.M., Andreotti, P.F. (2005) Interaction of pathogenic fungi with host cells: Molecular and cellular approaches. FEMS Immunol Med Microbiol 45, 383-394.

Mendoza, L., Vilela, R., Voelz, K., Ibrahim, A.S., Voigt, K., Lee, S.C. (2015). Human fungal pathogens of Mucorales and Entomophthorales. Cold Spring Harbor Perspect Med 5, a019562.

Missall, T.A., Lodge, J.K., Mcewen, J.E. (2004). Mechanisms of resistance to oxidative and nitrosative stress: implications for fungal survival in mammalian hosts. Eukaryot Cell 3, 835-846.

Miyazaki, T., Hayashi, O., Ohsima, Y., Yadome, T. (1979). Studies on fungal polysaccharides: the immunological determinant of the serologically active substances from *Absidia cylindrospora*, *Mucor hiemalis* and *Rhizopus nigricans*. Microbiol Soc 111, 417-422.

Morace, G., Borghi, E. (2011). Invasive mold infections: virulence and pathogenesis of Mucorales. Int J Microbiol 2012, 349278.

Morin-Sardin, S., Rigalma, K., Coroller, L., Jany, J.-L., Coton, E. (2016). Effect of temperature, ph, and water activity on *Mucor* spp. Growth on synthetic medium, cheese analog and cheese. Food Microbiol 56, 69-79.

Müller, F.-M.C., Seidler, M., Beauvais, A. (2011). *Aspergillus fumigatus* biofilms in the clinical setting. Med Mycol 49 (S1), S96-S100.

Muszewska, A., Piłsyk, S., Perlińska-Lenart, U., Kruszewska, J.S. (2017). Diversity of cell wall related proteins in human pathogenic fungi. J Fungi 4, 6.

Nagy, G., Farkas, A., Csernetics, Á., Bencsik, O., Szekeres, A., Nyilasi, I., Vágvölgyi, C., Papp, T. (2014). Transcription of the three HMG-CoA reductase genes of *Mucor circinelloides*. BMC Microbiol 14, 93.

Nagy, G., Szebenyi, C., Csernetics, Á., Vaz, A.G., Tóth, E.J., Vágvölgyi, C., Papp, T. (2017). Development of a plasmid free CRISPR-Cas9 system for the genetic modification of *Mucor circinelloides.* Sci Rep 7, 16800.

Naz, T., Nosheen, S., Li, S., Nazir, Y., Mustafa, K., Liu, Q., Garre, V., Song, Y. (2020). Comparative Analysis of β-Carotene Production by Mucor circinelloides Strains CBS 277.49 and WJ11 under Light and Dark Conditions. Metabolites 10, 38.

Navarro-Mendoza, M.I., Pérez-Arques, C., Murcia, L., Martínez-García, P., Lax, C., et al. (2018). Components of a new gene family of ferroxidases involved in virulence are functionally specialized in fungal dimorphism. Sci Rep 8, 7660.

Neph, S., Kuehn, M.S., Reynolds, A.P., Haugen, E., Thurman, R.E., Johnson, A.K., Rynes, E., Maurano, M.T., Vierstra, J., Thomas, S., et al. (2012). Bedops: high-performance genomic feature operations. Bioinformatics 28, 1919-1920.

Netea, M.G., Brown, G.D., Kullberg, B.J., Gow, N.A. (2008) An integrated model of the recognition of *Candida albicans* by the innate immune system. Nat Rev Microbiol 6, 67-78.

Nguyen, T.T.T., Lee, H.B. (2018). Isolation and characterization of three zygomycetous fungi in korea: *Backusella circina*, *Circinella muscae*, and *Mucor ramosissimus*. Mycobiology 46, 317.

Nodet, P., Capellano, A., Févre M. (1989) morphogenetic effects of congo red on hyphal growth and cell wall development of the fungus *Saprolegnia monoica.* J Gen Microbiol 136, 303-310.

Ohtaki, S., Maeda, H., Takahashi, T., Yamagata, Y., Hasegawa, F., Gomi, K., Nakajima, T., Abe, K. (2006a). Novel hydrophobic surface binding protein, hsba, produced by *Aspergillus oryzae*. Appl Environ Microbiol 72, 2407-2413.

Oka, T. (2018). Biosynthesis of galactomannans found in filamentous fungi belonging to Pezizomycotina. Biosci Biotechnol Biochem 82, 183-191.

Onaga, G., Wydra, K., Koopmann, B., Chebotarov, D., Séré, Y., von Tiedemann, A. (2017). High temperature effects on pi54 conferred resistance to *Magnaporthe oryzae* in two genetic backgrounds of *Oryza sativa*. J Plant Physiol 212, 80-93.

Orlowski, M. (1991). *Mucor* dimorphism. Microbiol Rev 55, 234-258.

Osherov, N., Yarden, O. (2010). The cell wall of filamentous fungi. Cell Mol Biol Fungi 224-237.

Pak, J., Tucci, V.T., Vincent, A.L., Sandin, R.L., Greene, J.N. (2008). Mucormycosis in immunochallenged patients. J Emerg Trauma Shock 1, 106-113.

Park, H. (2017). The intraphagocytic long-term survival of the mucormycotic agent *Lichtheimia corymbifera*. PhD dissertation. F. Schiller University, Jena, Germany

Patino-Medina, J.A., Valle-Maldonado, M.I., Maldonado-Herrea, G., Pérez-Arques, C., Jácome-Galarza, I., et al. (2019). Role of arf-like proteins (arl1 and arl2) of *Mucor circinelloides* in virulence and antifungal susceptibility. Fungal Genet Biol 129, 40-51.

Patiño-Medina, J.A., Vargas-Tejeda, D., Valle-Maldonado, M.I., Alejandre-Castañeda, V., Jácome-Galarza, I.E., Villegas-Moreno, J., Nuñez-Anita, R.E., Ramírez-Díaz, M.I., Ortiz-Alvarado, R., Meza-Carmen, V. (2019). Sporulation on blood serum increases the virulence of *Mucor circinelloides*. Microb Pathol 137, 103737.

Pattanayak, V., Lin, S., Guilinger, J. P., Ma, E., Doudna, J. A., & Liu, D. R. (2013). High-throughput profiling of off-target DNA cleavage reveals RNA-programmed Cas9 nuclease specificity. Nature Biotechnol 31, 839-843.

Paulick, M.G., Bertozzi, C.R. (2008). The glycosylphosphatidylinositol anchor: a complex membrane-anchoring structure for proteins. Biochemistry 47, 6991–7000.

Petrikkos, G., Skiada, A., Lortholary, O., Roilides, E., Walsh, T.J., Kontoyiannis, D.P. (2012). Epidemiology and clinical manifestations of mucormycosis. Clin Infect Dis 54 (S1), S23-S34.

Petrikkos, G.L. (2009). Lipid formulations of amphotericin b as first-line treatment of zygomycosis. Clin Microbiol Infect 15, 87-92.

Pfeiffer, C.D., Fine, J.P., Safdar, N. (2006). Diagnosis of invasive aspergillosis using a galactomannan assay: a meta-analysis. Clin Infect Dis 42, 1417-1427.

Pontón, J., Omaetxebarría, M.J., Elguezabal, N., Alvarez, M., Moragues, M.D. (2001). Immunoreactivity of the fungal cell wall. Med Mycol 39 (S1), 101-110.

Prakash, H., Chakrabarti, A. (2019). Global epidemiology of mucormycosis. J Fungi 5, 26.

Rathore, A.S., Gupta, R.D. (2015). Chitinases from bacteria to human: properties, applications, and future perspectives. Enzyme Res 2015, 791907

Reed, C., Ibrahom A.F., Edwards, J.E. (2006). Deferasirox, an iron-chelating agent, as salvage therapy for rhinocerebral mucormycosis. Antimicrob Agents Chemother 50, 3968-3969.

Ribes, J.A., Vanover-Sams, C.L., Baker, D.J. (2000). Zygomycetes in human disease. Clin Microbiol Rev 13, 236-301.

Richardson, M.D., Rautemaa-Richardson, R. (2020). Biotic environments supporting the persistence of clinically relevant Mucormycetes. J Fungi 6, 4.

Rogers, T.R. (2008). Treatment of mucormycosis: current and new options. J Antimicrob Chemother 61, 35-39.

Roncero, M. I., Jepsen, L. P., Strøman, P., van Heeswijck, R. (1989). Characterization of a leuA gene and an ARS element from *Mucor circinelloides*. Gene 84, 335-343.

Ruiz-Vázquez, R.M., Nicolás, F.E., Torres-Martínez, S., and Garre, V. (2015). Distinct RNAi Pathways in the Regulation of Physiology and Development in the Fungus *Mucor circinelloides*. In Advances in Genetics, Friedmann T., Dunlap J.C., Goodwin, S.F., Eds. (Academic Press) pp. 55-102.

Saegeman, V., Maertens, J., Meersseman, W., Spriet, I., Verbeken, E., Lagrou, K. (2010). Increasing incidence of mucormycosis in University Hospital, Belgium. Emerg Infect Dis 16, 1456-1458.

Sahai, A.S., Manocha, M.S. (1993). Chitinases of fungi and plants: their involvement in morphogenesis and host-parasite interaction. FEMS Micriobol Rev 11, 317-338.

Scholtmeijer,K., Wessels, J., Wösten, H. (2001). Fungal hydrophobins in medical and technical applications. Appl Microbiol Biotechnol. 56, 1-8.

Skory C.D. (2002). Homologous recombination and double-strand break repair in the transformation of *Rhizopus oryzae*. Mol Gen Genomics 268, 397-406.

Seidl, V. (2008). Chitinases of filamentous fungi: a large group of diverse proteins with multiple physiological functions. Fungal Biol Rev 22, 36-42.

Singh, T., Saikia, R., Jana, T., Arora, D.K. (2004). Hydrophobicity and surface electrostatic charge of conidia of the mycoparasitic *Trichoderma* species. Mycol Progress 3, 219-228.

Skiada, A., Lanternier, F., Groll, A.H., Pagano, L., Zimmerli, S., Herbrecht, R., Lortholary, O., Petrikkos, G.L., and European Conference on Infections in Leukemia (2013). Diagnosis and treatment of Mucormycosis in patients with hematological malignancies: Guidelines from the 3rd European Conference on Infections in Leukemia (Ecil 3). Haematologica 98, 492-504.

Skiada, A., Lass-Floerl, C., Klimko, N., Ibrahim, A., Roilides, E., Petrikkos, G. (2019).Challenges in the diagnosis and treatment of mucormycosis. Med Mycol 56, 93-101.

Smith, C., Gore, A., Yan, W., Abalde-Atristain, L., Li, Z., He, C., et al. (2014) Whole-genome sequencing analysis reveals high specificity of CRISPR/Cas9 and TALEN-based genome editing in human iPSCs. Cell Stem Cell 15, 12-13.

Snarr, B.D., Qureshi, S.T., Sheppard, D.C. (2017). Immune recognition of fungal polysaccharides. J Fungi 3, 47.

Soane, B.D., Ball, B.C., Arvidsson, J., Basch, G., Moreno, F., Roger-Estrade, J. (2012). No-till in northern, western and south-western Europe: a review of problems and opportunities for crop production and the environment. Soil Till Res 118, 66-87.

Song, R., Zhai, Q., Sun, L., Huang, E., Zhang, Y., Zhu, Y., Guo, Q., Tian, Y., Zhao, B., Lu, H. (2019). CRISPR/Cas9 genome editing technology in filamentous fungi: progress and perspective. Appl Microbiol Biotechnol 103, 6919-6932.

Spellberg, B., Ibrahim, A.S. (2010). Recent advances in the treatment of mucormycosis. Curr Infect Dis Rep 12, 423-429.

Spellberg, B., Fu, Y., Edwards, J.E., Ibrahim, A.S. (2005). Combination therapy with amphotericin b lipid complex and caspofungin acetate of disseminated zygomycosis in diabetic ketoacidotic mice. Antimicrob Agents Chemother 49, 830-832.

Spreer, A., Rüchel, R., Reichard, U. (2006). Characterization of an extracellular subtilisin protease of *Rhizopus microsporus* and evidence for its expression during invasive rhinoorbital mycosis. Med Mycol 44, 723-731.

Staden, R., Beal, K.F., Bonfield, J.K. (2000). The Staden Package. Methods Mol Biol 132, 115-130.

Sunde, M., Pham, C.L.L., Kwan, A.H. (2017). Molecular Characteristics and Biological Functions of Surface-Active and Surfactant Proteins. Annu Rev Biochem 86, 585-608.

Sze, K.H., Lam, W.H., Zhang, H., Ke, Y.H., Tse, M.K., et al .(2017). *Talaromyces marneffei* Mp1p is a virulence factor that binds and sequesters a key proinflammatory lipid to dampen host innate immune response. Cell Chem Biol 24, 182-194.

Takahashi, T., Maeda, H., Yoneda, S., Ohtaki, S., Yamagata, Y., Hasegawa, F., Gomi, K., Nakajima, T., Abe, K. (2005). The fungal hydrophobin rola recruits polyesterase and laterally moves on hydrophobic surfaces. Mol Microbiol 57, 1780-1796.

Tchigvintsev, A., Tchigvintsev, D., Flick, R., Popovic, A., Dong, A., Xu, X., Brown, G., Lu, W., Wu, H., Cui, H., et al. (2013). Biochemical and structural studies of conserved MAF proteins revealed nucleotide pyrophosphatases with a preference for modified nucleotides. Chem Biol 20, 1386-1398.

Torres-Narbona, M., Guinea, J., Martínez-Alarcón, J., Muñoz, P., Gadea, I., Bouza, E., and MYCOMED Zygomycosis Study Group (2007). Impact of zygomycosis on microbiology workload: a survey study in Spain. J Clin Microbiol 45, 2051-2053.

van der Auwera, G.A., Carneiro, M.O., Hartl, C., Poplin, R., Angel, G.D. et al. (2013). Identification of GPI anchor attachment signals by a Kohonen self-organizing map. Curr Protoc Bioinform 43, 11.10.1-11.10.33.

van der Auwera, G.A., Carneiro, M.O., Hartl, C., Poplin, R., Del Angel, G., Levy-Moonshine, A., Jordan, T., Shakir, K., Roazen, D., Thibault, J., et al. (2013). From fastq data to high confidence variant calls: the genome analysis toolkit best practices pipeline. Curr Protoc Bioinformatics 43, 11.10.1-11.10.33.

van Heeswijck, R., Roncero, M.I.G. (1984). High frequency transformation of *Mucor* with recombinant plasmid DNA. Carlsberg Res Commun 49, 691.

Vellanki, S., Billmyre, R.B., Lornezne, A., Campbell, M., Turner, B., Huh, E.Y., Heitman, J., Lee, S.C. (2020). A novel resistance pathway for calcineurin inhibitors in the human-pathogenic Mucorales *Mucor circinelloides.* mBio 11, 1.

Vellanki, S., Navarro-Mendoza, M.i., Garcia, A.E., Murcia, L., Perez-Arques, C. (2018). *Mucor circinelloides*: growth, maintenance, and genetic manipulation. Curr Protoc Microbiol 49, e53.

Voigt, K., Wolf, T., Ochsenreiter, K., Nagy, G., Kaerger, K., Shelest, E., Papp, T. (2016). 15 Genetic and metabolic aspects of primary and secondary metabolism of the zygomycetes. In Biochemistry and Molecular Biology, Hoffmeister, D., Ed. (Cham: Springer International Publishing), pp. 361–385.

Walther, G., Wagner, L., Kurzai, O. (2019). Outbreaks of mucorales and the species involved. Mycopathologia https://doi.org/10.1007/s11046-019-00403-1

Wang, B., Liang, X., Gleason, M.L., Zhang, R., Sun, G. (2017). Genome sequence of the ectophytic fungus *Ramichloridium luteum* reveals unique evolutionary adaptations to plant surface niche. BMB Genomics 18, 729.

Watsom, C.L., Letey, J. (1970). Indices for characterizing soil-water repellency based upon contact angle-surface tension relationships. Soil Sci Society Am J 34, 6.

Weerakkody, L.R., Witharana, C. (2019). Over expression of the multicopy associated filamentation maf gene of caldimonas manganoxidans MS1 and determination of the biological effect of MAF proteins on the viability of bacterial cells. 4th International Research Symposium on Pure and Applied Sciences, Faculty of Science, University of Kelaniya, Sri Lanka.

Wolff, A.M., Appel, K.F., Petersen, J.B., Poulsen, U., Arnau, J. (2002). Identification and analysis of genes involved in the control of dimorphism in *Mucor circinelloides* (syn. *racemosus*). FEMS Yeast Res 2, 203-213.

Woo, P.C.Y., Lau, S.K.P., Lau, C.C.Y., Tung, E.T.K., Chong, K.T.K., Yang, F., Zhang, H., Lo, R.K.C., Cai, J.-P., Au-Yeung, R.K.H., et al. (2016). Mp1p is a virulence factor in *Talaromyces* (*penicillium*) *marneffei*. Plos Negl Trop Dis 10, e0004907.

Wood, P.J. (1980). Specificity in the interaction of direct dyes with polysaccharides. Carboh Res 85, 271-287.

Wösten, H.A.B. (2001). Hydrophobins: multipurpose proteins. Annu Rev Microbiol 55, 625-646.

Xu, W., Liang, G., Peng, J., Long, Z., Li, D., Fu, M., Wang, Q., Shen, Y., Lv, G., Mei, H., et al. (2017). The influence of the mating type on virulence of *Mucor irregularis*. Sci Rep 7, 10629.

Yamazaki, T., Kawamura, Y., Minami, A., Uemura, M. (2008). Calcium-dependent freezing tolerance in *Arabidopsis* involves membrane resealing via synaptotagmin *syt1*. Plant Cell 20, 3389-3404.

Yoshimi, A., Miyazawa, K., Abe, K. (2017). Function and biosynthesis of cell wall α-1,3-glucan in fungi. J Fungi 3, 63.

Yuen, K-Y., Chan, C-M., Chan, K-M. Woo, P.C.W, Che, X-Y., Cao, S.P.L.L. (2001) Characterization of afmp1: a novel target for serodiagnosis of aspergillosis. J Clin Microbiol 22, 621-635.

Zhang, M., Ma, Q.Z., Zhai, N.P., Xu, C., Zang, R., Gen, Y.H., Wu, H.Y. (2018). Occurrence of outbreak of leaf spot caused by *Corynespora cassiicola* in strawberry in China. Plant Dis 102, 2037.

9. LIST OF PUBLICATIONS

Full papers

Nagy, G*; **Vaz**, **AG***; Szebenyi, C; Takó, M; Tóth, EJ; Csernetics, Á; Bencsik, O; Szekeres, A; Homa, M; Ayaydin, F et al. (2019). CRISPR-Cas9-mediated disruption of the HMG-CoA reductase genes of *Mucor circinelloides* and subcellular localization of the encoded enzymes. Fungal Genet Biol 129, 30-39. (* Divided first authorship.)

Nagy, G; Szebenyi, C; Csernetics, Á; **Vaz**, **AG**; Tóth, EJ; Vágvölgyi, C; Papp, T. (2017). Development of a plasmid free CRISPR-Cas9 system for the genetic modification of *Mucor circinelloides*. Sci Rep 7, 16800.

Abstracts

Nagy, G; Kiss, S; Szebenyi, C; Verghase, R; **Vaz, AG**; Jáger, O; Ibragimova, S; Gu, Y; Ibrahim, AD; Vágvölgyi, C; et al. (2020). Construction of a mutant library to examine the pathogenicity of *Mucor circinelloides* using CRISPR/Cas9 system. Fungal genetics, host pathogen interaction and evolutionary ecology pp. 289-290.

Nagy, G; Szebenyi, C; **Vaz, AG**; Jáger, O; Ibragimova S; Gu, Y; Ibrahim, AD; Vágvölgyi, C; et al. (2019). Development of a plasmid free CRISPR/Cas9 system for the genetic modification of opportunistic pathogenic mucormycotina species. In K., Márialigeti; O., Dobay, Eds., Acta Microbiol Immunol Hung Budapest, Hungary: Akadémiai Kiadó, pp. 169-169.

Szebenyi, C; Nagy, G; Tóth, EJ; Werner, T; **Vaz**, **AG**; Vágvölgyi, C; Papp, T. (2019). Disruption of the cotH genes of the filamentous fungus, *Mucor circinelloides* by a plasmid-free CRISPR/CAS9 system. HFP2019: Molecular Mechanisms of Host-Pathogen Interactions and Virulence in Human Fungal Pathogens. p. 146.

Vaz, **AG**; Takó, M; Szebenyi, C; Tóth, EJ; Vágvölgyi, C; Papp, T; Nagy, G. (2019). Functional characterization of a novel hydrophobic surface binding protein in Mucorales. HFP2019: Molecular Mechanisms of Host–Pathogen Interactions and Virulence in Human Fungal Pathogens. p. 1596.

Szebenyi, C; Nagy, G; Tóth, EJ; Kiss, S; **Vaz, AG**; Vágvölgyi, C; Papp, T. (2018). Molecular and functional analysis of the coth genes encoding spore coat-like proteins in the zygomycete fungus *Mucor circinelloides*. A Magyar Mikrobiológiai Társaság 2018. évi Nagygyűlése és a XIII. Fermentációs Kollokvium: Absztraktfüzet p. 597.

Szebenyi, C; Nagy, G; Toth, EJ; **Vaz**, **A**; Vegh, AG; Farkas, G; Vagvolgyi, C; Papp, T. (2018). Disruption of *cotH* genes of *Mucor circinelloides* via a plasmid-free CRISPR/Cas9 system. Med Mycol 56 (S2), S28-S28.

Szebenyi, C; Nagy, G; Tóth, EJ; Kiss, S; **Vaz**, **A**; Vágvölgyi, C; Papp, T. (2018). Identification and analysis of the cotH genes encoding spore coat-like proteins in *Mucor circinelloides*. In: Attila, Gácser; Ilona, Pfeiffer (eds.) 6th CESC 2018 Central European Summer Course on Mycology and 3rd Rising Stars in Mycology Workshop: Biology of pathogenic fungi, Szeged, Hungary: JATEPress Kiadó, p. 49.

Vaz, **AG**; Takó, M; Szebenyi, C; Vágvölgyi, C; Papp, T; Nagy, G. (2018). Functional characterization of a novel hydrophobic surface binding protein in Mucorales. A Magyar Mikrobiológiai Társaság 2018. évi Nagygyűlése és a XIII. Fermentációs Kollokvium: Absztraktfüzet p. 69.

Vaz, **AG**; Takó, M; Szebenyi, C; Vágvölgyi, C; Papp, T; Nagy, G. (2018). Characterization of a novel hydrophobic surface binding protein in Mucorales. Attila, Gácser; Ilona, Pfeiffer (eds.) 6th CESC 2018 Central European Summer Course on Mycology and 3rd Rising Stars in Mycology Workshop: Biology of pathogenic fungi, Szeged, Hungary: JATEPress Kiadó, p. 55.

Nagy, G; Szebenyi, C; **Vaz**, **AG**; Tóth, E; Homa, M; Vágvölgyi, C; Papp, T. (2017). A CRISPR/Cas9 system for disruption of carb gene in *Mucor circinelloides*. In: 7th Congress of European Microbiologists (FEMS 2017), p. 2125.

Szebenyi, Cs; Nagy, G; **Vaz**, **A**; Tóth, E; Vágvölgyi, C; Papp, T. (2017). Disruption of genes cotH1 and cotH2 of Mucor circinelloides via the CRISPR/Cas9 system. ACTA MICROBIOLOGICA ET IMMUNOLOGICA HUNGARICA 64: 1 pp. 172-173., 2 p.

Szebenyi, Cs; Nagy, G; **Vaz**, **A**; Tóth, E; Kiss, S; Vágvölgyi, C; Papp, T. (2017). A Mucor circinellodes cotH1 és cotH2 gén deléciója CRISPR/Cas9 rendszer segítségével - Disruption of the cotH1 and cotH2 genes of M. circinelloides usong a CRISPR/Cas9 system. MIKOLÓGIAI KÖZLEMÉNYEK-CLUSIANA 56: 1 pp. 136-138., 3 p.

Szebenyi, Cs; Nagy, G; **Vaz**, **A**; Tóth, E; Kiss, S; Vágvölgyi, Cs; Papp, T. (2017). Disruption of coth1 and coth2 genes of Mucor circinelloides by using a CRISPR/Cas9 system. 7th Congress of European Microbiologists (FEMS 2017), p. 1783.

Szebenyi, Cs; Nagy, G; **Vaz**, **A**; Tóth, E; Kiss, S; Vágvölgyi, Cs; Papp, T. (2017). Targeted genome editing via the CRISPR/CAS9 system in Mucor circinelloides. [Department, of Public Health Faculty of Medicine University of Szeged] (eds.) 19th Danube-Kris-Mures-Tisa (DKMT). Euroregional Conference on Environment and Health: Program and abstracts. Szeged, Hungary: University of Szeged, Faculty of Medicine, p. 30.

Vaz, **A**; Takó, M; Szebenyi, Cs; Vágvölgyi, Cs; Nagy, G; Papp, T. (2017). Characterization of novel type surface proteins in Mucorales. [Department, of Public Health Faculty of Medicine University of Szeged] (eds.) 19th Danube-Kris-Mures-Tisa (DKMT) Euroregional Conference on Environment and Health: Program and abstracts. Szeged, Hungary: University of Szeged, Faculty of Medicine, p. 57.

Vaz, **AG**; Takó, M; Szebenyi, Cs; Vágvölgyi, Cs; Papp, T; Nagy, G. (2017). Új típusú hidrofób sejtfelszíni fehérje funkcionális vizsgálata járomspórás gombákban - Functional analysis of a novel hydrophobic surface binding protein in Mucorales. Mikológiai Közlemények-Clusiana 56: 1 pp. 161-162, 2 p.

Nagy, G; Hassan, M; Kumar, D; **Vaz, AG**; Bartha, E; Vágvölgyi, C; Voigt, K; Papp, T; Csernetics, Á. (2016). Molecular background of virulence in human pathogenic Mucoralean fungi. Annual Conference 2016 of the Association for General and Applied Microbiology (VAAM)p. 84.

Nagy, G; Hassan, M; Kumar, D; **Vaz**, **AG**; Bartha, E; Csernetics, Á; Vágvölgyi, C; Voigt, K; Papp, T. (2016). Characterization of virulence genes in opportunistic human pathogenic Mucoralean fungi. 13th European Conference on Fungal Genetics (ECFG13), Bacterial Fungal Interactions Workshop, Abstract Book p. 161.

SUPPLEMENTARY MATERIALS

Table S1: Primers used in this study.

Name of the primer	Sequence 5'-3'	Length of the amplicon (bp)	Used for
McHSB1_RT1	CCCGAGTTTGATGCCATTCT	159	Primers for qRT-PCR analysis
McHSB1_RT2	GGAGTTGTTGATTTGAGTGACCA		
McHSB2_RT1	TCAACACTGTAAGCACCCTTG	192	
McHSB2_RT2	CAGCATCCAAATGAGTAGCGG		
McHSB3_RT1	CTTACTATTGCTGCCTCAGTCA	197	
McHSB3_RT2	GTTTCAAGAGTTTGTTCACTGGAG		
McHSB4_RT1	CATTGTCGTCCATTGTCACCA	195	
McHSB4_RT2	CAGATGCAAAGGAGGTGTTGA		
McActinF	CACTCCTTCACTACCACCGCT		
McActinR	GAGAGCAGAGGATTGAGCAGC		
McHSB1HEfw	TTTCTGAGGAGAAAAGAGCTGCCCTCGACAAGAG AGCCGTCT	536	Primers of *hsbA* to construct the expression vector for heterologous expression in *P. pastoris*
McHSB1HErev	TTCTCTAGATCGGATCCTCTTGGAACCAAGATACC ATAAGCGGTCTTGGCAGAG		
McHSB2HEfw	TTTCTCGAGGAGAAAAGAGCTGCTCTTGATAAGA GAGCCATCT	539	
McHSB2HErev	TTTTCTAGATCGGATCCTCTTGGAACCAAGATACC ATAAGAGGTCTTGGCTG		
5AOX 1	GACTGGTTCCAATTGACAAGC	588	To amplify *aox1* gene of *Pichia* transformant for positive clone selection
3AOX1	GCAAATGGCATTCTGACATTC		
McHSB1oefw	TTCCTCGAGATGCGTGCCTTCTCCACTTTAATC	640	Primers to construct pAV1, pAV2 and pAV3 plasmids for the overexpression of the *hsbA* genes
McHSB1oerev	TTCATCGATTTAGATACCATAAGCGGTCTTGGC		
McHSB2oefw	TTCCTCGAGATGCGCGCTTTC TCTACATTACTC	636	
McHSB2oerev	TTCATCGAT TTAGATACCATAAGCGGTCTTGGC		
McHSB3oefw	TTCCTCGAGATGCGCGCCTCTCTCTCTTT	573	
McHSB3oerev	TTCATCGATTTAAATACCGTAAGCGGTCTTGGCAG AGGC		
Gpdp	CATGAAGTGTGAGACATTGCGA		Primer for the analysis of the overexpressed mutants
McHSB1/1 (promoter)	AATGTGCTGTTGGTTACACGA	1109	Primers to construct the disruption cassette for *hsbA*1
McHSB1/2 (promoter)	CAGAGTTGATGTCGTCAATACAG		
McHSB1/3 (pyr)	GTCCAACTCTGTATTGACGACATCAACTCTGTGCC TCAGCATTGGTACTTG	2055	
McHSB1/4 (pyr)	CTTGGTTTGGGTATCCAAGTTCTTGATGTCGTACA CTGGCCATGCTATCG		

McHSB1/5 (terminator)	GACATCAAGAACTTGGATACCC	1129	
McHSB1/6 (terminator)	GGTTTGGACATCTCAACACCT		
McHSB1/7 (nested)	GTACTCTTCCATACATTCCATTCTG	3864	
McHSB1/8 (nested)	AAGCGCATAGTAAACTGACC		
McHSB2/1 (promoter)	AAATAGCCTGAGCAGTTGTTTGAG	1108	Primers to construct the disruption cassette for *hsbA*2
McHSB2/2 (promoter)	GGCTTTAACAATGGCAAGTTGAG		
McHSB2/3 (pyr)	GCTGCTGCTCAACTTGCCATTGTTAAAGCCTGCCTCAGCATTGGTACTTG	2065	
McHSB2/4 (pyr)	TGGTTTGAGAGTCCAGGTTCTTGATGTCACGTACACTGGCCATGCTATCG		
McHSB2/5 (terminator)	GTGACATCAAGAACCTGGAC	1138	
McHSB2/6 (terminator)	TGAATGACAAGATACACGCC		
McHSB2/7 (nested)	AATGGCCAATGGTATTAGTTCCC	3891	
McHSB2/8 (nested)	AGCTATAATCTGTACCGCACTG		
McHSB3/1 (promoter)	CAAACGAATGTTGGGATTTCTC	1155	Primers to construct the disruption cassette for *hsbA*3
McHSB3/2 (promoter)	TTTGATTTGATTTGTTTGTTGTTGA		
McHSB3/3 (terminator)	GTTAGCATAGCTAGTCTTTATCCCT	1106	
McHSB3/4 (terminator)	CATGGTACAAATGGCTTACGG		
McHSB3/5 (pyr)	CAATCAAATCTCAACAACAAACAAATCAAATCAAATGCCTCAGCATTGGTACTTG	2065	
McHSB3/6 (pyr)	CATGGCAAGTAGGGATAAAGACTAGCTATGCTAACGTACACTGGCCATGCTATCG		
McHSB3/7 (nested)	CTCCGCCCTATTAAAGAAGCA	3829	
McHSB3/8 (nested)	ACTTATGCCAAATGTCGTGAG		

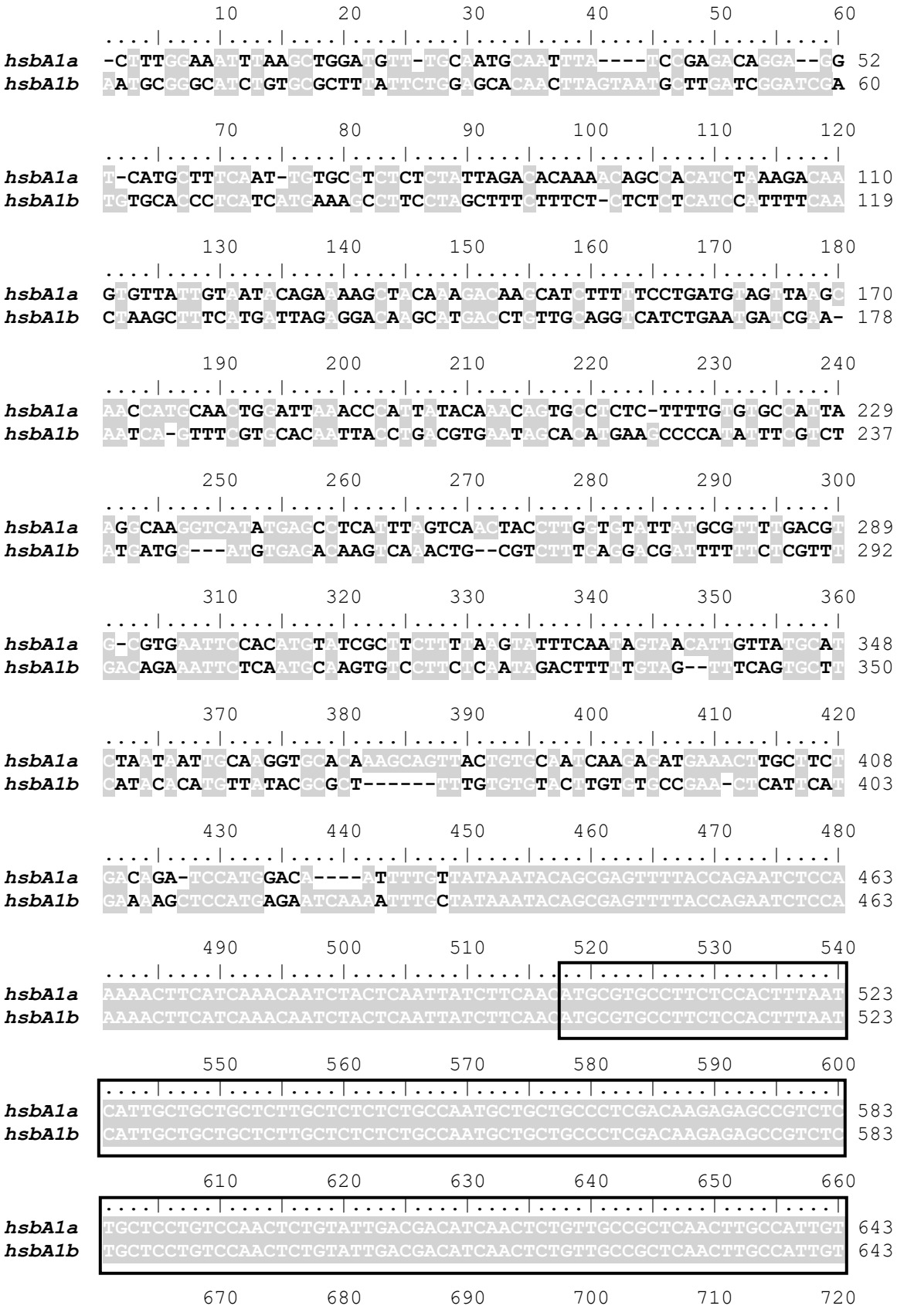
10 20 30 40 50 60
hsbA1a -CTTTGGAAATTAAGCTGGATGTT-TGCAATGCAATTTA----TCGAGACAGGA--GG 52
hsbA1b AATGCGGGCATCTGTGCGCTTTATTCTGGAGCACAACTTAGTAATGCTTGATCGGATCGGA 60
70 80 90 100 110 120
hsbA1a T-CATGCTTTCAAT-TGTGCTTCTCTATTAGACACAAAACAGCCACATCTTAAGACAA 110
hsbA1b TGTGCACCTCATCATGAAAGCCTTCCTAGCTTTCTTTCT-CTCTCTCATCCCTTTTCAA 119
130 140 150 160 170 180
hsbA1a GTGTTATTGTAATACAGAAAAGCTACAAGACAAGCATCTTTTCCTGATGTAGTATAGC 170
hsbA1b CTAAGCTTTCCTGATTAGTGGAAAGCATGACCTGTTGTAGGTCATCTGAATGACCGAA- 178
190 200 210 220 230 240
hsbA1a AACCATGCAACTGTGATTAAACCCATTATACAAACAGTGTCCTC-TTTTGTGTGCCATTA 229
hsbA1b AATCA-GTTTCGTGCACAATTACCTGCGTGAATAGCACAGAAGCCCCCATATTTCGTCT 237
250 260 270 280 290 300
hsbA1a AGGCAAGGTCATATGAGCCTCATTTTGTCAACTACCTTGCTTTTTATGCGTTTTGACGT 289
hsbA1b ATGATGG---ATGTGAGAAAAGTCAAACTG--CGTCTTTCAGGACGATTTTTCTCGTTT 292
310 320 330 340 350 360
hsbA1a G-CGTGAATTCCACATGTTTCGCTTCTTTTAAGTATTTCAAAAGTAACATTGTTATGCAT 348
hsbA1b GACAGAAATTCTCAATGCCAGTGTCCTTCTCCATAGACTTTTTGTAG--TTTCAGTGCTT 350
370 380 390 400 410 420
hsbA1a CTATTATTGCAAGGTGCAAAAGCAGTTACTGTGCAATCAAGAAATGAAACTTGCTTCT 408
hsbA1b CATTCACATGTTTACGCGCT------TTTGTGTGTACTTGTTGTCCGAAA-CTCATTCAT 403
430 440 450 460 470 480
hsbA1a GACAGA-TCCATCGACA----ATTTTCTTATAAATACAGCGAGTTTTACCAGAATCTCCA 463
hsbA1b GAAAAGCTCCATCAGAATCAAAATTTCCTATAAATACAGCGAGTTTTACCAGAATCTCCA 463
490 500 510 520 530 540
hsbA1a AAAACTTCATCAAACAATCTACTCAATTATCTTCAAGATGCGTGCCTTCTCCACTTTAAT 523
hsbA1b AAAACTTCATCAAACAATCTACTCAATTATCTTCAAGATGCGTGCCTTCTCCACTTTAAT 523
550 560 570 580 590 600
hsbA1a CATTGCTGCTGCTCTTGCTCTCTCTGCCAATGCTGCTGCCCTCGACAAGAGAGCCGTCTC 583
hsbA1b CATTGCTGCTGCTCTTGCTCTCTCTGCCAATGCTGCTGCCCTCGACAAGAGAGCCGTCTC 583
610 620 630 640 650 660
hsbA1a TGCTCCTGTCCAACTCTGTATTGACGACATCAACTCTGTTGCCGCTCAACTTGCCATTGT 643
hsbA1b TGCTCCTGTCCAACTCTGTATTGACGACATCAACTCTGTTGCCGCTCAACTTGCCATTGT 643
670 680 690 700 710 720

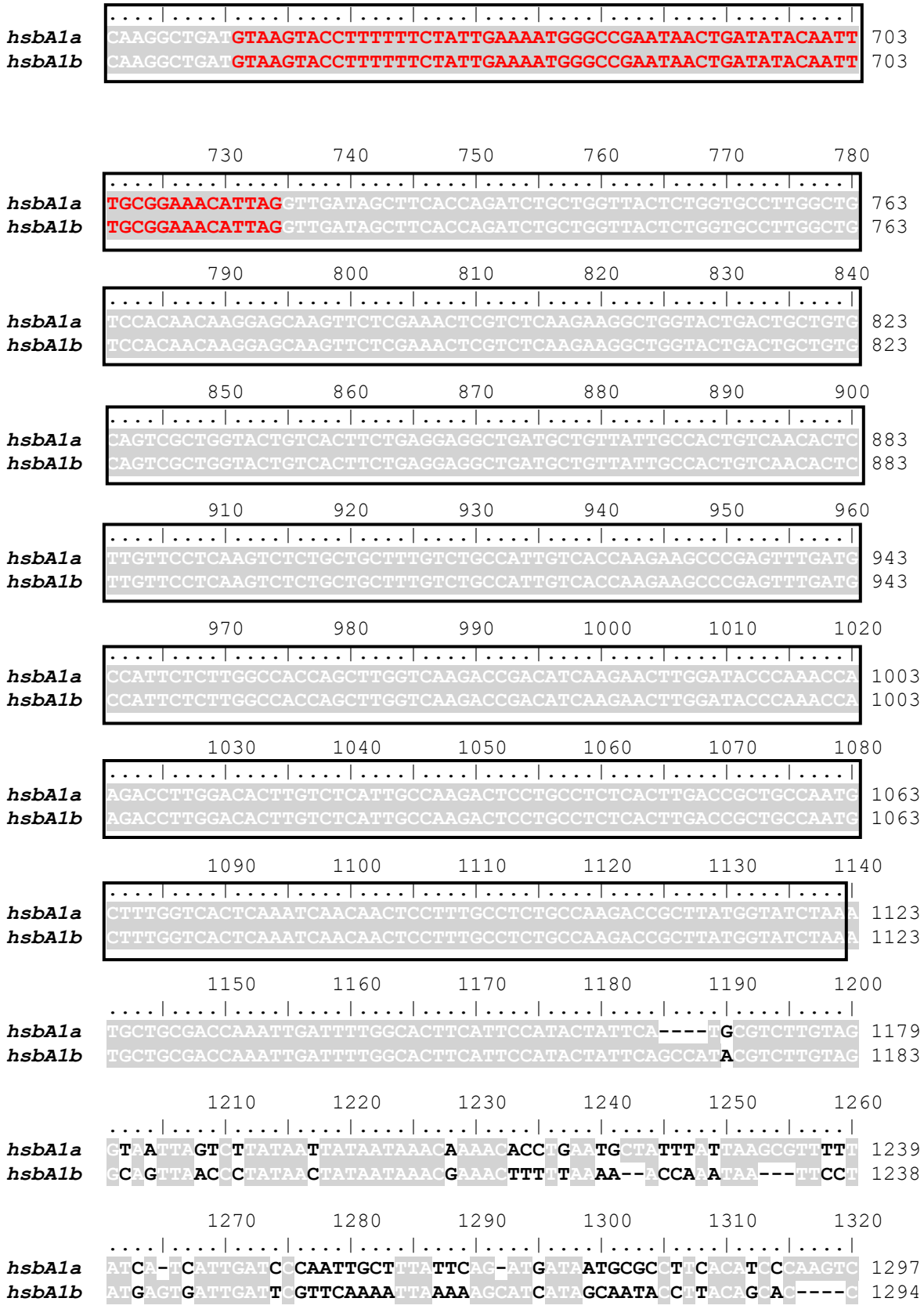
hsbA1a CAAGGCTGATGTAAGTACCTTTTTTCTATTGAAAATGGGCCGAATAACTGATATACAATT 703
hsbA1b CAAGGCTGATGTAAGTACCTTTTTTCTATTGAAAATGGGCCGAATAACTGATATACAATT 703
730 740 750 760 770 780
hsbA1a TGCGGAAACATTAGGTTGATAGCTTCACCAGATCTGCTGGTTACTCTGGTGCCTTGGCTG 763
hsbA1b TGCGGAAACATTAGGTTGATAGCTTCACCAGATCTGCTGGTTACTCTGGTGCCTTGGCTG 763
790 800 810 820 830 840
hsbA1a TCCACAACAAGGAGCAAGTTCTCGAAACTCGTCTCAAGAAGGCTGGTACTGACTGCTGTG 823
hsbA1b TCCACAACAAGGAGCAAGTTCTCGAAACTCGTCTCAAGAAGGCTGGTACTGACTGCTGTG 823
850 860 870 880 890 900
hsbA1a CAGTCGCTGGTACTGTCACTTCTGAGGAGGCTGATGCTGTTATTGCCACTGTCAACACTC 883
hsbA1b CAGTCGCTGGTACTGTCACTTCTGAGGAGGCTGATGCTGTTATTGCCACTGTCAACACTC 883
910 920 930 940 950 960
hsbA1a TTGTTCCTCAAGTCTCTGCTGCTTTGTCTGCCATTGTCACCAAGAAGCCCGAGTTTGATG 943
hsbA1b TTGTTCCTCAAGTCTCTGCTGCTTTGTCTGCCATTGTCACCAAGAAGCCCGAGTTTGATG 943
970 980 990 1000 1010 1020
hsbA1a CCATTCTCTTGGCCACCAGCTTGGTCAAGACCGACATCAAGAACTTGGATACCCAAACCA 1003
hsbA1b CCATTCTCTTGGCCACCAGCTTGGTCAAGACCGACATCAAGAACTTGGATACCCAAACCA 1003
1030 1040 1050 1060 1070 1080
hsbA1a AGACCTTGGACACTTGTCTCATTGCCAAGACTCCTGCCTCTCACTTGACCGCTGCCAATG 1063
hsbA1b AGACCTTGGACACTTGTCTCATTGCCAAGACTCCTGCCTCTCACTTGACCGCTGCCAATG 1063
1090 1100 1110 1120 1130 1140
hsbA1a CTTTGGTCACTCAAATCAACAACTCCTTTGCCTCTGCCAAGACCGCTTATGGTATCTAAA 1123
hsbA1b CTTTGGTCACTCAAATCAACAACTCCTTTGCCTCTGCCAAGACCGCTTATGGTATCTAAA 1123
1150 1160 1170 1180 1190 1200
hsbA1a TGCTGCGACCAAATTGATTTTGGCACTTCATTCCATACTATTCA----TGCGTCTTGTAG 1179
hsbA1b TGCTGCGACCAAATTGATTTTGGCACTTCATTCCATACTATTCAGCCATACGTCTTGTAG 1183
1210 1220 1230 1240 1250 1260
hsbA1a GTAATTAGTCTTATAATTATAATAAACAAAACACCTGAATGCTATTTATTAAGCGTTTT 1239
hsbA1b GCAGTTACCCTATAACTATAATAAACGAAACTTTTAAAA--ACCAATAA---TTCCT 1238
1270 1280 1290 1300 1310 1320
hsbA1a ATCA-TCATTGATCCCAATTGCTTTATTCAG-ATGATAATGCGCCTTCACATCCAAGTC 1297
hsbA1b ATGAGTGATTGATTCGTTCAAAATTAAAAGCATCATAGCAATACCTTACAGCA----C 1294

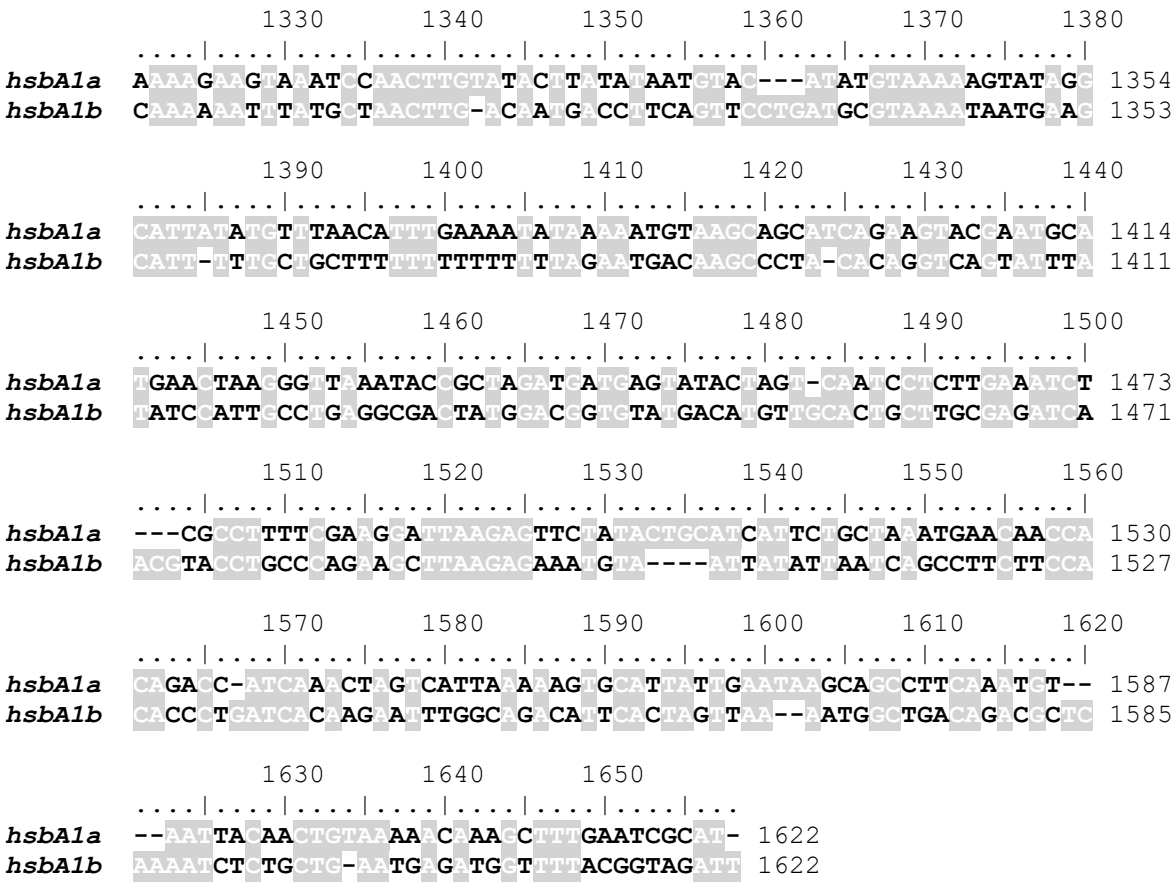

Figure S1: Nucleotide sequence of the *hsbA1a* and *hsbA1b* genes and their adjacent regions. Gene sequences are shown in the box, intron sequence is highlighted with red characters.

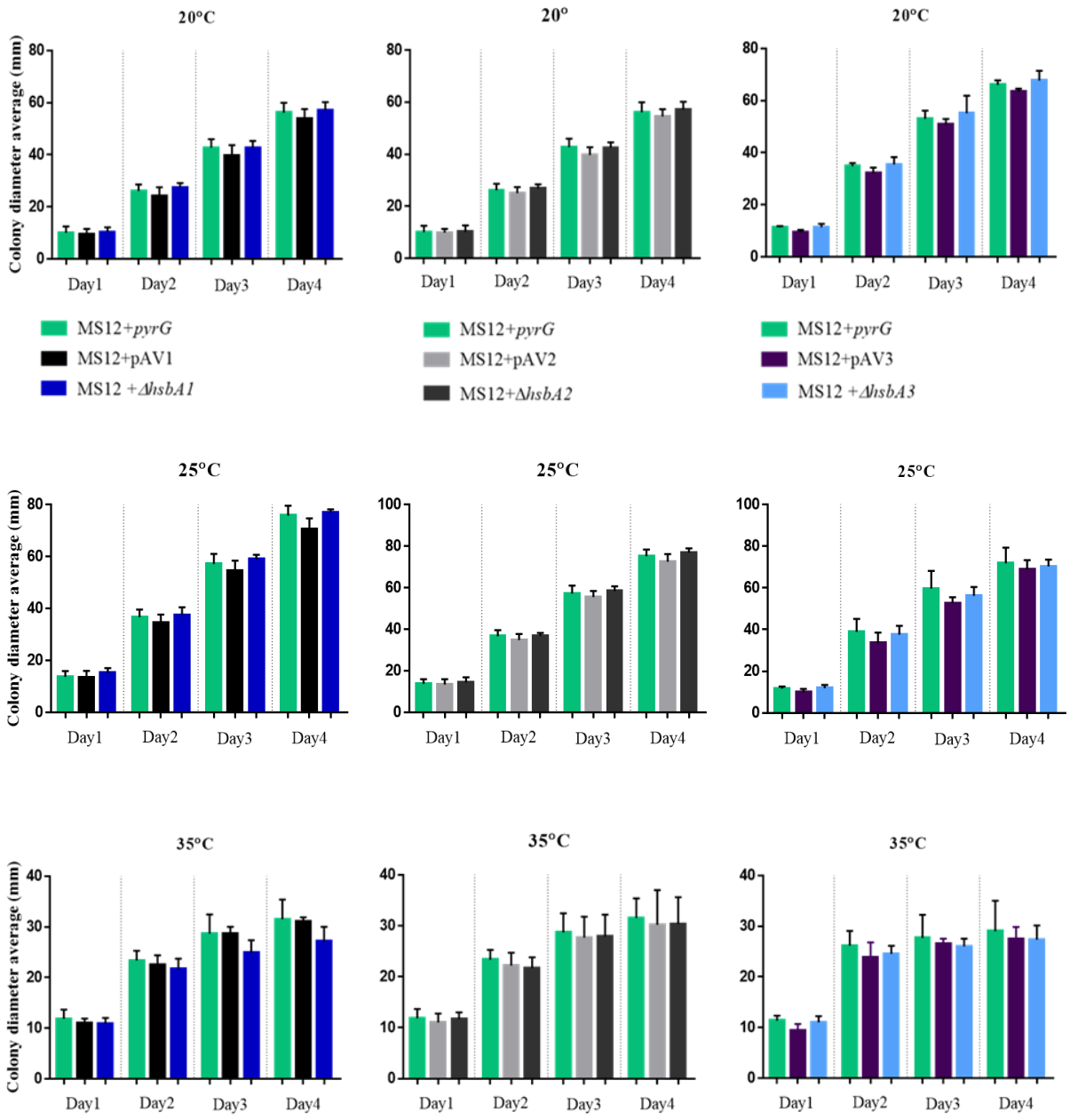

Figure S2: Colony diameter of the hsbA mutants and the MS12+*pyrG* strain at 20 °C, 25 °C and 35 °C. Strains were grown on YNB plates for four days. The presented values are averages; colony diameters were measured during three independent cultivation (error bars indicate standard deviation). Values were compared with the corresponding value of the MS12+*pyrG* strain according to the statistical method statistical method one-way ANOVA.